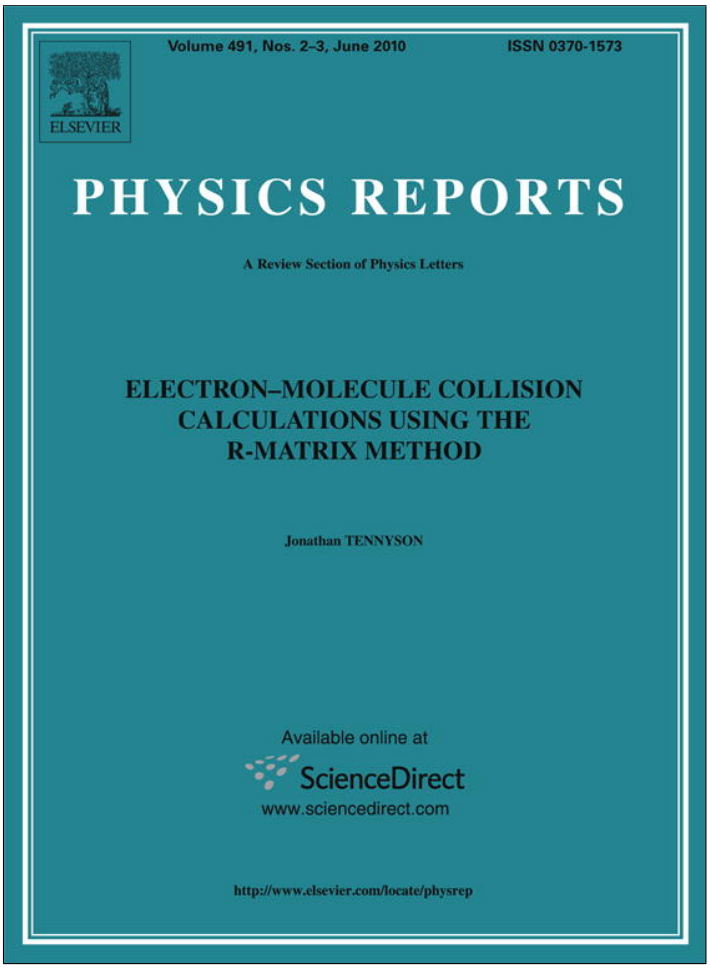

Physics Reports 491 (2010) 29–76

Contents lists available at ScienceDirect

Physics Reports

journal homepage: www.elsevier.com/locate/physrep

Electron–molecule collision calculations using the **R**-matrix method

Jonathan Tennyson *

Department of Physics and Astronomy, University College London, Gower Street, London WC1E 6BT, UK

ARTICLE INFO

Article history:
Accepted 10 December 2009
Available online 10 February 2010
editor: S. Peyerimhoff

Keywords:
Resonances
Cross sections
Eigenphases
Quantum chemistry
Close coupling
Pseudo-states
Electron scattering
Positron scattering
Quantum defects
Rydberg states
Photoionization

ABSTRACT

The **R**-matrix method is an embedding procedure which is based on the division of space into an inner region where the physics is complicated and an outer region for which greatly simplified equations can be solved. The method developed out of nuclear physics, where the effects of the inner region were simply parametrized, into atomic and molecular physics, where the full problem can be formulated and hopefully solved ab initio. In atomic physics **R**-matrix based procedures are the method of choice for the ab initio calculation of electron collision parameters. There has been a number of **R**-matrix procedures developed to treat the low-energy electron–molecule collision problem or particular aspects of this problem. These methods have been extended to both positron physics and the **R**-matrix treatment of vibrational motion.

The physical basis of the **R**-matrix method as well as its theoretical formulation are presented. Various electron scattering models within an **R**-matrix formulation including static exchange, static exchange plus polarization and close coupling are described with reference to various computational implementations of the method; these are compared to similar models used within other scattering methods. The need for a balanced treatment of the target and continuum wave functions is emphasised. Extensions of close-coupling based models into the intermediate energy regime using pseudo-states is discussed, as is the adaptation of **R**-matrix methods to problems involving photons.

The numerical realisation of the **R**-matrix method is based on the adaptation of quantum chemistry codes in the inner region and asymptotic electron–atom scattering programs in the outer region. Use of bound state codes in scattering calculations raises issues involving continuum basis sets, appropriate orbitals, integral evaluation, orthogonalization, Hamiltonian construction and diagonalization which need to be addressed. The algorithms developed to resolve these issues are described as are ones associated with the outer region where methods to characterize resonances have received particular attention.

Results from a few illustrative calculations are discussed: (i) electron collisions with polar systems with water as an example; (ii) electron collisions with molecular ions focusing on H_3^+; (iii) electron collisions with organic species such as methane and uracil and (iv) positron–molecule collisions. Finally some outstanding issues that need to be addressed are mentioned.

Contents

* Tel.: +44 20 7679 7155; fax: +44 20 7679 7145.
E-mail address: j.tennyson@ucl.ac.uk.

0370-1573/$ – see front matter © 2010 Elsevier B.V. All rights reserved.
doi:10.1016/j.physrep.2010.02.001

1. Introduction

Electron collisions with molecules are the dominant process in cool plasmas and discharges. They occur naturally in our own atmosphere through auroras [1] and lightning [2]. In the natural world it is now widely accepted that low-energy electron collisions are the major cause of radiation damage within cells [3]. In space, besides planetary auroras [4], vast tracks of the interstellar medium are weakly ionized plasma where the cold chemistry of molecular ions predominates. Electron collisions control much of this chemistry [5]. Hotter regions in the interstellar medium, such as shocks [6] and planetary nebulae [7], can also be sensitive to electron–molecule collision processes.

The list of technologies that rely on electron collisions is long: some are well established such as the spark plugs that fire internal combustion engines or their use in electric lighting. Electron–molecule collisions initiate many laser processes and are routinely used in discharges to stimulate interesting chemistries. A prime example is the use of electron collisions to initiate the plasma etching processes upon which much of the worlds hi-tech industries rely. The importance of electron–molecule collisions, particularly at low energy, has of course stimulated significant work both experimentally [8] and theoretically [9].

When considering electron collisions it is useful to divide the collision energies involved into three regimes. The easiest to treat theoretically is the high-energy region where the collisions are effectively impulsive and very simplified calculations based on perturbation theory or the impact approximations which neglect exchange interactions usually give reliable results [10–12]. Such approximations are not useful in the low-energy regime, which can be defined as the region below the ionization threshold of the target, and intermediate energy, which spans the target ionization threshold and the region directly above it.

The physics involved with low-energy collisions is complicated with many subtle effects and many possible outcomes. It is perhaps not surprising that the prototypical processes listed below are mainly sensitive to collisions in this energy regime. In approximate order of increasing electron impact energy, the processes that need to be considered in electron–molecule scattering below the threshold electron impact ionization are:

Elastic Scattering
$AB + e^- \rightarrow AB + e^-$

Rotational Excitation
$AB(j'') + e^- \rightarrow AB(j') + e^-$
where j denotes the rotational state of the target.

Vibrational Excitation
$AB(v'' = 0) + e^- \rightarrow AB(v') + e^-$
where v denotes the vibrational state of the target.

Dissociative attachment if AB is neutral
$AB + e^- \rightarrow A^- + B$
$A + B^-$
or dissociative recombination for a positively charged target
$AB^+ + e^- \rightarrow A + B.$

Electronic Excitation
$AB + e^- \rightarrow AB^* + e^-$
where the asterisk is used to denote an electronically excited state.

Impact dissociation:
$AB + e^- \rightarrow A + B + e^-$
which in practice usually goes via electronic excitation.

A common feature of all these processes is that they can be considered to go via a common intermediary, AB^-. The **R**-matrix method, described in this article, for treating electron–molecule collisions is built around obtaining accurate wave functions for this intermediary and hence gives a theoretical framework capable of modelling all the above processes.

A variety of theoretical procedures have been developed for treating low-energy electron–molecule scattering and related processes such as photoionization [13]. It is not my purpose to review them all here but I will instead single out those methods which are based on the use of a close-coupling expansion (see below for a discussion of what precisely this is), since such procedures appear to offer the most general treatment of the low-energy collision process.

Besides the **R**-matrix method, there are two other close-coupling expansion based methods which are in widespread use for electron–molecule collision studies. These methods are based on the Kohn variational principle, whose users sometimes badge themselves as the "Kohn club" [14,15], and the Schwinger variational principle [16–18]. These methods have much in common, and indeed some underlying deeper equivalences with the **R**-matrix method [19]. The numerical equivalence of the three procedures was demonstrated sometime ago when there was a concerted attempt to simultaneously solve the two-state model for electron impact electronic excitation of molecular hydrogen [20–22]. The overall agreement between the three methods, which has been demonstrated subsequently in bilateral comparisons (see [23] for example), was very good. However it is important to realise that just because calculations agree for a given, well defined model, this does not actually mean they give the right answer as defined by experimental measurement. The development of reliable models for electron–molecule collisions remains a major activity, see [24–26] for example. Although the three methods give similar answers under favourable conditions, there are particular problems which are best addressed by each of the methods.

For example the **R**-matrix method is based on the division of space into an inner and outer region, and requires that the wave function of the target molecule is totally contained with this inner region. This can cause problems with the treatment of highly extended target wave functions, which may arise from a geometrically large molecule or from a very spatially extended wave function such as found in Rydberg states. Conversely, the inner region problem is solved independent of the energy of the scattering electron and the dependence on this energy need only be considered in the outer region where obtaining solutions is relatively quick and simple. This is a major advantage of the method and one which makes it particularly appropriate for studying systems with complicated energy dependence of the scattering observables such as problems with many resonances. Both these considerations make the **R**-matrix method particular appropriate for considering electron collisions with positively charged ions since these have compact target wave functions and display complicated resonance structures.

The review is structured as follows. The next section describes the basic principles of **R**-matrix theory and some of its historical development. Section 3 gives the theoretical formalism used in electron–molecule scattering calculations based on the **R**-matrix method while Section 4 discusses theoretical models in common use for scattering calculation. Section 5 presents numerical and algorithmic issues that arise in the practical implementation of this formalism and Section 6 briefly discusses a sample of the many electron–molecule calculations that have been performed using **R**-matrix based methods. In the Conclusion I discuss some outstanding issues and possible future developments of method. The Appendix gives and overview of the UK molecular **R**-matrix codes.

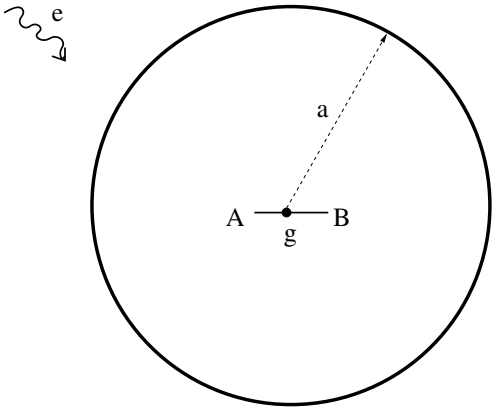

Fig. 1. The **R**-matrix method divides space into an inner region which contains the wave function of the target molecule, here denoted AB, and an outer region. The boundary is given by a sphere of radius a centered on the target center-of-mass, given by g. Only the scattering electron can be present in the outer region.

2. Basics of R-matrix theory

The **R**-matrix method is in widespread use in scattering theory. Before considering the method in detail it is useful to sketch out the basic principles of **R**-matrix based procedures.

Consider a radial scattering wave function, $F_i(r)$, where the subscript i denotes the channel or the different, asymptotic quantum states of the colliding particles before and/or after the collision. In its simplest form the **R**-matrix links the radial wave function to its derivative. At some point, $r = a$, this can be written

$$F_i(a) = \sum_j R_{ij}(a, E) a \frac{\mathrm{d}F_j}{\mathrm{d}r}\bigg|_{r=a}, \tag{1}$$

where the dependence of the **R**-matrix on both distance and energy has been made explicit. There is actually a degree of flexibility in the precise definition of the **R**-matrix which is something I return to below. In matrix notation equation (1) is

$$\mathbf{F}(a) = \mathbf{R}(a, E) a \frac{\mathrm{d}\mathbf{F}}{\mathrm{d}r}\bigg|_{r=a}, \tag{2}$$

or alternatively for any radial distance as

$$\mathbf{R}(r, E) = \frac{\mathbf{F}(r)}{r\mathbf{F}'(r)}, \tag{3}$$

where a prime has been used to denote the derivative. Inverting the **R**-matrix definition of Eq. (3) shows that the inverse of the **R**-matrix equals the logarithmic derivative of the radial function and illustrates the relationship of the **R**-matrix to log-derivative methods [19].

The **R**-matrix is actually used in two distinct but inter-related ways. For scattering problems, propagating the **R**-matrix itself is much more inherently stable than propagating either the wave function or its derivative [27]. This is because in numerical applications the functions themselves rapidly become contaminated by the exponential growth of noise from closed, that is energetically inaccessible, channels associated with the problem. The **R**-matrix element for such channels is simply a constant. This property has led to the widespread use of **R**-matrix propagation, and closely related procedures, for reactive scattering problems [28–33], but this not what is normally meant by **R**-matrix methods.

R-matrix methods rely on the division of space into an inner and outer region, see Fig. 1. The inner region is defined as the volume of a sphere of radius a centered at the center-of-mass of the target molecule. This region is constructed so that the wave function of all but one of the particles is entirely contained within it. This wave function is usually designated the target wave function and defined as containing N electrons. Conversely only a single scattering particle can be found in the outer region. This means that the physics of the outer region is relatively simple. However, as all the $N+1$ electrons in the problem can exist in the inner region, the physics of this region is necessarily complicated. Implicitly this method assumes that the Pauli principle, which asserts that all electrons are identical and any many electron wave function must be anti-symmetric to interchange of these electrons, is only obeyed in the inner region. In the outer region it is assumed that one electron can be considered to be distinct. This electron therefore moves in a local potential arising from the long-range interaction between it and the target. In this procedure it is the **R**-matrix, whose expression in terms of inner region solutions is derived in the next section, which is used to provide the link between the inner and outer region. That this **R**-matrix is in a suitable form to propagate to larger distances is a convenience but not a necessary part of the method.

The **R**-matrix method has a number of distinct advantages, a major one being that given basis sets that span the appropriate energy range, the inner region problem needs to be solved only once and the energy dependence is obtained

entirely from solution of the much simpler outer region problem. The ability to generate solutions at a large number of energies at little extra computational cost is a major advantage.

The origins of the **R**-matrix method are usually traced to a series of papers by Wigner [34–36] on resonance reactions in the mid-1940's. The formulation given by Wigner and Eisenbud [36] is particularly general although, as noted in that paper, it has similarities with work by Kapur and Peierls [37] several years earlier. These studies were all aimed at addressing scattering problems in nuclear physics where the precise form of the short-range interaction between the particles involved was unknown. No attempt was therefore made to obtain direct solutions of the inner region problem, instead the **R**-matrix was parametrized on the boundary between the two regions and the energy dependence of the problem was studied in the outer region. Such semi-empirical implementations of the **R**-matrix method were also used in atomic [38] and molecular [39–43] physics. These approaches are still in use for parameterizing resonances in electron collisions with larger molecules [43,44], but otherwise have been displaced by **R**-matrix procedures where explicit, *ab initio* solutions are found for the inner region problem. The **R**-matrix method was widely adopted for studying nuclear reactions [45,46], and remains in use today in nuclear physics both in semi-empirical [47] and first principles formulations [48].

R-matrix theory was indeed formulated as a full variational theory within the context of nuclear physics [49]; however the ability to write down the precise Hamiltonian for the scattering process made such formulations much more powerful in the context of atomic physics [50,51]. In particular, the major advance in application of **R**-matrix theory to atomic and molecular problems came with the formulation of a full *ab initio* electron–atom scattering theory by Burke et al. [52,53] at the start of the 1970's. This work led to rapid development of very sophisticated electron atom scattering codes; Burke and Berrington [54] reviewed this work up to the early 1990's.

The *ab initio* atomic **R**-matrix calculations have become very sophisticated and widely used. The **R**-matrix methodology was adopted [55], and indeed developed [56], by the international Opacity Project which treated all atomic process important in the atmospheres of hot stars [57,58]. **R**-matrix calculations remain a major source of atomic data for astrophysical studies which has meant continuous development of both the algorithms and the underlying theory employed [59–61]. Much of this work is outside the scope of the present review but reference will be made atomic developments which have impinged directly on procedures used for electron–molecule calculations. There are actually many such examples since, given the higher symmetry and relative simplicity of atomic problems, a significant number of advances originally developed and tested for atomic problems are now used for studies involving molecules.

Following the early work by Schneider in formulating an *ab initio* **R**-matrix for electron–molecule collision problems [62–64], Burke, Mackey and Shimamura [65] presented a full, multicentered formulation of the **R**-matrix method for diatomic molecules based on the use of Slater type orbitals (STOs) to represent the target wave function. The early work on the application of *ab initio* **R**-matrix methods to both atoms and molecules was reviewed by Burke and Williams [66].

The choice of STOs to represent the target wave functions, as implemented initially by Noble et al. [67], effectively limited the original molecular **R**-matrix codes to diatomic molecules. It was not until the early 1990's that a general, polyatomic **R**-Matrix procedure was developed, initially by Nestmann et al. [68]. This procedure used Gaussian Type Orbitals (GTOs) to represent both the target and continuum functions in the inner region. An alternative GTO based procedure was implemented by Morgan et al. [69] a few years later. The differences between these two procedures are discussed below; where appropriate, mention will also be made of a number of other more specialised, electron–molecule **R**-matrix procedures [70–74] that have been developed more recently.

Before leaving the general topic of **R**-matrix theory it should be noted that the theory has also found applications to problems in the condensed phase [75]. Within the context of solid-state physics the **R**-matrix method can be considered one of a number of embedding methods that are available for studying the local electronic structure of condensed matter problems [76]; as such **R**-matrix methods have not really made a major impact in this area. Some applications of **R**-matrix calculations have also been made to the problem of electron collisions with molecules on surfaces [77–79]; however these studies are generally based on adaptations of gas-phase calculations rather then being distinct implementations of an **R**-matrix procedure. Finally I note that an **R**-matrix theory has even been proposed for device physics [75].

The basic step in the **R**-matrix method is the division of configuration space into two regions [54]. A sphere centered at the molecular center-of-mass is used to define the inner region. For the method to be successful this sphere must contain the wave function of the entire N-electron target; for small molecules sphere of radius of about 10 a_0 is usually sufficient.

3. Theoretical foundations

While every effort is made below to define symbols and acronyms as they are first used in the text, a significant number of both of these are introduced. Tables 1 and 2 therefore respectively list the most important symbols and acronyms used below.

3.1. Derivation of basic equations and formal definition of the *R*-matrix

The derivation of the standard expression for the **R**-matrix linking the inner region to the outer region is as follows. Consider the general Schrödinger equation given by an $N+1$ electron Hamiltonian within the frozen nuclei approximation:

$$(\mathbf{H} - E)\mathbf{w}(E) = 0. \tag{4}$$

Table 1
Glossary of important symbols.

Symbol	Meaning
$A_k(E)$	Coefficient of the inner region scattering wave function for energy E.
a	Radius of the **R**-matrix sphere.
a_{ijk}	Coefficient of ith target times jth continuum orbital in the kth inner region wave function.
b	Boundary condition term in the **R**-matrix, usually set to zero.
b_{ik}	Coefficient of ith L^2 configuration in the kth inner region wave function.
$B_i(E)$	Buttlecorrectiontothe**R**-matrixassociatedwithchannel$i$.
c_{nms}	Coefficient of the mth CSF in the nth target wave function of symmetry s.
$C(j_1j_2j_3; m_1m_2m_3)$	Clebsch–Gordan coefficient.
E_k	**R**-matrixpole;energyof**R**-matrixstateψ_k^{N+1}.
E_i^N	Energy of ith target state.
E_i^r	Energy of ith resonance.
$F_i(r)$	Outer region radial wave function for channel i.
$f_{ij}(r)$	Radial part of continuum basis function, v_{ij}.
J	Total angular momentum of the system.
j	Target rotational angular momentum.
K_{ij}	**K**-matrixelementcouplingopenchannels$i$and$j$.
k_i	Wavenumber of scattering electron associated with channel i.
l_i	Orbital angular momentum of the scattering electron associated with channel i.
M_s	Number of CSF in CI wave function of target state with symmetry s.
N	Number of electrons in the target.
N_s	Number of target state with symmetry s included in the close-coupling expansion.
Q_{ij}^λ	Target multipole moment of order λ between target states i and j.
r_f	End radius for **R**-matrix propagation.
$R_{ij}(r, E)$	**R**-matrix linking channels i and j at scattering energy E and radius r.
T_{ij}	**T**-matrixelementcouplingchannels$i$and$j$.
u_{ij}	Continuum orbital number j associated with target state i.
$v_{ij}(r, \theta, \phi)$	Continuum basis function number j associated with target state i.
$w_{ik}(a)$	Boundary amplitude of kth inner region function for channel i.
Y_{lm}	Spherical harmonic.
Z	Net charge of the target.
α	Basis function exponent or the fine structure constant.
α_{ij}	Element of the dipole polarizability tensor.
α_{ij}^λ	Asymptotic potential coefficient of order λ between channels i and j.
β	Photoionization asymmetry parameter.
$\delta(E)$	Eigenphase sum as function of electron scattering energy.
η_{ms}	Configuration state function (CSF) contributing to target states of symmetry s.
Γ_i	Width of ith resonance.
λ	Order of target moment, =1 for dipole, =2 for quadrupole.
Λ	Projection of electron angular momentum onto molecular axis, and hence symmetry; linear molecules only.
ψ_k^{N+1}	kth inner region **R**-matrix wave function.
Φ_i^N	ith N-electron, target wave function.
θ_i	Coulomb phase associated with channel i.
σ	Scattering or photoionization cross section.
μ	Quantum defect; also used to denote the dipole operator.
χ_i^{N+1}	$N + 1$ electron L^2 configuration state function (CSF).
$\Xi_{\frac{1}{2}}$	One electron spin function.

If one wants to consider this equation over a finite spherical volume which has a surface at $r = a$ then one has to add an extra term, as derived by Bloch [80], to keep the operator Hermitian. The Bloch term, which is a one electron operator, takes the form:

$$L(b) = \sum_{i=1}^{N+1} \frac{\hbar^2}{2ma} \delta(r_i - a) \left(\frac{\mathrm{d}}{\mathrm{d}r_i} - \frac{b-1}{r_i} \right), \tag{5}$$

where m is the mass on an electron. Below atomic units are assumed to m and $\hbar$ are set to unity and dropped from most equations. The constant b is arbitrary and often taken as zero.

Including the Bloch term in the Schrödinger equation (4) gives

$$(\mathbf{H} + \mathbf{L} - \mathbf{E})\mathbf{w} = \mathbf{L}\mathbf{w}, \tag{6}$$

which is the Schrödinger equation for the space contained within the sphere given by $r \leq a$; below the operator $\mathbf{H} + \mathbf{L}$ will be referred to as the inner region Hamiltonian. This equation has the formal solution

$$\mathbf{w} = (\mathbf{H} + \mathbf{L} - \mathbf{E})^{-1}\mathbf{L}\mathbf{w}. \tag{7}$$

As Eq. (7) is for the finite region given by $r \leq a$, it is only satisfied at discrete values of the energy, E. Denoting the energy of each solution E_k and its associated wave function $\mathbf{w}_k$, these satisfy the equation:

$$\langle \mathbf{w}_k | \mathbf{H} + \mathbf{L} | \mathbf{w}_{k'} \rangle = \delta_{kk'} E_k \tag{8}$$

Table 2
Definition of important acronyms.

Acronym	Definition
ANR	Adiabatic nuclear rotation.
BBM	Burke, Baluja and Morgan (**R**-matrix propagator).
CAS	Complete active space.
CC	Close coupling.
CI	Configuration interaction.
CSF	Configuration state function.
DCS	Differential cross section.
DNA	Deoxyribonucleic acid.
GRACE	Graphical **R**-matrix atomic collision environment.
GTO	Gaussian type orbital.
IERM	Intermediate energy **R**-matrix.
IVO	Improved virtual orbital.
LUMO	Lowest unoccupied molecular orbital.
LW	Light–Walker (**R**-matrix propagator).
MCQD	Multichannel quantum defect.
MC-SCF	Multi-configuration self-consistent field.
MRD-CI	Multi-reference (singles and) doubles configuration interaction.
MO	Molecular orbital.
MRMPS	Molecular **R**-matrix with pseudo-states.
MVO	Modified virtual orbital.
NO	Natural orbital.
PDR	Photon dominated region.
PPS	Polarized pseudo-states.
PSCF	Polarized self-consistent field.
RMPS	**R**-matrix with pseudo-states.
SCF	Self-consistent field.
SE	Static exchange.
SEP	Static exchange plus polarization.
SP	Static plus polarization.
SSRM	State-selected **R**-matrix.
STO	Slater type orbital.
TDCC	Time-dependent close coupling.

where the integration implied by the Dirac brackets runs only over the finite volume defined by $r \leq a$. The eigenfunctions of the inner region Hamiltonian. $\mathbf{w}_k$, define a complete basis set inside the **R**-matrix sphere and the solution of the Schrödinger equation (4) can be expanded in this basis set:

$$\mathbf{w}(E) = \sum_k A_k(E)\mathbf{w}_k. \tag{9}$$

Inserting Eq. (8) into Eq. (7) gives

$$\mathbf{w}(E) = \sum_k \frac{|\mathbf{w}_k\rangle\langle\mathbf{w}_k|\mathbf{L}|\mathbf{w}\rangle}{(E_k - E)} \tag{10}$$

where use has been made of the resolution of the identity given by $\sum_k |\mathbf{w}_k\rangle\langle\mathbf{w}_k|$. Eq. (10) can be re-written as

$$F_i(a) = \frac{1}{2}\sum_k \frac{w_{ik}(a)}{E_k - E}\sum_j w_{jk}(a)\left[r\frac{\mathrm{d}F_j}{\mathrm{d}r} - bF_j\right]\Bigg|_{r=a} \tag{11}$$

by explicitly substituting in for the Bloch operator using the definition (5) and projecting the inner region wave functions, $\mathbf{w}_k$, onto the individual states of the target, which will be denoted Φ_i^N below.

In Eq. (11), $F_i(r)$ is the radial wave function in the outer region, i.e. $r \geq a$, associated with asymptotic channel i and $w_{ik}(a)$ are the amplitudes of the inner region functions at $r = a$, known as the boundary amplitudes. Both $F_i(r)$ and $w_{ik}(a)$ will be discussed further below. Eq. (11) can be re-written

$$F_i(a) = \sum_j R_{ij}(a, E)\left[r\frac{\mathrm{d}F_j}{\mathrm{d}r} - bF_j\right]\Bigg|_{r=a} \tag{12}$$

using the following substitution

$$R_{ij}(a, E) = \frac{1}{2}\sum_k \frac{w_{ik}(a)w_{jk}(a)}{E_k - E}. \tag{13}$$

Eq. (13) is the standard form of the **R**-matrix on the boundary. An alternative derivation of this expression, which avoids the need to explicitly define a Bloch term, is given by Burke et al. [52]. It should be noted that the eigenenergies of the inner

region problem, E_k, represent singularities in the **R**-matrix; for this reason these energies are usually referred to as **R**-matrix poles. To ensure smoothness in the region of an **R**-matrix pole it is necessary for the at least one of the other terms, the boundary amplitude in Eq. (13) or the derivative in Eq. (12), to also pass through zero. The precise behaviour of the **R**-matrix in this region has been analyzed by Burke and Seaton [81]. It should be noted that condition (11) is valid regardless of **w** in the outer region. Finally, it should also be noted that the above derivation make no use of any boundary condition for $r > a$. Eq. (13) serves as the inner boundary condition for the differential equations in the outer region and therefore can be used as the starting point to search bound states as well as to solve scattering problems.

The main task of the inner calculation is to provide the necessary numerical values to construct the **R**-matrix of Eq. (13) on the boundary. The necessary information is the **R**-matrix pole positions, E_k, and the associated surface amplitudes, $w_{ik}(a)$, of the inner region wave functions, which are denoted ψ_k^{N+1} below, as well as data on the target molecule itself. These parameters are all independent of the scattering energy which is why the inner region problem needs only be solved once for each total space-spin symmetry of the scattering problem.

3.2. The inner region

The inner region wave function is constructed using the close-coupling approximation [82], which is common to other accurate, *ab initio*, low-energy electron–molecule methods [13]. Within this framework the inner region wave function is usually written

$$\psi_k^{N+1} = \mathcal{A} \sum_{ij} a_{ijk} \Phi_i^N(\mathbf{x}_1 \dots \mathbf{x}_N) u_{ij}(\mathbf{x}_{N+1}) + \sum_i b_{ik} \chi_i^{N+1}(\mathbf{x}_1 \dots \mathbf{x}_{N+1}), \tag{14}$$

where the target contains N electrons and functions are labelled as N or $N+1$ according to whether they refer to the target or the compound scattering system respectively. Eq. (14) contains most of the physics of the problem and considerable care is required in its construction. Each of the terms making up this equation is defined below, but each is also discussed in turn in considerably more detail later in the article.

Φ_i^N is the wave function of ith target state. u_{ij} are the extra orbitals introduced to represent the scattering electron. The precise choice of the continuum orbitals, u_{ij}, is labelled by the target state index i as it depends on the symmetry of the particular target state, since the two must couple together to give the correct overall spatial and spin symmetry of the total wave function ψ_k^{N+1}. Furthermore the electrons, whose space-spin coordinates are represent by $\mathbf{x}_i$, must obey the Pauli principle and are therefore anti-symmetrized by operator $\mathcal{A}$. In practical implementations for generating the configurations which make up this term it is often necessary to impose a constraint on the coupling of the first N electrons to ensure that the target wave function does not get contaminated by states with the same configuration but different space-spin symmetry.

The second summation in Eq. (14) involves configurations which have no amplitude on the **R**-matrix boundary and where all electrons are placed in orbitals associated with the target. Since they are confined to a finite volume of space they will be referred to as L^2 configurations below. Such configurations, the choice of which is quite subtle, are essential in even the simplest scattering model as they allow for relaxation of the orthogonalization between the continuum orbitals and those belonging to the target given that the continuum orbitals are forced to be orthogonal to the target ones, see Section 5.2.2. In more sophisticated models the L^2 configurations are also used to model the effects of target polarization.

In order to match correctly with the asymptotic channels in the outer region, the continuum basis functions are written as a partial wave expansion using polar coordinates (r, θ, ϕ):

$$v_{ij}(r, \theta, \phi) = f_{ij}(r) Y_{l_i, m_i}(\theta, \phi) \Xi_{\frac{1}{2}} \tag{15}$$

where the (l_i, m_i) match with the asymptotic channel associated with the ith target state and these angular momentum quantum numbers. The function $\Xi_{\frac{1}{2}}$ is a one half electron spin function; since all calculations are non-relativistic the definition of this function can remain purely formal but it is necessary to ensure the correct spin coupling to the target state in expressions such as Eq. (14). Procedures, which largely concern orthogonalizing the continuum orbitals to the target orbitals, for turning continuum basis functions, v_{ij}, into the continuum orbitals, u_{ij}, used in Eq. (14) are discussed in Section 5.2.1 below.

The continuum basis set needs to be placed at the origin of the **R**-matrix sphere. It is usual for this origin to be the molecular center-of-mass although other choices are possible [83]. Although the center-of-charge and center-of-mass often coincide, there are situations when they do not which can introduce important physical effects. For example there is no permanent target dipole moment when an electron scatters off the H_2^+ molecular ion. However electrons scattering off its deuterated isotopologue HD^+ do experience a target dipole, with important physical consequences [84]. In the latter case this effect is reproduced by centering the **R**-matrix, and hence placing the continuum basis, on the HD^+ center-of-mass, which is not its center-of-charge. In practice, calculations where the center-of-mass is extremely close to one of the nuclei have actually used that nucleus as the center as this is found to give better numerical stability [83].

A major reason for using the partial wave expansion for low-energy electron–molecule studies is its rapid convergence for most problems. This means that it is usually only necessary to consider a few partial waves in the expansion. For example all **R**-matrix calculations on electron collisions with polyatomic molecule have thus far only considered up to g-waves, i.e. $l \leq 4$, with little evidence for loss of accuracy. However, here is one case where such low-l expansions are insufficient and that is

for collisions with species with a significant dipole moment. Methods which allow for the long-range, partial wave mixing effect of dipoles without the need to consider higher partial waves in the **R**-matrix inner region are well established [85,86] and will be discussion below in Section 5.5.

3.3. The boundary

The boundary is the point where the energy-independent solutions from the inner region are used to construct an energy-dependent **R**-matrix. As already shown in Eq. (1), the **R**-matrix relates the radial wave function to its derivative. For the most general set of boundary conditions at $r = a$, the relationship can be written [70]

$$d\mathbf{F}(r) + e\mathbf{F}'(r) = \mathbf{R}(b\mathbf{F}(r) + a\mathbf{F}'(r)) \tag{16}$$

where matrix notation has been combined with the use primes to denote first derivatives with respect to r. The constants a, b, d and e are in principle arbitrary. For example the choice $b = -e = 1$, $a = d = 0$ gives expressions similar to the log-derivative method of Manolopoulos and Wyatt [87,88]. In the most general form, the matrix linking the solutions has been termed the **Z**-matrix [89]. A **Z**-matrix approach was tested by Huo and Brown [70] for electron–molecule scattering who found it did not give any particular advantage over the use of a standard **R**-matrix. In its most general form the **R**-matrix is given by $d = 1$, $e = 0$, but in practice is usually implemented with $b = 0$ as in Eq. (1).

To construct the **R**-matrix on the boundary it is necessary to know the **R**-matrix pole positions, E_k, the boundary amplitude, w_{ik}, plus a Buttle or any other correction if needed. The pole positions come directly from diagonalizing the inner region Hamiltonian, but constructing the boundary amplitudes require some manipulation. The boundary amplitudes for channel i are defined by the overlap integral

$$w_{ik}(a) = \left\langle \Phi_i^N Y_{l_i,m_i} \Xi_{\frac{1}{2}} | \psi_k^{N+1} \right\rangle, \tag{17}$$

where ψ_k^{N+1} is the wave function of the kth**R**-matrix pole, see Eq. (14) and Φ_i^N is the target wave function for channel i. The integral runs over all space-spin coordinate except the radial coordinate of the scattering electron, r; ψ_k^{N+1} is evaluated at $r = a$. In practice this integral is not usually directly evaluated as the boundary amplitudes are computed from the continuum orbitals, u_{ij} see Section 5.2.2, and the coefficients of the inner region wave function, a_{ijk} see Eq. (14), using the expression

$$w_{ik}(a) = \sum_j u_{ij}(a) a_{ijk}, \tag{18}$$

where i labels asymptotic channels and k numbers the inner regions solutions, ψ_k^{N+1}. This means that

$$F_i(a) = \sum_k A_k(E) w_{ik}(a) \tag{19}$$

corresponds to the energy-dependent wave function of the projectile in the ith channel at the boundary.

The remaining information that is required to set-up the outer region problem concerns properties of the target. The target state energies relative to the ground state are needed as they give the energies of the asymptotic channels. The multipole moments associated with these target states are also required as they determine the outer region, long-range or asymptotic potential which is given by the multipole expansion:

$$V_{ij}(r) = \sum_{\lambda=0} \frac{\alpha_{ij}^{\lambda}}{r^{\lambda+1}}. \tag{20}$$

The asymptotic potential coefficients are defined as [65]

$$\alpha_{ij}^{\lambda} = \left(\frac{2l_i + 1}{2l_j + 1}\right)^{\frac{1}{2}} C(l_i \lambda l_j; m_i m_\lambda m_j) C(l_i \lambda l_j; 000) Q_{ij}^{(\lambda)} \tag{21}$$

where $C(l_1 l_2 l_3; m_1 m_2 m_3)$ is a Clebsch–Gordan coefficient. $Q_{ij}^{(\lambda)}$ is the target moment for which it usual to only consider dipoles, $\lambda = 1$, and quadrupoles, $\lambda = 2$, and, of course, for charged targets the Coulomb potential given by $\lambda = 0$. If $i = j$, $Q_{ij}^{(\lambda)}$ represents a permanent moment of the ith target state, whereas if $i \neq j$ it is a transition moment. These outer region potential coefficients provide the coupling between the channels in the outer region, see Eq. (23) below. Thus, for example, the dipole couplings between target states introduces target polarizabilities in the outer region, see Eq. (49). It is actually possible to include the asymptotic polarizability directly into the outer region potential by adding term in r^{-4} with appropriate coefficients and angular behaviour [90,91].

Finally mention should be made of a procedure developed recently by Nestmann and Beyer [92] as part of the Bonn **R**-matrix code. This method projects the coupling between the open and closed channels onto the open channels only, giving a greatly simplified outer region problem where closed channels do no need to be considered. This method is particularly useful if one has a negligibly weak potential in the outer region but important coupling between open and closed channels in the inner region [91].

3.4. The outer region

In the outer region the wave function can be written:

$$\psi^{N+1}(E) = \sum_{i=1}^{n} \Phi_i^N(\mathbf{x}_1 \ldots \mathbf{x}_N) F_i(r_{N+1}) Y_{l_i,m_i}(\theta, \phi) \Xi_{\frac{1}{2}}, \tag{22}$$

where the sum runs over the n-channels of the problem. For molecular problems, there are usually several channels associated with each target state, which means that even a one-state problem normally involves solving a multichannel outer region problem.

Substituting the wave function of Eq. (22) into the Schrödinger equation of the problem and projecting on the target state wave functions yields the following system of n-coupled differential equations for the radial functions, $F_i(r)$, [52]:

$$\left[-\frac{\mathrm{d}^2}{\mathrm{d}r^2} + \frac{l_i(l_i+1)}{r^2} - k_i^2\right] F_i(r) = 2\sum_{j=1}^{n} V_{ij}(r) F_j(r), \tag{23}$$

where V_{ij} represents the long-range potential constructed from the target properties and given by Eq. (21). In principle, the outer region consists of setting up and solving this set of differential equations. In practice, the **R**-matrix is used to solve the equations which, as discussed below, means that for most purposes it is not actually necessary to explicitly obtain $F_i(r)$.

Having obtained the **R**-matrix on the boundary in the form of Eq. (13), the problem is how to obtain the final, energy-dependent solutions to the scattering problem. The outer region problem for electron–molecules can be written in terms of equations which are formally the same as those for electron–atoms, and can be solved using the same procedures. In practice however there are two differences which make the molecular problem computationally more demanding: the first is that, due to the lower symmetry of the target, molecular problems always have several degenerate channels associated with each target state; the second is that the long-range potentials are much stronger. This is particularly true for scattering off molecules with a large permanent dipole for which special procedures often have to be employed.

The standard procedure for tackling the outer region problem uses two stages. First the **R**-matrix is propagated from the boundary given by $r = a$ to some large $r = r_f$ [93,94], where r_f is chosen such that the non-Coulombic potential can be neglected for asymptotic region defined by $r > r_f$. There are a number of methods available for obtaining asymptotic solutions [95–98]; the most commonly used procedure is based on the use of an asymptotic expansion due to Gailitis [98,99]. It should be noted that while the Gailitis procedure gives the outer region wave function at r_f, the use of **R**-matrix propagation avoids specifying this wave function in the region $a < r < r_f$.

Before attempting to solve the outer region problem it is necessary to gather together the information for doing this. Besides the **R**-matrix on the boundary, information is needed on the asymptotic channels of the problem and outer region potentials. Asymptotic channel i is defined by a state of the separated target molecule and a partial wave of the scattering electron, (l_i, m_i). If the target state associated with channel i has energy E_i^N, then the wavenumber of the scattering electron associated with this channel is given by

$$k_i^2 = 2(E - E_i^N) \tag{24}$$

where E is the energy of the scattered electron and the energy of the lowest target state is taken to be zero by convention. A channel is said to be open if $k_i^2 \geq 0$ since it can be reached asymptotically and closed if $k_i^2 < 0$. For a standard scattering problem and energy normalization of the wave function, the outer region solutions go asymptotically, as denoted by the symbol $\sim$, to

$$F_{ij} \sim \frac{1}{\sqrt{k_i}} \left(\sin\theta_i \delta_{ij} + \cos\theta_i K_{ij}\right) \tag{25}$$

for open channels and

$$F_{ij} \sim 0 \tag{26}$$

for closed channels, ones for which $E_i < 0$. For neutral targets the channel angle θ_i is given by

$$\theta_i = k_i r - \frac{1}{2} l_i \pi; \tag{27}$$

where as for collisions with a target of net charge $Z - N$, it has the more complicated form

$$\theta_i = k_i r - \frac{1}{2} l_i \pi - \eta_i \ln(2k_i r) + \sigma_i \tag{28}$$

with

$$\eta_i = \frac{Z - N}{k_i} \tag{29}$$

$$\sigma_i = \arg \Gamma(l_i + 1 + \mathrm{i}\eta_i) \tag{30}$$

where σ_i is sometimes referred to as the Coulomb phase.

The critical parameter in Eq. (25) is the **K**-matrix. This is a symmetric matrix whose dimension is the number of open channels. All the scattering observables can be extracted by starting from the **K**-matrix. The parameters which will concern us below include the **S**-matrix which is given by

$$\mathbf{S} = \frac{(\mathbf{1} + \mathrm{i}\mathbf{K})}{(\mathbf{1} - \mathrm{i}\mathbf{K})} \tag{31}$$

and the eigenphase sum. The eigenphase sum, δ, is obtained from the sum of the eigenvalues of the **K**-matrix, K^D_{ii}, as:

$$\delta(E) = \sum_i \arctan(K^D_{ii}). \tag{32}$$

Eigenphase sums provide a very useful diagnostic of scattering calculation; an example is presented in Fig. 9.

3.5. Resonances

The temporary trapping of an electron to form a quasibound or short-lived state is known as a resonance. The formation and behaviour of resonances is the key to many processes in electron–molecule scattering. Resonances are generally characterized qualitatively by type and configuration, and quantitatively by their symmetry, position, E^r, and width, Γ. Obtaining these parameters is a major objective of many calculations.

Some processes such as dissociative attachment [100] and dissociative recombination [101,102] are thought to be entirely driven by resonances, although in practice there are occasional exceptions [103,104]. Other processes, notably electron impact vibrational excitation [100], can have their cross section hugely enhanced by the presence of resonances. Indeed cross sections for all processes can show features, usually enhancements, due to resonances.

There are different types of resonances whose modelling requires different theoretical treatments. The simplest resonances are called shape resonances. In this case the electron is trapped behind a barrier in the electron–molecule potential. The usual situation is that the barrier is a centrifugal one caused by the angular momentum of the incoming electron meaning that s-wave scattering cannot give rise to shape resonances. However, recent calculations found that resonances in the C_2^{2-} anion are trapped by a barrier caused by the interaction between the attractive polarizability and the repulsive Coulomb potential leading, in this case, to shape-like resonances in both s and higher partial waves [105].

The more chemical view of shape resonance is that the incoming electron occupies a low-lying unoccupied orbital of the target, often the LUMO or lowest unoccupied molecule orbital. This picture is consistent with that of the one of trapping by a (centrifugal) barrier except with additional constraint that this low-lying orbital should not be an s-orbital. Shape resonances are generally rather short lived meaning that they appear as broad features as a function of energy in the scattering observables. They also provide the most common route for dissociative attachment [100].

Feshbach resonances, which are generally narrower than shape ones, are caused by the simultaneous excitation of the target and trapping of the scattering electron. In a classic Feshbach resonance this involves electronic excitation of the target which then binds an extra electron. In this case the electronically excited state is known as the parent state; although care must be taken not to over-work this concept [106]. Feshbach resonances are a particularly important feature of scattering from positively charged ions. In this case there are an infinite Rydberg series of resonances associated with each value of (l_i, m_i) and each electronically excited state of the target. Most of these excited states inevitably lie in the electronic continuum and manifest themselves as resonances. These Feshbach resonances provide the main or "direct" route to dissociative recombination [102].

Quantum defect theory [107] provides the natural framework for dealing with the series of Feshbach resonances converging on a particular "parent" excited target state. Indeed Jungen and co-workers have developed specific multichannel quantum defect theory based **R**-matrix methods for dealing with electron collisions with diatomic ions [72,108,109]. Even if quantum defect theory is not used in the actual calculations, it can be almost impossible to make sense of the many resonances that occur without parameterizing the data using quantum defects [110–112].

For a resonance the quantum defect, μ, is actually complex with the imaginary part quantifying the resonance width. Dividing the quantum defect into real and imaginary parts:

$$\mu = A + \mathrm{i}B, \tag{33}$$

then the effective quantum number, ν, is given by

$$\nu = n - \mu, \tag{34}$$

where n is an integer specifying the principal quantum number of the resonance electron whose energy is given by

$$E^r = E^N_p - \frac{Z^2}{2\nu^2}, \tag{35}$$

where the energy of the resonance, E^r, and parent target state, E^N_p, are given in Hartree and Z is the charge on the target ion. The width of the resonance, again in Hartree, is given by

$$\Gamma = \frac{B}{\nu^3}. \tag{36}$$

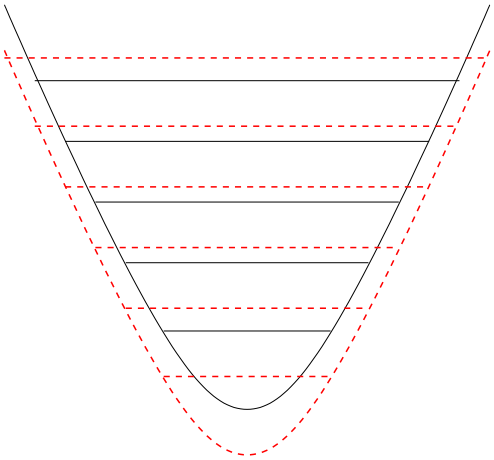

Fig. 2. Nuclear excited Feshbach resonances occur when the $N+1$ electron state, given by the dashed curve, is weakly bound compared to the N electron state, given by the solid curve. Under these circumstances, excited vibrational states of $N+1$ electronic state, denoted by the dashed horizontal lines, which lie above the lowest vibrational N electron state, appear as narrow resonances.

A resonance fitting procedure which gives E^r and Γ requires knowledge of both the parent target state and the principle quantum number, n, to give the quantum defect. These are usually, but not always, obvious.

Complex quantum defect theory can also be used to characterize entire resonance series by analyzing the **S**-matrix just above threshold [107], which has been found particularly useful for problems where the resonances of interest are associated with high values of n [110,113].

It should be noted that there is a rather less common class of resonances, known as core-excited shape resonances, which are essentially a combination of both a shape and Feshbach resonances. These resonances, like Feshbach resonances, are associated with electronic excitation of the target but, like shape resonances, the electron is trapped by a barrier in the potential at an energy above that of the excited state "parent".

Molecules, unlike atoms, can support another class of Feshbach resonances. These are the so-called nuclear excited Feshbach resonances and occur when a molecular target supports one or more very weakly bound state. Under this circumstance vibrational excitation of this state can lead to complex structures of very narrow resonances; Fig. 2 illustrates this situation. Positive ions always support weakly bound states and nuclear Feshbach resonance are important for dissociative recombination, where they form a key part of the so-called indirect process [102,114].

Nuclear excited Feshbach resonances can be responsible for very complicated near-threshold structures whose study requires treatment beyond the standard Born–Oppenheimer separation of electronic and nuclear motion. Electron collisions with hydrogen halides have provided a particularly fruitful area of study with several **R**-matrix calculations revealing the very complicated nature of, in particular, the vibrational [83,92,115–118] and rotational [119,120] excitation processes due these resonances.

Before leaving the topic of resonances mention should be made of one other class of resonances which are often the unavoidable and sometimes the deliberate feature of electron–molecule collisions calculations, that is pseudo-resonances. Pseudo-resonances are spurious resonances that are the well-known artifact of an incomplete theoretical model. In principle, pseudo-resonances can occur in a calculation which probes scattering energies above an open channel which is absent from that particular calculation. In practice means of coupling to that channel are also generally required which means that the static exchange model does not display pseudo-resonances despite the omission of all excited channels. The presence of one or more pseudo-resonances in a calculation is not necessarily disastrous. It is possible to smooth over pseudo-resonances [26,121], and indeed the intermediate energy **R**-matrix method makes a virtue out of their presence [122,123]. However in general pseudo-resonances are a nuisance which it is better to avoid.

Obtaining precise values for resonance positions, widths and symmetries is a significant objective of many theoretical treatments. The technical details of how this can be done are discussed in Section 5.4.2. Of course **R**-matrix methods can be used to search for bound states which, for example, can be particularly useful for tracking resonance states as they drop to zero energy and below [124,125].

Finally mention should be made of virtual states. These features, which are neither bound states nor resonances, manifest themselves as poles in the **S**-matrix at negative imaginary values of the momentum, k, see Fig. 7. A virtual state has a strong influence on very low energy scattering where they cause a sharp rise in the cross section.

3.6. Processes involving photons

At low photon energies, photoionization:

$$AB + h\nu \rightarrow AB^+ + e^-$$

and its reverse process, radiative recombination, can be thought of as involving a half electron collision. Indeed, at low energies structures can be expected in the angularly resolved photoionization cross sections due the electron dynamics very similar to that found in electron–molecule collisions [126].

In the dipole length approximation, angularly resolved photoionization cross section can be written [127]

$$\frac{\mathrm{d}\sigma^L}{\mathrm{d}\Omega} = 4\pi^2\alpha a_0^2\omega \left|\langle\Psi_E^{(-)}|\boldsymbol{\mu}|\Psi_0\rangle\right|^2 \tag{37}$$

where α is the fine structure constant, a_0 is the Bohr radius, ω the energy of the incident photon and the dipole matrix element, $\langle\Psi_E^{(-)}|\boldsymbol{\mu}|\Psi_0\rangle$, has the wave function of bound state, Ψ_0, see Section 5.4.4, in the ket and the outgoing wave function, $\Psi_E^{(-)}$, in the bra. When averaged over molecular orientation and spin, the angular dependence is given by

$$\left(\frac{\mathrm{d}\sigma^L}{\mathrm{d}\Omega}\right)_{\mathrm{Av}} = \frac{\sigma}{4\pi}[1+\beta P_2(\cos\theta)] \tag{38}$$

where θ is the angle between the incoming photon and the ejected electron. As implied by the formula, the angular dependence is entirely given by the asymmetry parameter β.

Although it is possible to consider transitions in the outer region [128], it usual to assume that this initial bound state wave function. Ψ_0, is contained within the **R**-matrix sphere. Within this assumption, an **R**-matrix formulation of the use of Eq. (37) to calculate energy-dependent angle-dependent photoionization cross sections was given by Burke and Taylor for atoms [129] and generalized to molecules by Burke [127,130]. The first thing to note in this formulation is that the continuum wave function $\Psi_E^{(-)}$ does not satisfy the standard asymptotic conditions, Eq. (25), since it only represents a half-collision. The half-collision boundary conditions are straightforward but in practice the outgoing wave function is related the standard full collision wave function, Ψ_E, via the **K**-matrix by:

$$\Psi_E^{(-)} = \frac{1}{(1+\mathrm{i}\mathbf{K})}\Psi_E. \tag{39}$$

In applications which use an electron–molecule scattering outer region code to study photoionization [130,131], it has proved easier to introduce this factor after the wave function has been calculated than to apply new boundary conditions from the start.

In the inner region the matrix element for the m_γth component of the dipole are given by [127]

$$D_{jl_jm_lm_\gamma}^{\Gamma_0(-)} = \left(\frac{4\pi}{3}\right)^{\frac{1}{2}}\left\langle\Psi_{jl_jm_l}^{SM_S(-)}|\mu_{m_\gamma}|\Psi_0\right\rangle \tag{40}$$

where Γ_0 gives the quantum numbers of the initial state and the final state channel is given by the jth state of the ion coupling to partial waves (l_jm_l). Such matrix elements can be computed as part of a standard quantum chemistry code, with possible allowance for finite volume of the inner region [130].

For calculating the photoionization cross section, it is easier to work in terms of the angular momentum transfer j_t [132] which means transforming the dipoles:

$$D_{jl_jj_tm_\alpha}^{\Gamma_0(-)} = \sum_{m_\gamma m_l} C(1l_jj_t;-m_\gamma m_l m_l-m_\gamma)D_{jl_jm_lm_\gamma}^{\Gamma_0(-)} \tag{41}$$

where the unit angular momentum in the dipole and the properties of the Clebsch–Gordan coefficient serve to limit the values of j_t to l_j and $l_j\pm1$. Within the momentum transfer framework, the angular resolved photoionization cross section is written in the dipole length form as

$$\frac{\mathrm{d}\sigma^L}{\mathrm{d}\Omega} = 4\pi^2\alpha a_0^2\sum_{l_jl'_jj_tm_\alpha}\frac{1}{2j_t+1}\exp(\mathrm{i}(\sigma_{l_j}-\sigma_{l'_j}))D_{jl_jj_tm_\alpha}^{\Gamma_0(-)}D_{jl'_jj_tm_\alpha}^{\Gamma_0(-)\,*}\Theta(j_tl_jl'_j;\theta) \tag{42}$$

where the σ_l's are the initial and final Coulomb phases and

$$\Theta(j_tl_jl'_j;\theta) = \frac{2j+1}{4\pi}[(2l_j+1)(2l'_j+1)]^{\frac{1}{2}}(-1)^{j_t}\sum_K\begin{Bmatrix}1 & 1 & K\\ l_j & l'_j & K\end{Bmatrix}C(11K;000)C(l_jl'_jK;000)P_K(\cos\theta) \tag{43}$$

where $\{\ldots\}$ is a Wigner 6j symbol and the angular algebra restricts the angular dependence to $K=0$ and 2, as assumed in Eq. (38).

Within an **R**-matrix procedure this is all conveniently written in the following matrix form [129,133]:

$$\langle\Psi_E^{(-)}|\boldsymbol{\mu}|\Psi_0\rangle = \mathbf{y}_f^{-T}\mathbf{R}_f^{-1}\mathbf{w}_f\mathbf{G}_f\mathbf{V}_f^T\mathbf{M}\mathbf{G}_i\mathbf{w}_i^T\mathbf{R}_i^{-1}\mathbf{y}_i \tag{44}$$

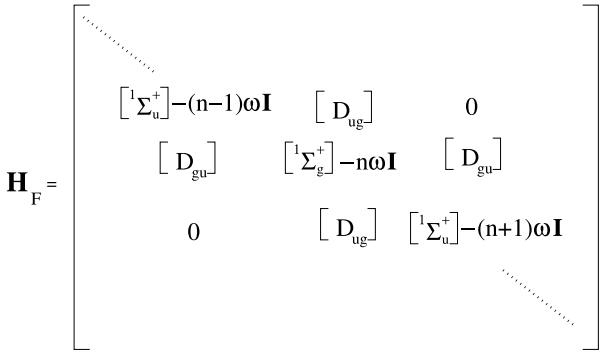

Fig. 3. Structure of the super-inner region matrix generated by the **R**-matrix Floquet method for the case of a symmetric linear molecule oriented parallel to the direction of the laser [135]; $[^1\Sigma_g^+]$ and $[^1\Sigma_u^+]$ represent the standard inner region Hamiltonian matrix of that symmetry; $[D_{ug}]$ and $[D_{gu}]$ represent the dipole couplings between states of $^1\Sigma_g^+$ and $^1\Sigma_u^+$ symmetry. The second term in the diagonal blocks gives the number of photons of frequency ω that dress each state.

where f labels the final, or continuum, state and i labels the initial, or bound, state. The matrices are given by:

$$y_{ji} = \sum_k v_{jk} x_k \tag{45}$$

and v_{jk} are the asymptotic functions with coefficients x_k which need to be evaluated at $r = a$. **R** is the **R**-matrix, see Eq. (57), with the associated matrix of boundary amplitudes **w**, see Eqs. (17) and (18). The **G**'s are diagonal matrices defined by:

$$G^i_{jk} = \frac{\delta_{jk}}{E_k - E_i} \tag{46}$$

and

$$G^f_{jk} = \frac{\delta_{jk}}{E_k - E_i - w}, \tag{47}$$

where E_i is the initial, i.e. target state, energy and $E_i + w$ is the final, i.e. continuum state, energy. Finally **M** is the is the reduced transitions state element which can be calculated entirely in terms of the inner region wave functions

$$M_{kk'} = \langle \psi^f_k | \boldsymbol{\mu} | \psi^i_{k'} \rangle. \tag{48}$$

The above discussion is all for the weak field case. The development of high intensity lasers have focused increasing attention on the behaviour of atoms and molecules in strong fields for which the perturbation theory which underlies the above formulation is no longer valid. Burke et al. [134] developed an **R**-matrix Floquet theory to treat the case were multiphoton effects are important. This theory takes advantage of the structure of the **R**-matrix method and, as above, also assumes that the interaction with the photon can be considered as an inner region problem. However in the inner region the coupling between states of the system differing by a single photon are explicitly considered. Fig. 3 illustrates the structure of the **R**-matrix Floquet super-matrix for the simplest case, that of a symmetric linear molecule oriented parallel to the direction of the laser field; for the more complicated case of perpendicular orientation see Colgan et al. [135]. The **R**-matrix Floquet method has been very extensively used to study atoms in strong fields [136]. It has been extended to molecules [135,137] where it uses appears to have so far been confined to studies of H_2 in strong laser fields [138].

The **R**-matrix Floquet method is not really viable for the strongest laser fields that can currently be achieved, as the large number of photons involved in this case leads to the Floquet super-matrix becoming unmanageably large. In this case it would appear that the only alternative which allows a proper treatment of the electronic structure of the target is to use time-dependent methods. A time-dependent formulation of the **R**-matrix method has been developed [60] and recently implemented for atoms [139]. Thus far there is no corresponding implementation for molecular problems.

3.7. Balance between N and N + 1 electron calculations

Implicit in all scattering procedures is obtaining a good balance between the representation of the target wave function, Φ^N_i, and the scattering wave function, represented in the inner region in the **R**-matrix method by ψ^{N+1}_k. Recent work by Cooper et al. [140], actually on positron scattering using a Kohn variational method, emphasizes the pitfalls of an unbalanced treatment. An unbalanced calculations will give unreliable results with, for example, resonances potentially becoming bound, or weakly bound states appearing in the calculation as resonances.

When considering the issue of balance it is important to remember that only for a very limited number of few, i.e. one and possibly two, electron targets is it possible to obtain energies and associated wave functions which approach anything like the exact solution to the problem. This means that in nearly all cases scattering calculations are working with approximate target wave functions and energies.

Within the **R**-matrix method the need for balance is rather simply seen in terms of the energies used in Eq. (13). The **R**-matrix poles, E_k, in this equation give an energy spectrum relative to the target energy. "Improving" the **R**-matrix pole energies in a variational sense, which means lowering them, will of course cause any resonance feature associated with a particular pole to also move to lower energy and potentially become bound. The effects of giving a better description of the scattering calculation than the target is often called "over-correlation" [141]. Conversely improving the target representation will cause the energy zero, E_0^N, to be lowered and hence the pole positions to effectively rise, with the converse effect on the associated properties. If the aim of a calculation is to compute resonance or bound state energies, then reliable results will only be obtained if the target and scattering calculations are performed at a similar level of approximation; I would describe such a model as balanced.

A balanced treatment is actually much harder to obtain for calculations, such as the ones considered here, which differ in the number of electrons being considered. To this end it is noticeable that the two main molecular **R**-matrix methods in general use take a significantly different approach to obtaining balanced calculations.

The Bonn codes use the selected state **R**-matrix (SSRM) approach [142] to determine the inner region **R**-matrix. This approach is based on the application of the Multi-Reference (single and) Double excitation Configuration Interaction (MRD-CI) method of Buenker and Peyerimhoff [143–145]. The MRD-CI method is a well used quantum chemistry procedure for target electronic structure calculations which considers single and double excitations from a multi-reference state of the target. A particular feature of Buenker and Peyerimhoff's MRD-CI method is the truncation of the configuration space at some threshold, optionally followed by an extrapolation procedures. Balance is obtained in the Bonn **R**-matrix codes by using this procedure with the same threshold parameters simultaneously for both the target and scattering wave functions, see Pfingst et al. [142] for details. It should be noted that this procedure allows for the inclusion of a high level of correlation in the target wave functions [141].

The basis of the UK molecular **R**-matrix method is the hand specification of the configurations used in the target, see Gillan et al. [146] for example, and scattering models so that they are explicitly consistent with each other. The currently favoured approach for doing this is to use a complete active space configuration interaction (CAS–CI) model [147–149]. Within this model a set of valence orbitals are identified and all possible configurations consistent with the given space-spin symmetry of the target state are used to construct the target wave function. For a molecule with N electrons of which m are frozen as core electrons, this wave function can be written as:

$$(\text{core})^m(\text{CAS})^{N-m}.$$

Within this model it is easy to define L^2 configurations to include in the scattering calculation; these simply involve placing the extra electron in the CAS thus:

$$(\text{core})^m(\text{CAS})^{N-m+1}.$$

The CAS–CI model is the most commonly used method for constructing scattering models and, with a correctly chosen CAS, it can give very good target potential curves [150]. However the CAS–CI model has its limitations. While the model gives a reasonable representation of the valence states associated with most targets, extension of the active space beyond the valence orbitals generates very large numbers of extra configurations with little benefits in terms of an improvement in the calculation [151]. An obvious alternative is to include excitations out of the CAS, in the style of the MRD-CI method described above. Such approaches have been used successfully [152], but within the framework described above they definitely run the risk of over-correlation. This is because adding all the L^2 configurations implied by this target calculation leads to the inclusion of configurations which can contribute to the artificial lowering of the energy of the target state [148].

4. Scattering models

There are a variety of models that one can use for treating electron–molecule collisions. I will not consider all possible models, even when they have been implemented within an **R**-matrix approach such as the no-exchange approximation [153]. Instead I will concentrate on those models which have been routinely used for treating low-energy electron–molecule collisions.

The most basic model is the static exchange (SE) approximation. In this model the target wave function is not allowed to relax, or polarize, in response to the incoming electron but, as the name implies, exchange between this electron and those of the target is explicitly included. Within the SE approximation only a single, usually Hartree–Fock, target wave function is included in the close-coupling expansion of Eq. (14), and the only possible L^2 configurations are ones in which the scattering electron occupies otherwise unoccupied, or virtual, spin orbitals of the target. Using the language of second quantization and taking the target wave function as the vacuum state, then scattering necessarily adds another particle and these L^2 configurations can be described as one particle, zero holes or (1p,0h), configurations.

The SE model cannot treat many physical processes such as, obviously, electron impact electronic excitation. It also cannot model Feshbach resonances since these also implicitly involve electronic excitation of the target. The SE approximation does give shape resonances, although these are usually too high in energy since their position is lowered by the inclusion of attractive target polarization effects.

The SE approximation must be regarded as fairly crude but it has a number of uses. At high scattering energies, in particular at energies above the ionization threshold of the target, it avoids problems with pseudo-resonances which

affect more sophisticated models. It can be used to identify shape resonances and, unlike most other models which are implementation dependent, it is a rigorously defined model which can be used to make cross comparisons between codes and methods.

The logical advance on the SE approximation is to include target polarization effects giving the static exchange plus polarization (SEP) approximation. This can be done in a number of ways, for example by use of an optical potential [154] or a local polarization potential [74,155]. However, the natural method within an **R**-matrix formalism is via the use of the L^2 configurations in Eq. (14). Again assuming a Hartree–Fock target wave function, this approach takes advantage of Brillouin's theorem [156] which shows that configurations single excitations from a Hartree–Fock wave function do not interact with it. This means that it should be possible to include configurations involving single excitations of the target wave function without the risk of artificially improving the target. Polarization effects can therefore be included by promoting one electron from the target into a virtual orbital and also putting the scattering electron into a virtual orbital giving two particle, one hole or (2p, 1h), configurations. This approach is widely used in both **R**-matrix and other approaches although whether it really yields a balanced approach to the problem has been questioned [157].

This (2p, 1h) SEP approach outlined above has also been called the polarized self-consistent field (PSCF) method [158]. The PSCF method is sometimes used with the imposition of an extra restriction on the spin state of the excitations [159,160], although this has not generally been the case of applications made using the **R**-matrix method. In practice SEP calculations are not restricted to self-consistent field (SCF) target wave functions; SEP calculations with correlated wave functions can be achieved in a straightforward fashion within the Bonn **R**-matrix procedure [141].

The SEP approximation still cannot explicitly describe electron impact electronic excitation but is now capable of resolving both shape and Feshbach resonances. In this model Feshbach resonances arise from (2p, 1h) L^2 configurations which correspond to target excitations. Although this method is effective in resolving individual Feshbach resonance [161], in the case of ions for which infinite series of Feshbach resonances should be present, only the lowest few can be modelled. Besides these physical resonances, the SEP method is prone to display pseudo-resonances at higher energies. Furthermore models based on use of a Hartree–Fock target wave function suffer from the well-known problems with such wave functions at elongated bond lengths.

An obvious way to reduce problems with low-lying pseudo-resonances and at the same time to allow for electron impact electronic excitation is to include several target states in the wave function expansion. This approach is computationally more expensive than the SE and SEP approaches. However it has significant advantages over these methods; for instance Feshbach resonances are modelled in a straightforward fashion if the associated "parent" state is included in the close-coupling expansion. This means, for example, in electron collisions with ions all the Rydberg series associated with each electronically excited states are automatically considered in the calculation subject only the truncation of the partial wave expansion of Eq. (15) and the numerics of the outer region calculation.

The use of several electronic states in a close-coupling (CC) expansion introduces complications that are not encountered using a target represented by a single Hartree–Fock target state. First these states must all be represented by a common orbital set, for which there is no unique best choice, see Section 5.2.2 below. However, no matter what orbital set is used the simplicity of Brillouin's theorem is necessarily lost in a multistate wave function as a configuration which represents a single excitation from one state will constitute a multiple excitation from other states in the CC expansion. This makes the appropriate choice of L^2 configurations for CC wave functions much trickier. Issues that arise from the need to balance target and scattering wave functions are discussed in the next section.

In principle a CC expansion can give a complete treatment of the scattering process, and indeed this property has been exploited very successfully for atomic problems [162,163] for which it has been possible to derive complete basis sets. However, except in the special case of anions [164], there are always an infinite number of target states that should in principle be included in the CC expansion. This consideration limits standard CC treatments to energies below the target ionization threshold.

A difficulty associated with all methods of including polarization effects in the calculation is the difficulty of demonstrating convergence in the calculation [165,166]. One method of assessing the convergence of CC calculations with respect to the target state expansion is to calculate the target polarizability [167] using Eq. (49). With this formalism, and an accurate target wave function, the calculated polarizability should monotonically increase to the correct answer as target states are added. In practice simple CC calculations often significantly underestimate the target polarizability [168].

The issue of how to further improve the representation target and scattering wave functions in a balanced fashion remains one of active research. One approach which appears particularly promising, albeit computationally expensive, is the use of pseudo-states. This approach is discussed in section next.

4.1. Extension to intermediate energy

The intermediate energy regime, which straddles the ionization threshold of the target, is traditionally difficult to treat although for electron atom collisions there has been great progress on this problem in recent years [169]. Besides the convergent close-coupling technique of Bray and Stelbovics [162,163,170] alluded to above, two **R**-matrix techniques have been developed which each significantly extend the energy range for which it is now possible to perform reliable collision calculations. These are the intermediate energy **R**-matrix method (IERM) [122,171] and the **R**-matrix with pseudo-states method (RMPS) [172,173]. While the IERM has so far only been exploited for one electron targets and would therefore prove

difficult to generalize to polyatomic systems, the RMPS technique has been used for complex atoms where it has found rather general application. Finally I note that the Time-dependent Close-Coupling (TDCC) method of Pindzola and Robicheaux [174,175] has been applied to molecular problems [176]. However, of all these approaches, only the RMPS method has been routinely been applied to problems involving many active electrons.

The basic idea of the RMPS method is that an extra set of basis functions with zero amplitude for $r \geq a$ are placed at the center of the **R**-matrix sphere and are used to represent the continuum. Since the expansion is only over a finite volume, this continuum is discretized into what are called pseudo-states. Furthermore, since the target wave function is entirely confined to this spatial region, these pseudo-states represent the only part of the continuum which is directly accessible to physical states of the target. Although it is possible to project out different target channels [177], a standard assumption in the RMPS method is that electron impact excitation to a pseudo-state lying above the threshold to ionization can be considered to be ionizing [178]. In the atomic RMPS calculations the extra basis is generally represented by Sturmian orbitals [178] which have the form $r^l \exp(-\alpha r)$, which are similar to the Slater type orbitals (STOs) discussed below.

In practice, the use of the pseudo-states in **R**-matrix calculations predates the introduction of the RMPS method and attempts to perform calculations at intermediate energy. This is because the pseudo-states perform another important role in the calculations, which is to complete the representation of polarization effects by allowing for states omitted from the close-coupling expansion of Eq. (14). In this guise the extra states are often described as polarized pseudo-states (PPS) [179]. For atomic problems there are systematic methods for optimizing extra basis functions [180] which allow for the very efficient inclusion of polarization effects in scattering calculations. Such effects are particularly important for electron collisions with neutral atoms where the polarizability is the dominant long-range potential. Similar procedures have been proposed for molecules [181,182], albeit based exclusively on the use of Hartree–Fock wave functions for the target. Pseudo-States [183,184], or sometimes merely extra states [167], have been used in electron–molecule collision calculations but their design and use is altogether more haphazard. The option to simply manually include the polarizability in the outer region potential has also been used [91,185]. Of course, this does not help to improve the representation of polarization in the inner region which is probably more critical for obtaining reliable results [186].

The use of extra states to represent polarizabilities is based on the second-order perturbation theory expression for the static dipole polarizability, $\boldsymbol{\alpha}$:

$$\alpha_{ij} = 2 \sum_{n>0} \frac{\langle 0|\mu_i|n\rangle \langle n|\mu_j|0\rangle}{E_n - E_0} \tag{49}$$

for state $|0\rangle$ with energy E_0. In this expression the components of the polarizability tensor are given by the components of the transitions dipoles and the sum over excited states runs over *all* states of the system including the continuum. It is the need to include the continuum which usually restricts the usefulness of this expression but which is directly addressed in the RMPS method [168].

Recently Gorfinkiel and Tennyson [26,187] developed a molecular implementation of the RMPS technique which is also beginning to find rather general application [105,188–190]. The numerical implementation of this method is described in Section 5.3. Test calculations have shown the method to be very efficient at recovering the full polarizability of the target [26,168,189]. In practice, because of the availability of simple, analytic and reliable methods of calculating electron impact ionization cross sections for neutral molecules [191–193], the main use the RMPS calculations has been in converging polarization potentials and in extending the energy range above the ionization threshold that calculations of other cross sections, such as electron impact electronic excitation, can be reliably performed.

4.2. Relativistic effects

Nearly all electron–molecule calculations performed so far have concentrated on the molecules containing light atoms and have therefore ignored relativistic effects. Given the needs of the lighting industry, see for example Yang et al. [194] who discuss the requirement of studies of electron collisions with the heavy molecule GaI, there is a requirement for relativistic treatments of electron–molecule collision problems. A fully relativistic formulation of the **R**-matrix method was given by Chang [195] in the 1970's and has been widely used [196] and developed [197]. The soundness of this approach, which has been subject to criticism, has recently been reconfirmed [198].

Fandreyer and Burke [184] considered implementing relativistic effects in their study of electron collisions with HBr but appear not to have actually done so. The approach they advocate, which is in the spirit of many atomic **R**-matrix calculations, is to use angular momentum recoupling in the outer region [199]. This approach is similar to the widely used frame transformation to allow for the inclusion of rotational motion [200] and I would expect to see it implemented at some point.

4.3. The double *R*-matrix method

So far all discussion of electron–molecule collisions has been implicitly within a fixed-nuclei approximation. The basis for separating the electronic and nuclear motion in scattering problems was given by Chase [201] and is generally termed the adiabatic nuclear rotation (ANR) approximation. The underlying basis of Chase's ANR approximation is that the "period of

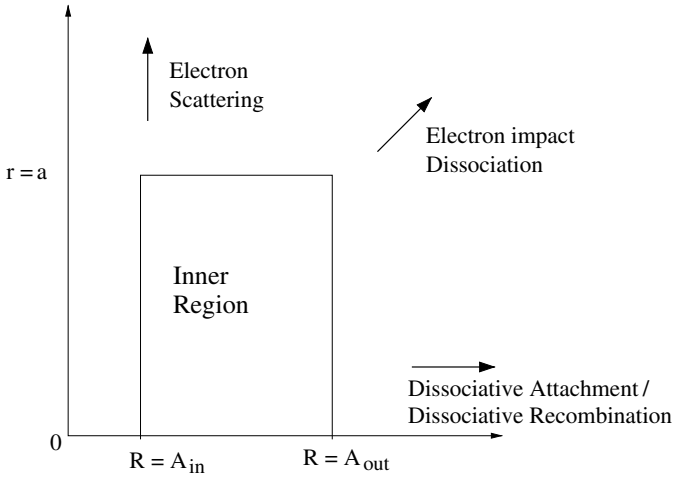

Fig. 4. The two-dimensional **R**-matrix method of Schneider, Le Dourneuf and Burke [215]: in this method the inner region is given for the scattering electron coordinate $0 \le r \le a$ and the nuclear coordinate $A_{\rm in} \le R \le A_{\rm out}$. The asymptotic processes as $r \to \infty$ and/or $R \to \infty$ are illustrated.

traversal of the scattered particle through the region of interaction is small compared with the target motion excitable in the collision". This condition is often satisfied in electron–molecule collisions and the ANR approach has been shown to work remarkably well, even in very detailed comparisons [202]. However there are two circumstances where the pre-conditions for the ANR approximation are not satisfied. The first is very close to threshold and second is in the region of a resonance.

In principle the energy region near a threshold can be treated using a generalization of the close-coupling equations to include nuclear motion. Full close coupling has been used to treat near-threshold vibrational and rotational excitation [203,204] but has been found to be largely unnecessary even close to threshold [202,205]. Instead rotational motion is largely dealt with by using a frame transformation [200,206,207], which rotates the scattering problem from body-fixed coordinates to laboratory coordinates. On the assumption that all rotational energy levels are degenerate, this transformation can be performed on the body-fixed **T**-matrix elements. For linear molecules the transformation of body-fixed **T**-matrix element $T^{\Lambda}_{l',l}$ is given by [208]:

$$T^{J}_{j'l',jl} \simeq \sum_{\Lambda=-l}^{l} A^{J\Lambda}_{j'l'}\, T^{\Lambda}_{l',l}\, A^{J\Lambda}_{jl}, \tag{50}$$

where Λ labels the total symmetry of the problem given by the projection of the total orbital angular momentum on the molecular axis; J is the total angular momentum of the system. j and j' are the initial and final rotational states of the target, and l and l' label the channels in the original calculation. In the linear molecule case, the transformation has the relatively simple form:

$$A^{J\Lambda}_{jl} = \sqrt{\frac{2j+1}{2J+1}}\, C(j\, l\, J;\, 0\ \Lambda\ -\Lambda). \tag{51}$$

Similar transformations for non-linear molecules depend on the symmetry of the molecule concerned; they can be found in the specialist literature [209,210].

The problem of how to treat nuclear motion in the region of a resonance, or indeed a very weak bound state which also leads to nuclear excited Feshbach resonances, is altogether more complicated. Here too it is necessary to consider lifetime effects. If the resonance is long lived compared to the target motion under consideration, then it is possible to treat resonance curves rather as if they are the potential energy curves of bound states and, for example, solve the nuclear motion equations to determine what vibrational states they support [211]. This sort of treatment is fairly standard in studies of dissociative recombination [101,212].

Conversely short-lived resonances are well known to support complicated structures due to the coupling between the resonance and the motion of the nuclei [213,214]; resonances that occur near thresholds show a complicated structures for similar reasons [100]. These problems can only be properly addressed by explicitly treating the non-adiabatic couplings between the electronic and nuclear motions.

Schneider, Le Dourneuf and Burke [215] developed a non-adiabatic **R**-matrix theory based on the use of an **R**-matrix formalism for both the electronic and nuclear motion. This theory was re-derived variationally by Nesbet [216] and demonstrated to work for the shape resonance in N_2^- [214,217] for which the low-lying shape resonance is broad and structured by non-adiabatic coupling between the nuclear motion of the nitrogen and the electronic resonance. The division of the **R**-matrix into two regions is illustrated in Fig. 4.

The basis of the non-adiabatic **R**-matrix approach involves identifying an inner region pole of the electronic problem which can be associated with the resonance of interest and solving for the nuclear motion using both the curve given by

this pole and the non-adiabatic couplings. The solutions of this problem are used to construct nuclear motion **R**-matrices on the boundary A_{out}, see Fig. 4. These **R**-matrices are essentially the same in form as the electronic ones discussed elsewhere in this article. The only major difference is that because the inner region for nuclear motion is considered only the range $A_{in} \leq R \leq A_{out}$, a Bloch term is also required at the inner boundary. In the method implemented by Morgan [214], these nuclear motions are simply represented in a basis of Legendre polynomials scaled to span the range A_{in} to A_{out}.

This two-dimensional **R**-matrix theory has been widely used to perform detailed and very successful studies of non-adiabatic processes in diatomic systems such as elastic scattering [92], rotational excitation [119,120] and vibrational excitation [83,92,115,117,118,214]. In all these cases the study has involved the treatment of a single, low-lying resonance curve. To my knowledge no attempt has been made to extend this to multidimensional, polyatomic problems.

The method has also been used for electron collisions with molecular ions [103,218–220] where, in particular, it was used to demonstrate the possibility of dissociative recombination occurring even in the absence of any suitable resonance curves [103]. As molecular ions have many resonance states, the application of the two-dimensional **R**-matrix method requires the treatment of more than a single **R**-matrix pole. This is actually technically quite demanding as it requires not only tracking the poles correctly as a function of geometry, which becomes increasingly difficult for many electron problems where the density of the poles can be high, but also ensuring that the associated wave functions vary smoothly so that their derivatives as a function of geometry can be evaluated to allow for the inclusion of non-adiabatic effects [103]. Ensuring the smoothness of the wave function requires enforcing phase consistency between neighboring geometries, which is complicated by the fact that there are up to five separate places in the calculation which can introduce an arbitrary phase in the wave functions. For this reason the method has ceased to be routinely used for problems with many resonances. Instead the alternative method of using **R**-matrix calculations to provide the input to multichannel quantum defect studies [212,221,222] has been preferred.

5. Numerical realisation

5.1. Different approaches

There are a number of current computational procedures for performing electron–molecule collisions calculations. The two most widely used are generically referred to in this article as Bonn code and the UK molecular **R**-matrix code. The Bonn code is the GTO based implementation of Nestmann, Peyerimhoff and co-workers [141,142,223,224] which is built on the MRD-CI quantum chemistry programs of Buenker and Peyerimhoff [143–145]; recent implementations of this code have used the program DIESEL [225]. The UK molecular **R**-matrix code(s) [226–228] actually encompass two methods which share the configuration generation, Hamiltonian construction and diagonalization and most of the outer region, but use completely distinct basis sets. The original code, which used STOs for the target and numerical continuum functions, was based on the Alchemy quantum chemistry code [229,230] as adapted by Noble [231] and others. This code can only treat electron collisions with diatomic targets. A more general GTO based code, capable of treating electron collisions with polyatomic code, was built about the Sweden Molecule quantum chemistry suite of Almlöf and Taylor [232,233] by Morgan et al. [69].

In principle, the most general other implementation appears to be the **Z**-matrix method of Huo and Brown [70] whose development seems not to have been pursued. Hiyama and Kosugi [73,234,235] developed an **R**-matrix code called GSCF4R, which uses a mixture of GTOs and multichannel quantum defect theory [107], to study the super-excited states which result from inner shell excitations of polyatomic molecules.

A much more extensive set of **R**-matrix based multichannel quantum defect codes for diatomic have been developed by Jungen and co-workers. This work has two strands. The study of rare earth halides such as CaF and BaF [108,236,237] and related systems [238] using semi-empirical procedures [236,237] and, increasingly, *ab initio* methods [239]. More recently earlier work on the super-excited states of H_2 [240] has been developed into a fully *ab initio* treatment of the problem [72,109,241,242]. This work uses spheroidal coordinates and performs a full treatment of nuclear motion. This work gives truly impressive agreement with corresponding very detailed experimental studies [243].

The most recent development has been of three-dimensional, finite element **R**-matrix approach by Tonzani and Greene [155] as represented by code FERM3D [74]. This approach is based on the use of potentials and is therefore limited to consideration of electron collisions with molecules in their electronic ground state. However it has proved useful for the systematic study of electron collisions with biomolecules with particular emphasis on the study of shape resonances [244,245]. This work has been used as input to multiple scattering calculations to model radiation damage to DNA induced by secondary low-energy electrons in the condensed phase [246].

In the descriptions below I will focus mainly on the Bonn and UK **R**-matrix procedures, and only mention the other methods when their algorithms add something significant to the discussion. The Appendix gives a brief outline of the UK molecular **R**-matrix codes which should help with understanding some of the algorithmic points discussed below.

5.2. Specialised algorithms: Inner region

5.2.1. Continuum basis sets

A fundamental issue when developing treatments of the electron–molecule scattering problem is the choice of suitable functions with which to represent the continuum. These continuum functions have to be complete over the energy range of

interest and, in the **R**-matrix method, span only the inner region. Conversely these functions must not be so complete that they cause problems of linear dependence with the functions chosen to represent the target wave functions. In practice, it is often impossible to work without using over-complete sets, which means that robust methods for removing the linearly dependent functions must be found. This is also not straightforward as removing functions can lead to the generation of incomplete basis sets. A final computational consideration in the choice of functions is the need to be able to evaluate rapidly and accurately a large number of multicentered and multidimensional integrals.

Although energy-dependent basis functions have been used for **R**-matrix calculations of electron–molecule collisions [247], this would seem to be somewhat against the spirit of the **R**-matrix method. Below only basis functions which span a given range of scattering energies, normally from zero to some upper limit, are considered.

In all the procedures described below the net result is to produce a set of continuum orbitals given by

$$u_{ij}(r,\theta,\phi) = N_{ij}\left(\sum_{i'j'} c_{iji'j'}\, v_{i'j'}(r,\theta,\phi) + \sum_k d_{ijk}\psi_k(\mathbf{x})\right) \tag{52}$$

where v_{ij} are the continuum basis functions written in terms of the partial wave expansion (15) and the form of whose radial functions, $f_{ij}(r)$, are discussed below; ψ_k are the target orbitals, including any virtual orbitals retained in the calculation, which are discussed in detail in Section 5.2.2. The coefficients $c_{iji'j'}$ and d_{ijk} result from the various orthogonalization procedures described, which involve both orthogonalization to the target MOs and within the continuum functions. The factor N_{ij} ensures that the orbitals are normalised to unity within the **R**-matrix sphere.

In atomic **R**-matrix calculations, a complete set of functions can be generated by solving a one-dimensional Schrödinger equation for an effective or model, but never-the-less fairly realistic, central potential. These numerically defined functions can be made rigorously orthogonal to the atomic wave function of the target using Lagrange multipliers [129]. This approach necessarily requires numerical evaluation of integrals, but as all these integrals are confined to a single center this is straightforward as only one-dimensional quadrature is required.

A significant number of different methods have been used to represent continuum functions in electron–molecule collision calculations. Since the first attempt to build a general electron–molecule collision code was based on the use of Slater type orbitals (STOs) for the target wave functions, STOs were also initially used to represent the continuum [67]. However, the difficulty of representing continuum functions by STOs expanded about a single center, combined with the limited accuracy of the associated integrals, meant that reliable results could only be obtained for low scattering energies with these continuum functions.

As an alternative Burke et al. [248] followed the procedure discussed above for atoms: they used numerical solutions of a radial Schrödinger equation based on the isotropic term in a single center expansion of the potential [249], $V_0(r)$, combined with enforced Lagrange orthogonalization to an expansion of the target wave function. These functions are obtained as numerical solutions of the differential equation

$$\left(\frac{\mathrm{d}^2}{\mathrm{d}r^2} - \frac{l_i(l_i+1)}{r^2} + V_0(r) + k_i^2\right) f_{ij}(r) = \sum_n \lambda_{jn} P_{ln}(r), \tag{53}$$

where λ_{jn} is a Lagrange multiplier and $P_{ln}(r)$ is the lth component of the nth target orbital. In order to obtain numerical solutions of this equation it is necessary to apply boundary conditions. The boundary conditions for all i and j used for this, and the generation of other numerical basis functions is:

$$\begin{aligned} &f_{ij}(0) = 0 \\ &\frac{a}{f_{ij}}\frac{\mathrm{d}f_{ij}}{\mathrm{d}r}\bigg|_{r=a} = b, \end{aligned} \tag{54}$$

where in practice b is always taken as zero.

This approach was successful in allowing calculations to be performed over an extended energy range. However, the enforced Lagrange orthogonalization of the continuum basis functions to the target led to very complicated continuum orbitals each of which were comprised of different continuum functions for each partial wave. The resulting continuum basis sets were therefore deemed to be too large to be tractable for most calculations. As a result subsequent calculations [161,250] dropped the Lagrange orthogonalization requirement, i.e. set the right hand side of Eq. (53) to zero. This approach yields much simpler basis sets typically comprising about 10 functions per partial wave. Subsequent work [251] also stopped using the isotropic target potential, choosing instead to use no potential for neutral targets and a Coulomb potential for charged targets. The resulting continuum functions are therefore simply numerical representations of Bessel or Coulomb functions, respectively, within the **R**-matrix sphere. A special integrals code was developed by Noble [231] to allow the use of these numerical basis functions. As the structure of the inner region wave function, Eq. (14), means that only one electron ever occupies a continuum orbital, this code makes a significant saving by not calculating any two electron integrals purely between continuum basis functions.

One important issue with using numerical functions is the need to define boundary conditions on the **R**-matrix sphere. The second boundary condition in Eq. (54) with $b = 0$ ensures that the continuum functions have a zero derivative on the

R-matrix boundary. This condition removes the Bloch term but is unphysical as it arbitrarily constrains the derivative of the wave function on the **R**-matrix boundary. The condition therefore has to be relaxed in order to get a complete treatment of the problem. This is done in a straightforward fashion using the perturbative correction due to Buttle [252]. This correction takes the form

$$B_i(E) = \frac{1}{2a} \sum_{j=N_{li}+1}^{\infty} \frac{(v_{ij}(a))^2}{k_i^2 - E} \tag{55}$$

where the sum runs over the solutions of Eq. (53) not used in the continuum basis set. In practice it is usual to least-squares fit this expression to a simple quadratic form:

$$B_i(E) = C_{i1} + C_{i2}E + C_{i3}E^2 \tag{56}$$

which appears to lead to little loss of accuracy.

The Buttle correction is added to the diagonal of the **R**-matrix formed at the boundary giving a revised expression for the **R**-matrix:

$$R_{ij}(a, E) = \frac{1}{2} \sum_k \frac{w_{ik}(a) w_{jk}(a)}{E_k - E} + \delta_{ij} B_i(E). \tag{57}$$

Although the use of Buttle corrections is often criticised in the literature, in my experience they give reliable results. Indeed it is straightforward to check if the correction is working well since they give a negligible contribution very close to any **R**-matrix pole. If the eigenphase sums pass smoothly through the **R**-matrix poles without any sign of underlying oscillations, then the Buttle correction is likely to be satisfactory. However, one drawback of using a Buttle correction is that the calculation is no longer strictly variational.

The dropping of enforced Lagrange orthogonalization to the target meant that other procedures had to be developed to ensure that the continuum orbitals remain orthogonal to the target molecular orbitals (MOs). The method generally chosen is to Schmidt orthogonalize the continuum orbitals to the target MOs having already ensured that the target MOs are themselves orthonormal. This procedure imposes weaker orthogonality conditions as no (linearly dependent) functions are dropped from the basis. It is in principle possible to identify the most linearly dependent functions as the result of this orthogonalization, or indeed other procedures such the alternative symmetric or Löwden orthogonalization, and drop them from the continuum basis sets. However, unpublished tests on such procedures for electron–H_2^+ scattering showed that functions could not safely be removed in this fashion without adversely affecting the results.

Many calculations have been performed on linear molecules using numerical functions and Schmidt orthogonalization [253]. However, this procedure is not sufficient to remove linear dependence problems with calculation on some molecular targets. This is particularly true for positively charged ions where the use of a Coulomb potential leads to low-lying "continuum" orbitals which in fact mimic delocalized bound states of the target. A further orthogonalization step, based on Lagrange orthogonalization to the actual target wave functions, rather than a spherical expansion of them, has therefore been implemented [254]. This method drops one continuum orbital for every target orbital selected to orthogonalized against; it works well provided only a minimal number of target orbitals are used. It is now routinely used for calculations on involving positively charged targets.

An alternative formulation for diatomic positive ions by Jungen and co-workers, which has its basis in quantum defect theory, also uses numerical functions for the radial coordinate [72,241].

The use of numerical functions to represent the continuum has proved very successful for calculations involving electron collisions with both atoms and linear molecules. Indeed they have been used successfully to span both extended **R**-matrix spheres [255–258] and very extended energy ranges [259]. However, for calculations involving non-linear molecular targets, use of numerical functions would require the evaluation of multicenter, multidimensional numerical integrals for which there are at present no robust procedures available. Alternatives are therefore needed.

Gaussian Type Orbitals (GTOs) have proved supremely successful for electronic structure calculations on polyatomic molecules [260]; this is mainly because of the ease and accuracy with which multicenter integrals over GTOs can be evaluated. In particular multicenter integrals over GTOs can be computed a factor of about 10^6 times more accurately than similar integrals over STOs or the STO/numerical function integrals discussed above, even when these latter integrals are restricted to the simpler linear molecule case. It was therefore anticipated from the earliest days of **R**-matrix calculations on molecules that GTOs might provide good continuum basis functions [62,63]. However the real development of GTOs for **R**-matrix calculations was by the Bonn group of Peyerimhoff and Nestmann [68,261]. Nestmann and Peyerimhoff optimized GTO basis sets by fitting them to appropriate radial wave function i.e. Bessel functions for scattering from neutral targets. A number of basis sets have been developed in this fashion for electron collisions with neutral targets and an **R**-matrix radius of 10 a_0 [141,261,262]. Faure et al. [263] developed a general procedure for generating such basis sets for both charged and neutral systems, and for different **R**-matrix radii. This procedure is now the most commonly used although Tarana and co-workers [91,189] noted that, due to the similarity of the problem with the standard quantum mechanical particle in a box problem, it was possible to adapt GTO basis functions developed for one **R**-matrix radius to other values of a using a simple scaling. It should be noted however that at the same time that the energy range covered by the basis also scales.

Tarana and Horáček [157] used a different method for optimizing the exponents of their GTOs. Their procedure involved testing the quality of their basis sets by performing electron scattering calculations from null targets. Such calculations should, of course, give zero eigenphase sums and cross sections for all scattering energies. This criterion not only formed the basis for the optimization but also explicitly gives the energy range of validity for a given continuum basis set.

There are two technical issues that need to be resolved with the use of GTOs: that of orthogonalization, and how to perform the integrals over a finite region and retain the accuracy inherent in the use of Gaussians. The solution to the orthogonalization problem advocated by the Bonn group [68] is based on the use symmetric or Löwden orthogonalization. The continuum functions are Löwden orthogonalized to the orthonormal target MOs. Orthogonalized functions which have eigenvalues of the overlap matrix that are lower than some deletion threshold, typically about 2×10^{-7}, are then removed from the basis. Finally the continuum orbitals are Schmidt orthogonalized to each other. This procedure appears to be robust and was also adopted in the UK molecular **R**-matrix codes [227]. Indeed, as discussed below, this procedure has also been adapted to cope with the inclusion of the extra set of GTOs required in the molecular **R**-matrix with pseudo-states method.

The issue of how to adapt Gaussian integral procedures to a finite volume was largely solved by Nestmann et al. [68] who wrote the integral over the inner region as the integral over all space minus the integral over the outer region. This latter contribution is usually known as the tail integral. Nestmann et al. realised that in the special circumstances required for low-energy electron scattering, when it is only necessary to consider a single electron in the outer region, it was possible to write these tail contributions in a straightforward fashion in terms of multipole moment integrals of the short-range GTOs. These integrals are actually routinely calculated in scattering calculation. This procedure was adopted by the Bonn group to correct one electron integrals, and in the UK molecular **R**-matrix codes to correct both one and two electron integrals [69].

The use of GTOs to represent the continuum orbitals is now widespread but is not ideal for all problems. In particular while numerical functions can cope with both large ($a > 20\,a_0$) **R**-matrix spheres and extended energy ranges [255,256,258], this has so far not proved possible with GTOs. This is because it is difficult to reproduce the nodal structure of the continuum orbitals using a linear combinations of nodeless GTOs over an extended range without encountering severe problems of linear dependence. It may be possible to make progress on representing highly oscillating functions at some distance from the expansion center by using clever contractions of GTOs, but it seems more likely that alternative basis functions may be required. To this end I note that B-spline basis functions have proved highly successful for atomic **R**-matrix calculations [264,265]. So far the application of B-splines to electron–molecule problems has been restricted to problems with one electron targets [266,267], but its extension to general problems is certainly worth investigating.

5.2.2. Target orbitals

The choice of an appropriate target basis set is restricted by the standard **R**-matrix requirement of keeping the wave function within the **R**-matrix sphere; this tends to rule out the use of very extended basis sets which usually contain a number of very diffuse functions. In addition in coupled states calculations, a single target basis and orbital set is required to represent all the states in the calculation. I note that in atomic calculations non-orthogonal sets of valence orbitals [268] are increasingly being used to circumvent this requirement; up until now all molecular **R**-matrix studies have been based on the used of orthogonal sets of orbitals.

The choice of which target molecular orbitals (MOs) to use in the calculation is quite difficult and it is probably true to say that a clear or unique answer to this problem has yet to emerge. The difficulties arise from the use of these MOs for several different purposes in the calculation. Before discussing this issue, it is worth classifying MOs into several categories according to their occupancy in the scattering calculation. Note that the classifications are similar to, but not precisely the same, as the orbital definitions used for bound state electronic structure calculations. One can define core orbitals as ones which are fully occupied or frozen in all configurations considered, valence orbitals are orbitals which are partially occupied in the target wave functions and hence are the ones used to represent electron–electron correlation in the target. In scattering calculations, virtual orbitals are defined as target orbitals which are not occupied in the target wave function and, for our purposes, are restricted to those virtual orbitals which are used in the scattering calculation. The remaining MOs are discarded and need not concern us. It should be emphasised that it is usual, and indeed generally necessary, to use the same MOs in the target and scattering calculations.

The simplest models use a target wave function calculated within the Hartree–Fock approximation in which case there are no valence orbitals and all target MOs are core ones. The self-consistent field (SCF) procedure used to generate these MOs also gives a set of unoccupied orbitals which, once orthogonalized to the occupied orbitals, can provide the virtuals for a scattering calculation. These virtuals are important for representing shape resonances, which can be thought of the entry of the scattering electron into a low-lying unoccupied MO; indeed inclusion of insufficient virtual orbitals in a calculation can lead to difficulties, or even failures, in getting a good representation of these shape resonances [166,269]. Given that the partial wave expansion used for the continuum orbitals is necessarily finite, the virtual orbitals also play a key role in representing high partial waves in the vicinity of the nuclear singularities, where the partial wave expansion is, at best, only slowly convergent.

Virtual orbitals in SCF calculations actually represent orbitals of the $N + 1$ electron systems i.e. anion states for a neutral target. In some sense this may appear appropriate for the representation of $N+1$ electron shape resonances but such orbitals are often more diffuse than required. Furthermore their extended nature can cause difficulties for **R**-matrix calculations. A number of alternative schemes for generating virtual orbitals including Improved Virtual Orbitals (IVOs) [14,270,271]

and Modified Virtual Orbitals (MVOs) [272,273] have been advocated although test performed by my group, see [166] for example, have found only small differences in the results obtained using these different choices.

The use of SCF target wave functions has considerable advantages in terms of defining polarization effects in the scattering calculations, see Section 3.7, but there are limits the accuracy and scope of target wave functions that can be modelled. Besides the well-known problems with bond-stretched SCF wave functions [260], it is difficult to get reliable excited state wave functions and energies within this model as single particle excitations from a Hartree–Fock ground state tend to significantly overestimate excitation energies. Good representations of the excited state are vital not only for electron impact excitation calculations but also for obtaining reliable Feshbach resonances. The simplest approach to treating excited states is to consider SCF wave functions with a single electron excitation; this approach has been extensively used [274], but does not in general give accurate excitation thresholds or excited state wave functions.

To move significantly beyond single electron excitation approximations, it is necessary to include configuration interaction (CI) effects in the wave function. This is not only to allow for electron correlation effects, which is the usual purpose of performing CI calculations [260], but also to allow for orbital relaxation effects. This is a particular issue in scattering calculations based on a close-coupling expansion since all target states must be represented using a single set of MOs; this means that the MOs will not be optimal, even in the limited SCF sense, for most if not all of the states. Indeed use of SCF MOs for multistate calculations tends to over-emphasize the ground state at the expense of excited states, leading to excitation energies which are too high.

There are a number of possible choices of orbitals appropriate for representing several electronic states simultaneously. The two that have been used are state-averaged Natural Orbitals (NOs) [156] and MOs from Multi-Configurational Self-Consistent Field (MC-SCF) calculations [260]. NOs are the orbital set which gives the fast convergence of a CI expansion; they are thus a particularly efficient choice of single particle states for use in construction of correlated electronic wave functions [275]. However, as one generally does not have the full-CI wave function for a given problem, the NOs generated are strictly pseudo-NOs or the best estimate of the NOs for the given wave functions. The NOs for a particular wave function are obtained by diagonalizing the density matrix using that wave function. State-averaged natural orbitals are obtained by diagonalizing the density matrix constructed using appropriately weighted wave functions for several electronic states. State-average NOs have been used for a number electron–molecule collision studies [276,277]. This procedure has particular advantages for calculations where the SCF procedure leads to a breaking of the degeneracy between pairs of symmetry-linked orbitals as it can be used to restore the correct orbital and hence electronic state degeneracies [278].

MC-SCF calculations are a generalization of the SCF procedure where orbitals for several electronic states are optimized simultaneously. It is now a standard first step in many electronic structure methods [260]. A common variant of the MC-SCF method is the Complete Active Space (CAS) SCF procedure where all states for a given active space, within which the electrons are freely distributed, is considered. Clearly the CAS-SCF procedure has some links with the CAS-CI method used to balance the target and scattering calculations [148] and discussed Section 3.7. MC-SCF orbitals have found increasing use in scattering calculations [166,279].

Before leaving the topic of orbitals there are few special cases that should be mentioned. The simplest case is one electron systems where the orbital actually represents the best possible wave function for the target with the given basis set. In this situation a separate orbital can simply be optimized for each electronic state of interest [161,280]. Systems with few electrons, typically between two and four, form another special case since for these systems it is possible to use target wave functions built on a full-CI representation [218,256,258]. In this circumstance the wave function is invariant to the choice of orbitals for a given basis set.

Finally it is worth considering the treatment of diffuse or Rydberg states since many molecules have low-lying excited states with a pronounced Rydberg character. Cooper and Kirby [281] developed a procedure for representing Rydberg states of molecules. They first derive valence NOs for the system and then add selected low exponent or diffuse functions to represent the Rydberg electron. These Rydberg orbitals are obtained by considering single excitations out of the valence space. In scattering calculation, such as the one performed by Rozum et al. on the CF radical [282], this meant identifying three different categories of target MOs: core, valence and Rydberg. In practice there are not many **R**-matrix calculations which include Rydberg states in the target model; this is because the correct treatment of many such states requires extended **R**-matrix spheres.

5.2.3. Constructing and diagonalizing the inner region Hamiltonian

Despite the fact that the inner region Hamiltonian for the scattering problem needs only to be constructed and diagonalized once for each total space-spin symmetry of the problem being considered, it is still the step that dominates the computer usage for most calculations. There are computer issues with both the construction and the diagonalization steps.

In the construction step, the use of correlated target wave functions results in the generation of very long configuration lists which, without special measures, can lead to Hamiltonian matrices which are computationally very expensive to evaluate. In principle, given that the target wave function appears as a single term in the inner region wave function, see Eq. (14), use of a very lengthy target CI expansion does not necessarily lead to a large final Hamiltonian matrix just complicated matrix elements. In practice this is not quite so since the number of L^2 terms included in the expansion of Eq. (14) is related to size of the target CI.

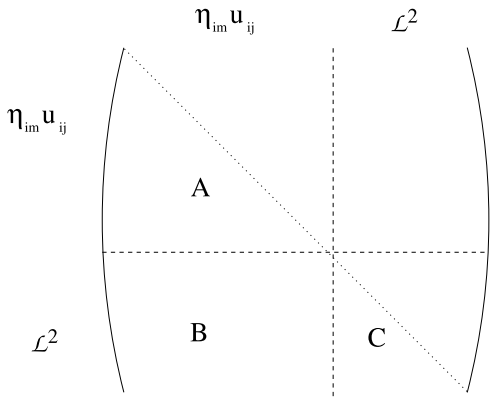

Fig. 5. The real symmetric Hamiltonian matrix contains three types of matrix elements: A continuum state – continuum state; B continuum state – L^2 and C L^2 – L^2.

The big problem with the diagonalization step is that in principle construction of the inner region **R**-matrix, Eq. (13), requires information on *all* the **R**-matrix poles and associated wave functions. This is quite impractical for large expansions and has resulted in the developments of methods [142,283,284] which obviate the need for a full matrix diagonalization.

Before discussing how the inner region Hamiltonian is constructed and diagonalized, it is worth noting that although quantum chemists have developed a number of very efficient algorithms for generating very large lists of configurations and evaluating the resulting matrix elements [260], they are in general not useful in the context of **R**-matrix calculations. The requirement for a balanced calculation, see Section 3.7, means that it is essential that total control is retained over configuration selection and that these configurations are generated in a specific order. Indeed, it is also usually necessary to enforce an extra constraint on the non-L^2 configurations which ensures the coupling of the first N electrons to identifiable target states which hence map to channels in the outer region.

Consider first the issue of constructing the Hamiltonian using a CI wave function: in this case the target wave function of symmetry s is built as a linear combination of M_s electron configurations, more formally configuration state functions (CSFs) which are denoted η below. The N-electron target wave function is then written

$$\Phi_{ns}^{N} = \sum_{m=1}^{M_s} c_{nms}\eta_{ms}(x_1 \ldots x_N), \tag{58}$$

where two indices on the target wave function, Φ_{ns} label the nth state of symmetry s and allow for inclusion of several target states of the same symmetry, which are represented by a single set of configurations, η_{ms}. The index n therefore runs over the N_s states of symmetry s. Note that elsewhere in this article the target state is denoted Φ_i^N for simplicity; in this notation i is used as a compound index denoting both n and s. The coefficients c_{nms} are obtained from a standard electronic structure calculation and appropriate models for generating this form are discussed in Section 3.7.

The first term in the expression for the **R**-matrix wave function, Eq. (14), runs over $\Phi_i(\mathbf{x}_1 \ldots \mathbf{x}_N)u_{ij}(\mathbf{x}_{N+1})$, which is the product of the target wave function and a continuum function. In the case of a CI target this means that the sum of configurations represented by Eq. (58) above is contracted into a single term. Conceptually and computationally the simplest way of building the Hamiltonian for the $N + 1$ electron problem which includes the target contraction is to first compute the greatly expanded Hamiltonian that deals with each configuration $\eta_{ms}(x_1 \ldots x_{N_i})u_{ij}(\mathbf{x}_{N+1})$ individually. This gives Hamiltonian matrix elements between the target times continuum configurations of the form $H_{smj,s'm'j'}$. These matrix elements can then be contracted to give the final matrix using the target states CI coefficients:

$$\tilde{H}_{nsj,n's'j'} = \sum_{m=1}^{M_s}\sum_{m'=1}^{M_{s'}} c_{nms}c_{n'm's'}H_{smj,s'm'j'} \tag{59}$$

where the need for two target state indices, i and n is discussed above. This operation is a contraction rather than a simple transformation since significantly fewer target states are retained in the final Hamiltonian, $\tilde{\mathbf{H}}$, than configurations used to expand the target wave function, i.e. $N_s \ll M_s$. This becomes increasingly true as the length of the target CI expansion increases.

In performing this contraction the Hamiltonian matrix is actually split into three blocks [65], see Fig. 5. Eq. (59) actually only gives the form of the contraction for block A; the off-diagonal block B links the target-continuum part of the Hamiltonian matrix with the L^2 configurations and requires a one-dimensional contraction involving only a single set of target CI coefficients. Block C which contains the Hamiltonian matrix elements between the purely L^2 configurations does not change between the original and contracted Hamiltonian matrices.

The size of this uncontracted Hamiltonian matrix, excluding the L^2 functions, is the product of the length of the target CI expansion, M_s, times the number of continuum functions summed over the symmetries of the target states included in

the CC expansion. The equivalent of this number is sometimes quoted as the size of the problem tackled in calculations; however, it is more usual for UK molecular **R**-matrix papers to quote the M_s separately. This product can become extremely large and the fully, uncontracted Hamiltonian unwieldy which places a serious constraint on the size of problem that can be addressed [124,146].

The present UK **R**-matrix molecular **R**-matrix codes uses a completely different and computationally very much more efficient method of performing the target contraction [285]. This method bears some conceptual similarities with the algorithm used in the RMATRX II atomic code [59] which was developed at approximately the time. The algorithm used in the molecular codes is built on the prototype configuration method [286,287] which was originally developed as part of the ALCHEMY quantum chemistry codes. The basic idea of the prototype configuration method is that many lists of configuration differ only in the occupancy of a single spin orbital. In the prototype method this list is represented by only the first two CSFs in the list. These two CSFs are used to construct all the symbolic matrix elements using Slater's rules [156] and to identify the integrals necessary for their evaluation; only at this point are the matrix elements generalized to all the configurations on the list and the appropriate integrals used. Given the structure of the **R**-matrix wave function, Eq. (14), the target-continuum configurations lend themselves very naturally to the prototype CI method [251] since there are usually between 25 and 50 continuum functions in this expansion.

However, the real advantage of the prototype CI method for constructing **R**-matrix Hamiltonians comes when it is combined with performing the target CI contraction at the symbolic matrix element level [285]. In this algorithm the following steps are performed:

(1) The list of all prototype configuration state functions (CSFs) are generated, including all L^2 CSFs.
(2) Symbolic matrix elements involving prototype CSFs are generated but all symbolic integrals involving only core and/or valence target orbitals are deleted.
(3) The prototype symbolic matrix elements are contracted using phase-corrected (see below) target coefficients; again the structure of Fig. 5 is appropriate.
(4) The prototype symbolic matrix elements are expanded to give the full set of matrix elements which are evaluated and stored. This step requires the consideration of eight separate classes of matrix elements [285].
(5) As a final step the energies of the appropriate target state are added to the non-L^2 diagonal elements of the matrix, which corrects for the deletion of the target integrals in step (2).

In practice steps 3 and 4 are looped over and the Hamiltonian matrix elements are written disk once calculated, as this reduces the memory requirements. It should be noted that the step of replacing the re-evaluation of all the target integrals by adding the previously computed target energies to the appropriate diagonal element significantly reduces the number of symbolic matrix elements that need to be evaluated, by about an order of magnitude. The saving on the time taken to construct Hamiltonian matrices with complicated target CI wave functions is even more significant. It is probably true to say that with this algorithm the codes are capable of handling more sophisticated target wave functions for small molecules than we really know how to use in the scattering calculations.

There is one further technical problem to do with the use of the CI target wave functions that needs to be addressed and that is to with consistency of phases between the N-electron target and $N + 1$ electron scattering wave function. Orel et al. [288] pointed out that without special measures the contraction scheme discussed above can suffer from problems due to differences in the phase of the target wave function which is implicitly calculated in the $N + 1$ electron calculation. Indeed early **R**-matrix calculations neglected this issue [183,256] giving rise to spurious results in some cases [289]; electronic excitation calculation on high symmetry systems are particularly sensitive to this problem. The solution proposed for this problem by Orel et al. [288], and originally adopted in the **R**-matrix codes [226,289], was to perform the target calculation with a dummy extra spin orbital but to set all integrals involving this orbital to zero. One drawback of the dummy orbital method is that it the target wave function to be recomputed for each combination of the target symmetry and the total symmetry.

A subsequent analysis [290] showed that provided the canonical or "dictionary" order [156] of the spin orbitals of the code is used, it is relatively straightforward to derive a phase map which can then be used to correct the problem. Furthermore this analysis suggested that there were some special cases where the dummy orbital method might not actually give the correct answer. This second procedure, dubbed the spin orbital method, has been used in all recent calculations with the UK molecular **R**-matrix codes.

Even with target contraction, the Hamiltonian matrices one wishes to diagonalize for the scattering problem can become very large, see Halmovà et al. [188] for example. Under these circumstances it becomes impossible to obtain all the eigenvalues and eigenvectors of the problem. A number of ways round this problem have been suggested.

One possible solution is to obtain the **R**-matrix as the solution to a linear equation problem rather than by direction diagonalization [50,291]. The problem with this method is that the linear equations have to be solved for each energy which, of course, removes one of the important advantages of the **R**-matrix method.

In the selected state **R**-matrix (SSRM) approach of the Bonn codes [142], the equation used to form the **R**-matrix, Eq. (13), is re-written as

$$R_{ij}(a, E) = \frac{1}{2}\sum_{k=1}^{m} \frac{w_{ik}^{CI}(a) w_{jk}^{CI}(a)}{E_k^{CI} - E} + \frac{1}{2}\sum_{k=m+1}^{n} \frac{w_{ik}^{SE}(a) w_{jk}^{SE}(a)}{E_k^{SE} - E}. \tag{60}$$

In Eq. (60), the first sum runs over the lowest m solutions of the MRD-CI configuration interaction problem; the second sum runs over solutions of the much simpler static exchange problem which are orthogonalized on the solutions of the CI problem. Typically [141,142], it would appear that inclusion of less than $m = 10$ CI roots are sufficient for getting reliable low-energy results for collisions with neutral molecules. Such studies are usually restricted to scattering energies below 10 eV.

Berrington and Ballance [283] proposed an alternative procedure which they called partitioned **R**-matrix theory. In this method, as above, only the lowest m poles are explicitly used to form the **R**-matrix, with the remaining terms allowed for using an error correction procedure. The expression used to construct the **R**-matrix on the boundary within partitioned **R**-matrix theory is:

$$R_{ij}(a,E) = \frac{1}{2}\sum_{k=1}^{m} w_{ik}(a)w_{jk}(a)\left(\frac{1}{E_k - E} - \frac{1}{E_0 - E}\right) + \delta_{ij}\left(\frac{s_i}{E_0 - E} + R_i^C\right). \tag{61}$$

In Berrington and Ballance's implementation, E_0 is the average energy of the poles not included in the first sum which can obtained from the trace of the Hamiltonian matrix; s_i is the amplitude of the excluded channels on the boundary and R_i^C is an error correction term.

Numerical tests by Berrington and Ballance [283] suggested that about one half of all the poles needed to be retained in the final sum to give converged results. Given the characteristics of iterative diagonalizers, this does not actually represent a significant computational saving compared to the standard formulation using all the poles. However, a reworking of the theory in the context of low-energy electron–molecule scattering [284] showed that it was possible to greatly improve on this. In the revised theory E_0 is defined as the average value of the diagonal target-continuum matrix elements whose energy is greater than E_m, i.e. the last pole explicitly included in the first sum. s_i is the total probability distribution of a given channel on the **R**-matrix boundary which is already not explicitly included in first sum and R_i^C is a revised error correction term, see Ref. [284] for details. With this formulation it is possible to reduce the number of poles explicitly required to well below 10% of the total in large calculations [292]. Test calculations suggest that the number of poles needed is more to do with the ability to span an appropriate energy range, typically two to three times the energy of interest, than to capture a particular percentage of the states. In particular addition of significant numbers of extra L^2 configurations, which tend to have diagonal elements at high energy, does not lead to the need to increase the value of m. The largest calculation attempted so far with this method involved diagonalizing a Hamiltonian of dimension 218 064 to obtain the lowest 5000 **R**-matrix poles [166]. This calculation took about a month on a desktop workstation, albeit one running a 64-bit operating system. It is to be anticipated that significantly larger calculations will be performed using this method in the future. In particular, I note that the iterative diagonalizer [293] used for partition **R**-matrix calculations is well suited to be used with massively parallel computers [294].

Given that for large problems the computer time tends to be dominated by diagonalizing the inner region Hamiltonian matrix, it is worth briefly comparing the SSRM and partitioned **R**-matrix method as implemented in the Bonn and UK **R**-matrix codes respectively. The SSRM takes a few, typically about 10, eigenvalues and eigenvectors from a very large Hamiltonian matrix. Initial matrices of dimension many million may be reduced to a few hundred thousand dimensional using selection thresholds [295]. This is a procedure that is well understood from bound state electronic structure calculations and is computationally efficient as the Hamiltonian matrix being diagonalized is extremely sparse. The partitioned **R**-matrix method typically takes more eigenpairs from a somewhat smaller [166] Hamiltonian matrix. Even though the target contraction procedure discussed above leads to this matrix being slightly less sparse, for large problems it is still found to contain more than 95% zero elements. The main computational issue is, however, the use of many coupled channels and extended energy ranges which lead to a significant increase in the number of eigenpairs required. As the time taken for the iterative diagonalization of a matrix is dominated by the time taken to converge the highest eigenvalues required, this means that coupled states, partitioned **R**-matrix calculations are the most demanding.

5.3. The *R*-matrix with pseudo-states method

Gorfinkiel and Tennyson [26,187] developed a molecular RMPS (MRMPS) method using the polyatomic (i.e. GTO) version of the UK molecular **R**-matrix code [227]. Keeping within the spirit, not mention the numerics, of this code we chose to represent the pseudo-states using a series of even-tempered GTOs [296]. In this type of basis set, α, the exponents of the GTOs are constructed as a geometric series as follows:

$$\alpha_i = \alpha_0\beta^{(i-1)} \quad i = 1,\ldots,L, \tag{62}$$

where, by choosing different values of the parameters α_0 and β, different basis sets can be systematically generated. These universal basis functions have a number of useful properties including one concerning completeness [297].

Adding a third, notionally complete, basis set to the problem of course increases difficulties with linear dependence. In the MRMPS procedure, the pseudo-continuum basis is added to the target orbitals and then orthogonalized using the same combination of symmetric and Schmidt orthogonalization that is routinely used for GTO continuum orbitals, see Section 5.2.1. The only change in this procedure is that numerical experiments showed that a relatively high deletion

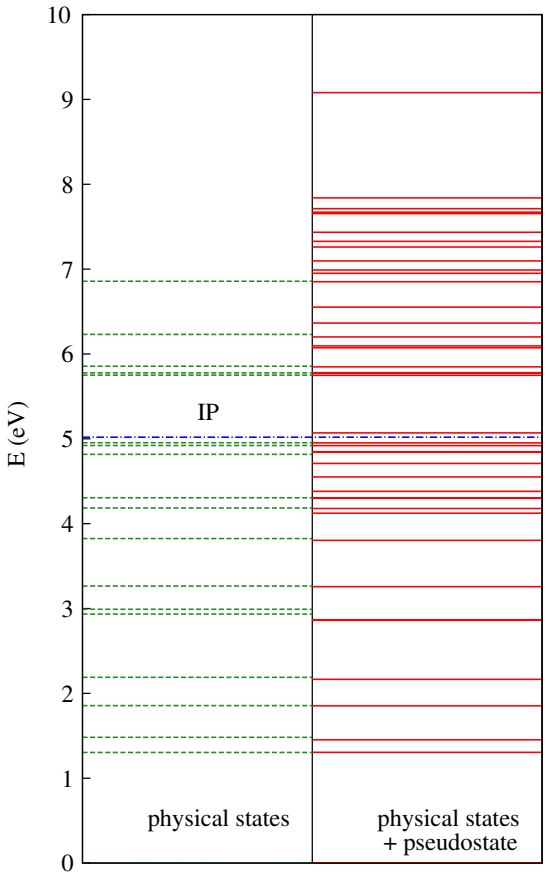

Fig. 6. Distribution of electronic states in Li_2. Left: states given by physical basis of GTOs; Right: states given when the physical basis is augmented by (10s, 10p, 6d, 5f) pseudo-states basis with $\alpha_0 = 0.0463$ and $\beta = 1.3$ [189]. IP denotes the ionization potential of Li_2. M. Tarana, private communication.

threshold, in the range 10^{-4} to 10^{-5}, is necessary to keep the calculation stable [187]. The resulting target MOs plus pseudo-orbitals (Pseu) are used to represent the target. Usually only configurations with one electron in a pseudo-orbital are allowed so target CSFs are give by the following configurations:

$$(\text{core})^m(\text{CAS})^{N-m},$$
$$(\text{core})^m(\text{CAS})^{N-m-1}(\text{Pseu})^1.$$

The states given by this treatment represent both the physical target states of the system and a pseudo-state representation of the continuum. This is illustrated in Fig. 6 for the case of the lithium dimer.

Having built the target states, the continuum orbitals are added to the basis set in the standard manner except that those continuum orbitals with exponents greater than α_0 are deleted from the basis to avoid duplication. The symmetric and Schmidt orthogonalization procedures are repeated and an appropriate number of continuum orbitals are deleted. For many electron molecules, choosing the appropriate configurations to use in the MRMPS scattering calculation can be quite difficult. Building from the target configurations given above, a complete set of L^2 configurations might be:

$$(\text{core})^m(\text{CAS})^{N-m+1},$$
$$(\text{core})^m(\text{CAS})^{N-m}(\text{Pseu})^1,$$
$$(\text{core})^m(\text{CAS})^{N-m-1}(\text{Pseu})^2.$$

However, this can give result in huge numbers of configurations which have proved computationally intractable for even relatively small targets [188]. At present the number of published studies using the MRMPS methods is small and the design of consistent but soluble models for MRMPS calculations remains a matter of trial and error.

Use of the MRMPS procedure leads to a significant increase in the number of channels that have to be considered in the outer region, especially when performing calculations at energies above the ionization threshold of the target. This tilts the balance of the calculation so that the outer region can come to dominate the computer time taken. This situation is familiar in atomic calculations on electron collisions with iron-peak ions such Fe^+ [298] and undoubtedly will in due course require similar coding strategies to ensure that the outer region calculations remain tractable.

Finally it is worth noting that pseudo-state expansions have long been known to provide a methods of calculating atomic polarizabilities [133]. This method has recently been applied to molecules using Eq. (49) and found to give good results for

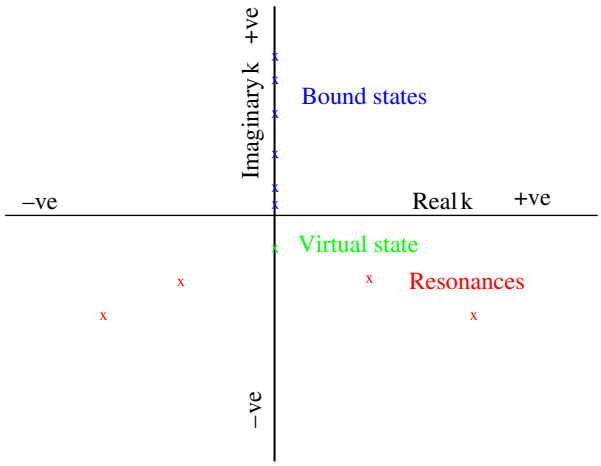

Fig. 7. The **S**-matrix in the complex wavenumber, k, plane: bound states lie on the positive imaginary axis, virtual states are found on the negative imaginary axis and resonance lie in the lower half of the diagram with complex values of k.

the static dipole polarizabilities of the ground and excited electronic states of a number of small molecules [168]. I note that the atomic procedure has also been extended so that pseudo-states can be used to calculate dynamic or frequency-dependent dipole polarizabilities as well as static ones [133]; this has yet to be done for molecular problems.

5.4. Specialised algorithms: Outer region

5.4.1. Continuum states

Having prepared the **R**-matrix on the **R**-matrix boundary $r = a$, a variety of methods are used to find numerical values for the scattering observables. The first step is usually to propagate the **R**-matrix. **R**-matrix propagation generally involves dividing the problem into a number of sectors and then solving the problem within each sector by diagonalizing a matrix problem. There is a direct trade-off between the number of basis functions needed in each sector and the size of the sector. The problem also scales with the number of asymptotic channels explicitly included in the outer region, for which reason it is sometimes useful to drop strongly closed channels from this step in the calculation [125,167].

There are two propagation procedures in general use which are respectively due to Light and Walker (LW) [27] and to Baluja, Burke and Morgan (BBM) [93]; both methods divide the region under consideration into sectors. The LW **R**-matrix propagator is a potential following method. It assumes a constant potential throughout a given sector, usually the value at the central point of the sector. The LW propagator is less efficient if the potential varies rapidly since it requires many sectors, but can be fast and effective for slowly varying potentials of the multipole form given by Eq. (20). The BBM propagator expands the solution vector in each sector in terms of a set of basis functions. It is consequently solution following and most effective near the target where the potential is varying most rapidly. In practical implementations [93,94] shifted Legendre polynomials are used to provide fast and flexible basis functions.

Electron–molecule calculations using the UK molecular **R**-matrix codes [227], the Bonn codes [142], and indeed **Z**-matrix calculations by Huo and Brown [70], all generally used BBM propagator in its original [93] or improved [94] form. Typically R-matrices for molecular problems are propagated to about $a_{\text{out}} = 100\ a_0$, although significantly larger values of a_{out} are sometimes necessary [113]. After propagation the solutions are matched to the asymptotic form of Eqs. (25) and (26) and the **K**-matrix is extracted [99].

I note that over the last decade atomic **R**-matrix calculations have had to address problems with very large numbers of asymptotic channels. These have been tackled using a mixture of improved algorithms [299] and massively parallel computers, for which **R**-matrix propagation is well suited [61,298,300,301]. In particular the algorithmic improvement is based on using a mixture of BBM and LW propagators. The explosive increase in the number of channels given by the application of RMPS methods to molecular problems, see Section 5.3, will undoubtedly lead to these procedures being implemented for electron–molecule problems.

Finally, before leaving the topic of **R**-matrix propagation mention should be made of situations where the **R**-matrix is propagated backwards, i.e. inwards to smaller r. Inwards propagation is useful in situations where further manipulations are performed in the outer region and these manipulations are r-dependent; the ability to propagate R-matrices in either direction allows the optimal choice of r. Thus Thümmel et al. [120] used a frame transformation to include rotational motion in their non-adiabatic treatment of low-energy scattering from the HF molecule. They found that their results were sensitive to the value of r chosen for the frame transformation. They concluded that propagating R-matrices inwards gave stable, converged results which, unlike results obtained using a frame transformation at larger r values, did not diverge. This procedure has been employed to include rotational motion in studies of other systems with low-lying resonances [118,302].

Caron and Sanche [303,304] proposed a theory for electron collisions from large molecules such as DNA [246], or indeed ice [305], based on multiple scattering. Their method breaks the molecule into subunits for which it is possible to obtain **T**-matrices and uses the ideas of multiple scattering to construct a super-**T**-matrix for the entire system. One issue that has to addressed when dealing with this procedure is that of replacing the long-range potential associated with each subunit by the asymptotic potential for the whole super-molecule. The **R**-matrix method lends itself well to this approach since once a subunit **R**-matrix has been constructed it can be propagated, usually backwards, to a distance suitable for including the subunit in the super-molecule [306,307].

5.4.2. Characterizing resonances

Although it is possible to characterize resonances by fitting to cross sections, the presence of many competing direct or non-resonant processes in electron–molecule collisions means that analyzing cross sections is not a good method for obtaining reliable resonance parameters. However, there are quite a few other methods available for obtaining these parameters. These methods can be divided in two classes: those which can be used as part of any electron–molecule scattering procedure, and those which take specific advantage of the structure of the **R**-matrix [308–311]. I will discuss the general methods first, but note that the ability to repeat the collision calculation on a fine energy grid at little extra computational cost, which is a feature of **R**-matrix methods, can be important for characterizing complicated resonance structures. This is particularly true for electron collisions with positively charged ions which have infinite series of resonances.

One formal definition of a resonance is that is constitutes a pole in the **S**-matrix in the complex plane with the real part of the energy representing the resonance energy, E^r and the imaginary part its half-width, $\frac{1}{2}\Gamma$. Fig. 7 illustrates the structure of poles in the **S**-matrix in the complex k-plane, where $E = \frac{1}{2}k^2$. Resonances also manifest themselves as an increase in the value of the eigenphase sum, see Eq. (32), by π. In practice eigenphases are arbitrary modulo π so resonances often actually appear as discontinuities in plots of the eigenphases sums, see Fig. 9 for example.

The standard method for characterizing an isolated resonance is to represent the eigenphase sum in the region of the resonance using the Breit–Wigner form [312]

$$\delta(E) = \delta_0(E) + \sum_{i=1}^{m} \tan^{-1} \frac{\Gamma_i}{2(E_i^r - E)}. \tag{63}$$

This expression was originally derived for single-channel problems but Hazi [313] showed that for multichannel problems it is correct to fit to the eigenphase sum, δ, as a function of collision energy, E. For molecular problems, with the degenerate channels, the background eigenphase, $\delta_0(E)$, can be quite large; it is often parametrized as a low-order polynomial [314,315]. Eq. (63) is written for m resonances; my experience is that direct fits to the Breit–Wigner form are generally not reliable for m greater than one, although several of the other procedures discussed below work well for the many resonance case.

Tennyson and Noble implemented a recursive procedure for detecting and performing Breit–Wigner fits to resonances in program RESON [314] which relies of the ability to quickly generate new energy points. This procedure scans $\delta(E)$ and marks those points where the numerically computed second derivative $\frac{d^2E}{d\delta^2}$ changes signs from positive to negative. A new, usually finer, grid is constructed about each of these points which is then used as the input to a Breit–Wigner fit. In principle the method can fit pairs of nearby resonances but such fits are generally found to be less satisfactory. Because the slope of the eigenphase can be discontinuous upon the opening of a new threshold, the procedure is restricted to scanning energy grids between thresholds.

Although RESON is fast and reliable for many situations, there are some cases where it struggles. These include resonances that straddle a threshold, cases where the background eigenphase is rapidly varying and overlapping or nearby resonance, for which the Breit–Wigner form is not really appropriate. The more recent VisRes package [316] gives a graphical interface for resonance fitting with an **R**-matrix framework. However, as it is only implemented as part of the Graphical **R**-matrix atomic collision environment (GRACE) [317], it does not appear to have been used for molecular problems.

An alternative, but related, approach is to fit resonance parameters directly to the **K**-matrix [318]. This method has been implemented by Barschat and Burke in program RESFIT [315]; it yields not only resonance positions and widths, but also partial widths for cases where there are several channels available for decay.

Smith [319] proposed a completely different procedure based on the classical concept of the time-delay of the scattering electron; resonances can be associated with a long time-delay, as indeed can processes near to a threshold. The time-delay method is another procedure which can give partial resonance widths. The time-delay matrix **Q** is formed from the scattering matrix, **S**, and the time operator, $-\mathrm{i}\hbar\frac{\mathrm{d}}{\mathrm{d}E}$, as:

$$\mathbf{Q} = -\mathrm{i}\hbar\mathbf{S}^* \frac{\mathrm{d}\mathbf{S}}{\mathrm{d}E}. \tag{64}$$

Smith [319] showed that the largest eigenvalue of the **Q**-matrix, q, represents the longest time-delay of the incident particle. He further showed that the probability of decay into a particular channel, the branching ratio β_i, is given by the square of the corresponding component of the eigenvector associated with q. Close to resonance, the time-delay has a Lorentzian form given by:

$$q(E) = \frac{\Gamma}{((E - E^r)^2 + (\Gamma/2)^2)}. \tag{65}$$

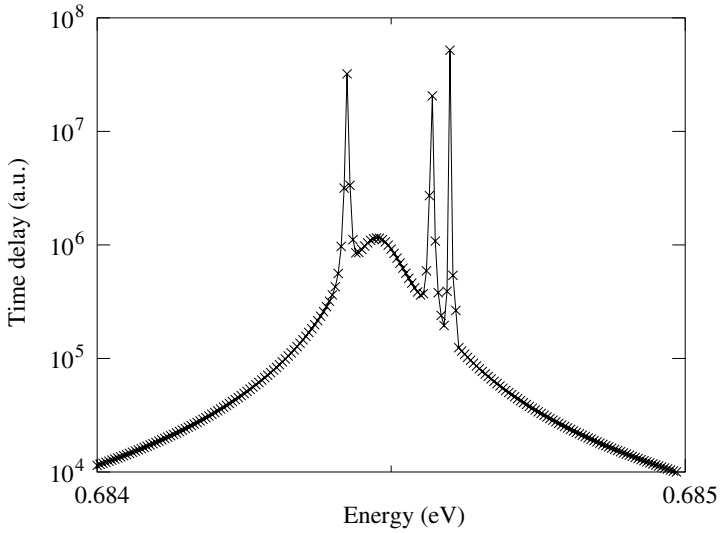

Fig. 8. Multiple resonances resolved using the time-delay method for super-excited states of the NO molecule with effective quantum numbers in the region of $n = 6$. The calculated time delays are denoted by crosses and the curves give the results of independent fits for each resonance. Note that in the time-delay method only the features with the longest time-delay are routinely analyzed. The broader resonance is largely d-wave ($l = 2$) in character with the narrower ones being mainly f ($l = 3$), g ($l = 4$) and h ($l = 5$) wave. I. Rabadán and D.T. Stibbe, private communication.

The time-delay method has several advantages over the more standard Breit–Wigner treatment [320]. The use of only one eigenvalue projects out the channel containing the resonance and therefore removes many of the problems associated with large backgrounds found in molecular problems. The method can cope with multiple resonances, which display themselves as several overlapping Lorentzians, as illustrated in Fig. 8, and can be used to fit resonance across a threshold once allowance has been for the spike in the time-delay caused by the threshold. Stibbe and Tennyson implemented a recursive time-delaying fitting procedure, TIMEDEL [321]. However, TIMEDEL is probably less useful than RESON as a black box program since special cases such as overlapping resonances or resonances straddling a threshold still require hand intervention to obtain a good fit.

One strategy for characterizing resonances is to directly inspect the **S**-matrix at complex energies. The **R**-matrix method lends itself to this readily since one can re-write the definition of the **R**-matrix of Eq. (13), $R_{ij}(a, E)$, taking E to represent a complex energy. Noble et al. [309] developed a procedure based the analytic continuation of **R**-matrix theory into the complex energy plane. Their complex energy **R**-matrix procedure is potentially rather powerful: it deals elegantly with overlapping resonances and can, uniquely, predict the number of resonances within a specified region of the complex energy plane. The method has been applied successfully to a number of one-off calculations [115,116,309,322], including ones to analyze the trajectory of **S**-matrix poles as function of molecular geometry [184,323]. Perhaps because it has never been implemented in one of the standard **R**-matrix packages, the method does not appear to be in routine use. However, this method was used by Morgan to identify [323] and study the behaviour of [324] the virtual state in CO_2. In particular, its behaviour as a function of geometry was successfully characterized using a procedure [115] similar to that of Noble et al. [309].

An even more **R**-matrix specific resonance fitting method is the QB method of Quigley and Berrington [310]. This method exploits the analytic properties of the **R**-matrix in the vicinity of a resonance and is particularly designed for collisions with charged systems. The QB method can be used to study resonances in molecular problems but as implemented [325] it makes a number of approximations concerning the outer region potential which are more appropriate for atomic ions than molecular ones. Ballance et al. [326] actually give an inter-comparison of results obtained using RESON [314], TIMEDEL [321] and the QB method [325] for super-excited states of molecular oxygen, while Ballance et al. [322] also compare with the complex energy **R**-matrix method. In subsequent work Ballance et al. [327] developed an adaptation of the QB method particularly for treating interloping molecular resonances. These workers also used the method study resonances associated with inner shell excitations [259]. The net conclusion of these studies is that in favourable circumstances all the procedures give very similar resonance parameters and the more important issues are one of robustness and numerical stability of each procedure.

Some analysis of resonances can performed within an **R**-matrix method without considering the outer region at all. In many cases a resonance position corresponds closely to an **R**-matrix pole. In this case it is possible to track the geometry dependence of the resonance using the results of the inner region calculation. Furthermore, if the wave function associated with pole is dominated by a single configuration, then it is straightforward to identify the configuration of the resonance. These ideas are important for the procedures designed to look at non-local effects which are discussed below.

However, it should be noted that by no means all **R**-matrix poles correspond to resonances. The easy availability of black box quantum chemistry codes which are designed to give accurate energies for electronic bound state makes it tempting to use these codes to study resonances. The codes readily yield eigenenergies in the electronic continuum, but the identification

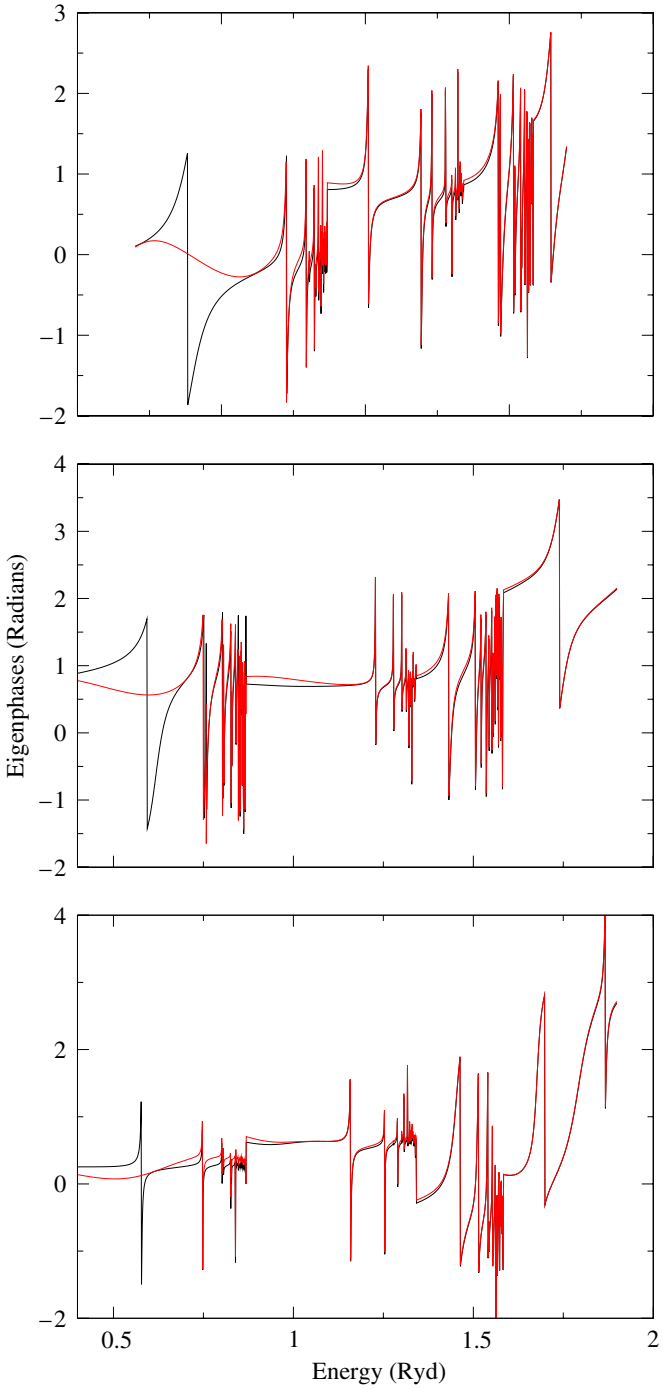

Fig. 9. Eigenphases sums for electron–H_2^+ collisions, for an H_2^+ bond length of 2.0 a_0, as a function of energy for $^1\Sigma_g^+$ symmetry (upper), $^1\Sigma_u^+$ symmetry (middle) and $^3\Pi_g$ symmetry (lower). Full curves are the complete eigenphase sum and the dashed curves are the "background" eigenphase sums obtained when the configuration associated with the lowest resonance of each is symmetry is removed from the calculation. Note that the resonances actually appear as apparent discontinuities in the eigenphases. N. Doss, private communication.

of these energies of resonances is fraught with problems [328]. In particular, a CI calculation will give a spectrum of energies in the continuum simply because the number of eigenenergies available must equal the size of the CI Hamiltonian matrix. As the underlying basis set used is expanded, the vast majority of these states, which can be described as target molecule plus free electron states, will simply drop in energy. Such states are generally of little physical significance and should be interpreted with extreme caution or, preferably, by making appropriate adaptations to the methodology [329].

So far the discussion of resonance has been entirely within the context of the fixed-nuclei approximation However, in resonant, vibrationally inelastic processes such as vibrational excitation, dissociative electron attachment (or dissociative recombination for positive ions), the electronic motion is strongly coupled with the nuclear motion. Under these circumstance the Born–Oppenheimer approximation is not valid and more general procedures are required. To describe resonant nuclear dynamics correctly, it is necessary to take non-local couplings into account. The non-local treatment of

the nuclear dynamics in electron–molecule collisions [330] yields a full description. In the simpler local complex potential approach, the coupling is characterized by the position and width of the electronic resonance as discussed above, which can then be calculated for a set of nuclear geometries. The fuller, non-local treatment requires the Feshbach–Fano separation of the fixed-nuclei scattering problem into a one-dimensional discrete state and a background, which usually achieved using the projection operator formalism [100]. The discrete state component and its coupling to the background continuum calculated as a function of nuclear geometries are then used to construct the non-local complex potential for the nuclear dynamics calculation. This separation can be characterized by the generalized energy-dependent resonance width which can be defined as:

$$\Gamma(E) = 2\pi \sum_q \left| \langle \Psi_q^{\rm bg}(E)|H|\phi_{\rm res}\rangle \right|^2 \tag{66}$$

where $\phi_{\rm res}$ is the wave function of the resonance and $\Psi_q^{\rm bg}(E)$ is the background wave function. Within an **R**-matrix procedure, $\phi_{\rm res}$ is usually taken to be represented by a single CSF in the inner region, meaning that $\Psi_q^{\rm bg}(E)$ is the wave function of the problem obtained by removing the CSF associated with $\phi_{\rm res}$. Fig. 9 illustrates the effect of this partitioning which has been used successfully as to treat complex collision problems [331,332].

Nestmann [311] combined the properties of the **R**-matrix method with the Feshbach–Fano projection operator approach to develop a method of calculating $\Gamma(E)$ which he subsequently used to study the dissociative attachment of ozone [333,334]. This method can be used to study the energy-dependent properties of resonances directly without the need to perform a full outer calculation [157,335,336]. Conversely, the evaluation of Eq. (66) directly is fairly straightforward in a standard **R**-matrix approach since the inner region Hamiltonian matrix elements between the resonance CSF and all other CSFs are routinely calculated. The only technical problem is therefore determining the energy-dependent background wave function, an issue which discussed in the next section.

For many studies it is desirable to calculate resonance parameters as a function of nuclear geometry. For diatomic systems the calculation of resonance curves has been routine for sometime [125,211,337,338] and more recent studies have begun characterizing multidimensional resonance surfaces [339].

Finally it is important to understand the conventions used for the energies in the denominator in Eq. (13), particularly when studying properties as a function of target geometry. For this purpose let us denote a general target geometry by $\mathbf{Q}$, with the equilibrium geometry of the target given by $\mathbf{Q}_e$. The ground state target energy at each geometry can be denoted $E_0^N(\mathbf{Q})$. By definition the asymptotic kinetic energy of the incoming scattering electron, E, is a zero when the electron is stationary and the target is in its ground state for the given geometry under consideration. Within this convention the energy of the **R**-matrix poles, E_k, at geometry $\mathbf{Q}$ are written relative to $E_0^N(\mathbf{Q})$ so that negative values of E_k represent **R**-matrix states which are bound relative to the target and positive values of E_k represent scattering states. When considering the variation with target geometry of resonance positions, $E^r(\mathbf{Q})$, in particular, and the scattering energy in general, it is important to allow for the change in the target energy as a function of geometry. For resonances this is done be defining the potential energy curve or surface of a resonance, $V^r(\mathbf{Q})$ as:

$$V^r(\mathbf{Q}) = E^r(\mathbf{Q}) + E_0^N(\mathbf{Q}) - E_0^N(\mathbf{Q}_e). \tag{67}$$

This transformation places everything on a common energy scale, which has its zero at the energy of the target at equilibrium, $E_0^N(\mathbf{Q}_e)$. Similar considerations are necessary when considering other energies as a function of target geometry [340].

5.4.3. Generating wave functions

The procedures described above do not actually yield continuum state wave functions; indeed avoiding calculating outer region wave functions is often regarded as a virtue of **R**-matrix methods. However, there are occasions when wave function are required. In this case it is necessary to integrate the wave functions inwards from r_f to the **R**-matrix boundary at $r = a$. This is usually done using Runge–Kutta–Nystrom integration [341].

In the inner region the continuum wave function for scattering energy E is given by

$$\Psi^{N+1}(E) = \sum_k A_k(E)\psi_k^{N+1} \tag{68}$$

where ψ_k^{N+1} is an energy-independent solution of the inner region problem, see Eq. (14). The problem of determining this wave function thus reduces to solving for $A_k(E)$ which can be expressed in terms of the radial functions evaluated on the boundary plus other boundary information as:

$$A_k(E) = \frac{1}{2a(E_k - E)} \sum_i w_{ik}(a) \left(a\frac{{\rm d}F_i}{{\rm d}r} - bF_i \right)\Bigg|_{r=a} \tag{69}$$

or alternatively as

$$A_k(E) = \frac{1}{2a(E_k - E)} \sum_{ij} w_{jk}(\mathbf{R}^{-1})_{ji}F_i(a). \tag{70}$$

These two expressions for $A_k(E)$ are formally equivalent but not necessarily numerically so since Eq. (69) becomes ill-determined whenever $E = E_k$. This indeterminacy is removed in Eq. (70) by the inverse **R**-matrix, which depends on $(E_k - E)$, but this expression also becomes ill-determined because of the behaviour of the inverse **R**-matrix as a function of energy. In practice it is possible to use a regularization procedure [81,342] for the kth pole whenever $E \approx E_k$ to ensure numerical stability.

5.4.4. Bound states

The ability to calculate bound states using the scattering wave functions is important for a variety of problems including the need to follow resonance curves to regions where they become bound [125], to characterize very weakly bound states [343] and the demands of photoionization [130,344], as well as other problems linking bound and continuum states [128,280,345,346]. Bound state finding, unlike other outer region problems, involves a search over energies.

In the inner region, the wave function of a bound state m can be written in terms of the solutions of the inner region problem as:

$$\Psi_m^{N+1} = \sum_k A_k(E_m)\psi_k^{N+1} \tag{71}$$

where E_m defines the energy of the given bound state and the coefficients $A_k(E_m)$ have to be determined by solving the outer region problem for $E < 0$.

In the outer region, bound state radial functions are required which tend to zero as r tends to infinity and which can be matched to the inner region functions at the **R**-matrix boundary. As in the continuum case, these are first obtained using a Gailitis expansion [99] at an appropriate radius. For reasons to do with numerical stability, this radius is usually taken to be smaller than for continuum problems; values about $r_f = 30\ a_0$ have been found to give reliable results. The functions, $P_{ij}(r)$, obtained at this radius are then integrated inwards by solving the asymptotic equations numerically, using the Runge–Kutta–Nystrom method [341]. This explicit calculation of the outer region wave function was not advocated for atomic problems in the method of Seaton [56] described below, but is necessary for molecules given the importance of their outer region potentials [345].

By imposing suitable boundary conditions Seaton [56] showed that at the **R**-matrix boundary:

$$\sum_j \left[P_{ij} - \left(\sum_k R_{ik}(E) Q_{kj} \right) \right] X_j = \sum_j B_{ij} X_j = 0 \tag{72}$$

where

$$Q_{kj} = \frac{\mathrm{d}P_{kj}}{\mathrm{d}r} - bP_{kj}, \tag{73}$$

and where b is the arbitrary constant introduced in the Bloch term of Eq. (5) and generally taken as zero. In the above all matrices are evaluated at the **R**-matrix boundary ($r = a$). **X** is a column vector needed to find the bound state coefficients $A_k(E)$ which are given by:

$$A_k(E) = \sum_i \frac{w_{ik}}{(E_k - E)} \sum_j \left(\frac{\mathrm{d}P_{ij}}{\mathrm{d}r} - bP_{ij} \right) X_j, \tag{74}$$

and w_{ik} and E_k are respectively the boundary amplitudes and **R**-matrix pole positions used to construct the **R**-matrix on the boundary, see Eq. (13).

Eq. (72) is only satisfied for certain discrete values of the energy, the bound state energies, which can be found by searching for zeros of the determinant of $\mathbf{B}(E)$. However, the **R**-matrix, Eq. (13) and hence the matrix $\mathbf{B}(E)$ of Eq. (72), is not clearly defined at energies close to the **R**-matrix poles. Burke and Seaton [81] analyzed this problem and reformulated it so that the contribution due to the **R**-matrix pole nearest in energy to E is treated separately in a fashion that is numerically stable.

The remaining issue is how to construct a suitable grid to search for bound states. For anionic systems this is fairly straightforward as strongly bound states lie close to, generally slightly above, individual **R**-matrix poles and the number of bound states is finite and usually small. The situation is less straightforward for electron collisions from molecular cations, which support an infinite series of bound states for each partial wave included in the continuum basis set. For this problem grids based on the use of effective quantum have been implemented [124,347].

The use of scattering calculations can actually be very effective for characterizing bound states of Rydberg systems. An illustration of this is the calculated transition frequencies in the HeH molecule, see Table 3, for which all states can be considered as Rydberg states of the closed shell HeH^+ molecular ion. As can be seen the **R**-matrix calculations give results closer to the observations than calculations with more standard quantum chemical procedures [348,349] which can struggle to find appropriate basis sets to represent very diffuse states.

As a final comment on bound states, it should be noted that it is possible to use the standard **R**-matrix inner region wave function of Eq. (14) to perform bound state quantum chemistry calculations. To do this it is only necessary to omit the subtraction of the outer region integrals from a standard inner region **R**-matrix calculation. Such calculations can be useful to provide checks and benchmarks.

Table 3
Electronically bound states of neutral HeH at the equilibrium geometry of the ion, $R_e = 1.455\ a_0$ calculated using the **R**-matrix method by Sarpal et al. [347]. Given are quantum defects, μ, and vertical excitation energy, T_e, relative to the ground state of the ion, $-2.951208\ E_h$. The last column gives the ionization potentials deduced from experimental data by Ketterle [350]. A fuller list, containing predicted energy levels, can be found in Sarpal et al. [347].

Assignment	Energy[a] (E_h)	μ	T_e (cm^{-1})	T_e (exp.) (cm^{-1})
1s X $^2\Sigma$	−3.232158	−0.334		
2s A $^2\Sigma$	−3.094013	0.129	31 339	31 695
2p B $^2\Pi$	−3.080895	0.036	28 460	28 888
2p C $^2\Sigma$	−3.035538	−0.435	18 506	18 837
3s D $^2\Sigma$	−3.011379	0.117	13 205	13 307
3p E $^2\Pi$	−3.008489	0.046	12 570	12 647
3d F $^2\Sigma$	−3.007627	0.023	12 381	12 430
3d G $^2\Pi$	−3.007228	0.012	12 294	12 355
3d H $^2\Delta$	−3.006284	−0.013	12 086	12 136
4p $^2\Pi$	−2.983156	0.044	7 011	7 058
4d $^2\Pi$	−2.982665	0.013	6 903	6 931
4d $^2\Delta$	−2.982263	−0.013	6 815	6 850

[a] Note $1\ E_h = 2.194746 \times 10^5$ cm^{-1}.

5.5. Scattering from polar molecules

Whereas the long-range Coulomb potential given by a charged target is relatively easily dealt with by matching to asymptotic Coulomb functions, scattering from a target molecule with a permanent dipole moment requires special treatment. This is because the dipole potential leads to strong coupling between channels which differ by one in l and the long-range nature of the dipole potential means that the partial wave expansion, Eq. (15), requires many more terms as it is necessary to extend the continuum basis to high l. It should be noted that it is possible to match asymptotically to dipole functions specifically adapted to the dipole moment of the potential under consideration [351]. These functions are obtained by solving a Schrödinger equation which includes the dipole interaction term which therefore introduces couplings between channels with l and $l \pm 1$. The resulting functions have to be represented by a numerically determined linear combination of spherical harmonics. Asymptotic dipole functions have been used in specialist applications involving the behaviour or near-threshold resonances [120], but appears not to have been employed as part of any general procedure for study scattering by polar molecules.

However, extending the partial wave expansion alone is still not sufficient to obtain correct cross sections for strongly polar molecules, since performing calculations which neglect the rotational motions of the target molecules leads to an overestimate of the cross section. This is because the effect of rotational motion is to wash out the asymptotic potential due to the permanent dipole; neglect of this motion leads to unphysical cross sections which diverge at low energy. In practice instead of explicitly including large numbers partial waves in the expansion, procedures have been developed based on the use of a frame transformation [200] and the adiabatic nuclear rotation (ANR) approximation to account for the rotational motion, and the dipole Born approximation to account for the contribution from high partial waves [85,200,352,353].

The standard procedure for implementing this correction [354] is to perform a detailed, **R**-matrix or similar, calculations for the lowest few symmetries, add this to the dipole Born approximation results for the problem and then subtract the partial dipole Born results for the symmetries included in the original calculations. This manipulation can be performed with the cross sections, the scattering amplitude or **T**-matrices and has been implemented in a number of published programs [209,355]. Studies have shown that this procedure is not necessary for rotational transitions with $\Delta J \geq 2$ as these are entirely determined by short-range interactions and can be satisfactorily converged by the original scattering calculations [356,357].

A series of **R**-matrix calculations have been performed on scattering from polar systems. These studies are largely aimed at astrophysical environments, such as photon dominated regions (PDRs), which are sufficiently diffuse for each collision to result in emission. Since the collision cross sections for molecular ions are particularly large, initial studies focused on ionic systems [356,358]. These calculation played an important part in the first measurement of electron density in a (shocked) region of the interstellar medium [359]. The **R**-matrix studies showed that the use of a Born top-up procedure is essential for $\Delta J = 1$ transitions, but unnecessary for transitions with $\Delta J > 1$ which are found to be totally driven by short-range, low partial wave effects. However these $\Delta J > 1$ transitions, which were routinely neglected in earlier studies based entirely on the dipole Coulomb–Born approximation [360], are indeed found to be important in some key systems [358,361,362].

One aspect of the ANR approximation is that it assumes all channels are degenerate. This is clearly not a good approximation at collision energies close to the excitation threshold and can result in the unphysical excitation of closed rotational channels. One approach is to correct for this using simple kinematic scaling [204]; however a recent study showed that simply cutting the rates at the appropriate threshold gives surprisingly good agreement when compared with a full, energy-resolved treatment [202]. This is now the recommended procedure.

In the absence of any measured cross sections, all astronomical studies have thus far had to rely on calculated cross sections for modelling the effect of rotational impact excitation. However recently Shafir et al. [84] measured the rate of rotational cooling of the HD^+ molecular by low-energy electrons in a storage ring. HD^+ has a permanent dipole moment

due to the separation between the center-of-mass and center-of-charge, and calculations found appreciable rotational (de-)excitation rates for transitions with both $\Delta J = 1$ and $\Delta J = 2$. Use of these calculations to model the measurements gave very good agreement [84]; this is the closest that there has been thus far has come to an experimental verification of this procedure. I note that similar studies involving vibrational de-excitation of H_2^+ did not find good agreement between theory [363,364] and experiment [365]; it would appear that the neglect of rotational motion in the theoretical treatments is the cause of this discrepancy [366].

Similar treatments of rotational effects in polar neutral molecules have been performed [357,367,368] and have been found to give excellent agreement with experiment [86,369]. Indeed these theoretical results were adopted in a recent compilation of cross sections for the water molecule [370].

5.6. Orientation effects

So far all discussion has considered only isotropic distributions of molecules and electron spins. However orientation of the molecular target or the electron spin can introduce new effects into the collision problem which require more detailed treatments to elucidate. Although it is possible to study such effects using a number of different methods, the **R**-matrix method presents some advantages since it is usually possible to compute the effects of orientation by manipulating quantities in the outer region portion of the code only.

Experimentally it generally requires special techniques to orient molecules. However experiments on electron collisions with the chiral molecule camphor reported cross sections that depended on the spin polarization of the beam of scattering electrons [371], an effect known electron circular dichroism. Even though subsequent experiments on camphor failed to reproduce this effect [372,373], the initial observations acted as a catalyst for considerable theoretical work in this area. This work has been comprehensively review by Blum and Thompson [374]. Related studies have considered collisions of polarized electron beams from molecules with unpaired electrons such as oxygen. **R**-matrix studies on this problem [375,376] have shown that electron spin polarization effects could be observable and that they are most pronounced in the vicinity of a resonance. Similar studies have considered molecules with a fixed orientation of the molecular axis [377].

Recently experimental focus has turned to the dynamics of molecules in ultrafast, high intensity lasers. In these experiments an electron which is ionized near the start of a laser pulse can undergo a re-collision with its parent molecule producing a variety of interesting effects [378]. Given that the strong laser field usually also orients the molecule under investigation, these re-collision events can be considered to be electron collisions with an oriented molecular ion. Furthermore, the dipole selection rules associated with the multiphoton ionization which precedes the re-collision leads to strict symmetry requirements on the re-collision event [379]. A formulation for considering this problem, which is shown to lead to pronounced orientation effects, has recently been presented [380], although issues remain about the best method of treating the Coulomb phase in this problem [381,382]. Furthermore it should be noted that as yet no photon dynamics have been included in any molecular **R**-matrix studies so any conclusions must therefore be regarded as preliminary.

5.7. Adaptation for positron physics

Positrons, the antiparticles of electrons, provide an important alternative probe of molecular structure and dynamics [383]. Low-energy positron–molecule collisions can not only drive the processes listed for electron in the introduction but also provide two further processes. These are:

Annihilation
$AB + e^+ \rightarrow AB^+ + 2\gamma$ or 3γ
where γ represents a γ ray or high-energy photon.

Positronium formation
$AB + e^+ \rightarrow AB^+ + Ps$

where positronium, Ps, is the quasi-atom formed between an electron and positron. The threshold for Ps formation is 6.8 eV below the ionization threshold of the target molecule. Conversely positrons cannot cause spin changing electronic excitations.

It is seemingly straightforward to adapt an electron–molecule scattering code to the requirements of positron scattering [90,185]; doing this involves dropping the anti-symmetrization requirement that leads to exchange integrals and changing the sign on all the Coulomb interactions involving positrons. Within this framework the inner region **R**-matrix wave function can written:

$$\psi_k^{N+1} = \sum_{ij} a_{ijk} \Phi_i^N(\mathbf{x}_1 \ldots \mathbf{x}_N) \tilde{u}_{ij}(\mathbf{x}_{N+1}) + \sum_i b_{ik} \chi_i^N(\mathbf{x}_1 \ldots \mathbf{x}_N) \tilde{\chi}_i^1(\mathbf{x}_{N+1}), \tag{75}$$

where the $\tilde{}$ is used to denote an orbital occupied by a positron. It is necessary to introduce a spin coupling constraint on the electron part of the L^2 term, denoted χ_i^N, to prevent contamination of the wave function with spin changing transitions. Although tests have been performed using distinct electron and positron orbital sets [185], most **R**-matrix calculations

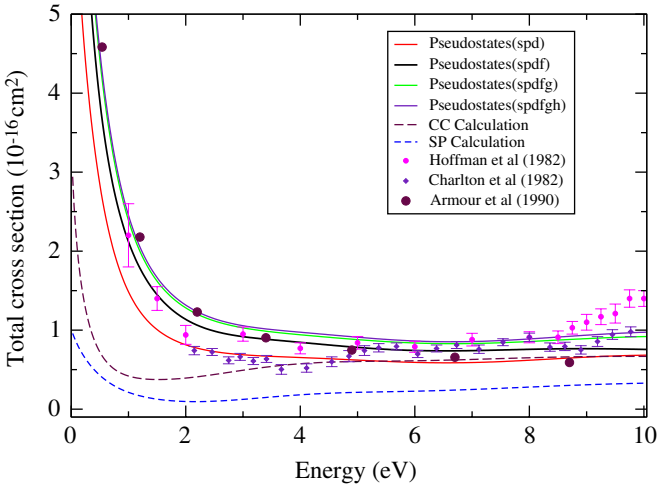

Fig. 10. Total cross sections for positron–H_2 collisions as a function of energy. Points with error bars are the measurements of Hoffman et al. [390] and Charlton et al. [391]; points without error bars are the calculations of Armour et al. [386]. The curves are **R**-matrix calculations due to Zhang et al. [190], see text for details. R. Zhang, private communication.

performed on positron scattering have used an orbital set common to both the electrons and the positron; they therefore follow the procedures used for electrons fairly closely.

The model described above has been used successfully to detect a positron bound state of the HF molecule [343] and to address issues with experimental acceptance angles for positron–polar molecule collisions [86,384]. However for most molecules completely *ab initio* procedures, including the **R**-matrix method, struggle to get reliable cross sections at low energy [385]. The reasons for this are well understood: whereas what is usually termed electron–electron correlation is really anti-correlation, the positrons are attracted to the electrons in the target and the motions of the particles should be strongly correlated. This behaviour is much more difficult to represent starting from one particle functions.

The high class solution to the positron–electron correlation problem is the explicit inclusion of the positron–electron coordinate in the trial wave function. Such methods have been used for positron scattering on both atoms and molecules with excellent results [386]; however they have only been used for systems with very few electrons. Although tremendous advances have been made in the use of explicitly correlations functions in molecular electronic structures calculations [387,388], there is as yet no implementation of such a method for positron collisions with either general atoms or molecules. Instead calculations have often relied on a modest, empirically motivated, adjustment to or tuning of their procedures to deliver reliable low-energy scattering results [389].

Recently Zhang and co-workers [190] have applied the molecular **R**-matrix with pseudo-state method (RMPS) to the problem of low-energy positron collisions. Their calculations are compared with other results in Fig. 10. At low energy the Kohn variational calculations of Armour et al. [386], which explicitly include the positron–electron distance, give excellent agreement with experiment, but are too low at higher energies since these calculations only considered contributions from the lowest total symmetry. Fig. 10 demonstrates how both the static plus polarization (SP) and close-coupling (CC) models seriously underestimate the cross section, particularly at low energies. This is because these models struggle to fully represent electron–positron correlation effects which are most important for slow positrons. Conversely the RPMS calculations show that, provided pseudo-states with high enough angular momentum are included in the basis set, excellent results can be obtained. In these calculations the pseudo-states are acting to put the positron–electron correlation into the wave functions. The need for states with high l can be understood by the well-known slow angular convergence of correlated motions with one particle basis sets [392]. It should be noted that the positronium formation channel becomes open at about 7.2 eV; above this the experimental cross sections, which measure this process, rise above the calculated ones, which neglect it.

6. Examples

The discussion below gives a very few illustrative results from electron–molecule collision calculations using the **R**-matrix method. There have been far too many such calculations to make a comprehensive compilation useful. The systems chosen below are designed to illustrate some of the strengths and weaknesses of the method and the discussion thus also make no attempt to present systematic reviews of calculations by other methods, or indeed measurements, for the same problem.

6.1. Water

Water is, of course, ubiquitous in the gas phase and an important component of bio-organisms. Electron collisions with water there have immense significance for a large variety of applications. The electron–water collision problem has also

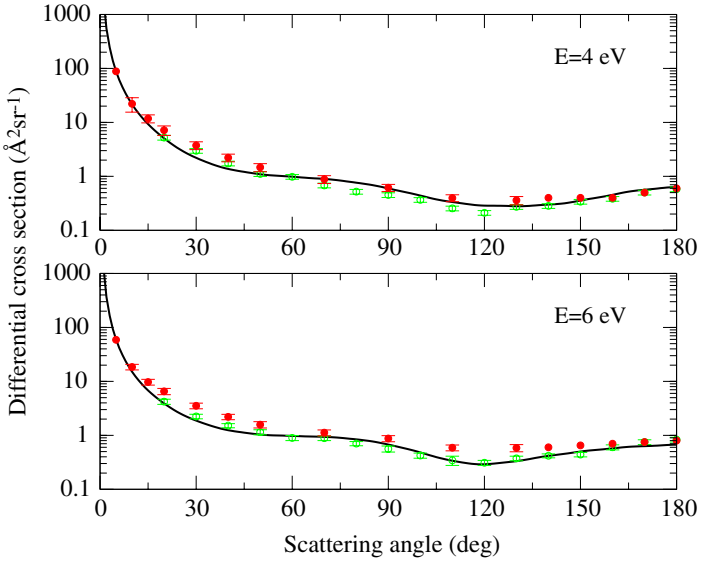

Fig. 11. Differential cross sections for electron collisions with water: solid curve, Born-corrected **R**-matrix calculation [86]; open circles, measurements of Cho et al. [393]; closed circles, measurements of Khakoo et al. [394].

become a benchmarks for the study of elastic, and rotationally inelastic, collisions with dipolar systems, and for detailed study of resonance driven processes such as dissociative attachment in more than one degree of freedom.

As discussed in Section 5.5, electron collisions with polar molecules require special methods because of the long-range nature of the dipole potential due to the target. Zhang et al. [86] recently discussed this problem with particular reference to water. They showed that for the differential cross section (DCS) there is good agreement between **R**-matrix calculations [369] and the most recent measurements [393,394]. Fig. 11 illustrates this for collisions at 4 and 6 eV.

The very strong forward peaking of the DCS means that the elastic cross sections are dominated by low angle collisions. The **R**-matrix calculations give good agreement with the measurements of Khakoo et al. [394] for the total cross section but suggest that Cho et al. [393] systematically underestimate the contributions from low angles. In practice, Khakoo et al. used the calculated Born cross section to estimate the contribution from low angles; this means that the good agreement between theory and "experiment" is not altogether surprising.

Electron collisional excitation of water is an important process not least for astrophysics where, for example, it is thought to be one of the possible processes driving water masers. The only experimental attempt to measure electron impact rotational excitation cross section assumed that it was only necessary to consider transitions with $\Delta J = 1$ [395]. Faure et al. [369] got excellent agreement with the total measured DCS in that and other studies, but showed that collisions with $\Delta J = 2$ also needed to be considered. The only reliable rotational excitation rates are therefore theoretical [367].

Electron collisions with water show a number of narrow resonances associated with the low-lying electronic states of the system. These Feshbach resonances have been subject to a series of studies using the **R**-matrix [150,276,396,397] and Kohn variational [339,398,399] methods. The most comprehensive of these have been the Kohn calculations which have formed the basis of extensive nuclear motion calculations using wavepackets [400,401]. I will restrict myself to one comment here on the electronic structure aspects of the calculations.

The Feshbach resonances in water can all be associated with excited target "parent" states [150]. The close-coupling procedure used in the **R**-matrix calculations automatically includes these target states in these calculations and the resonances are found to track their parent state from below. This means that, given a good analytic representation of the parent state potential energy surface, it is possible to represent the position of the resonance in a simple fashion as the binding energy relative to this surface. For some cases simply using a constant binding energy already gives a very good approximation to E^r as a function of geometry [402]. The Kohn calculations used independent representations of the target and resonance surfaces for which it is harder to get a balanced treatment and which, contrary to the close-coupling studies, can lead to the resonance crossing the parent state curve [339].

6.2. H_3^+: Collisions with an ion

The H_3^+ molecular ion is the dominant molecular ion in cold hydrogen plasmas; it is therefore an important species in environments from the edge of fusion plasmas to the interstellar medium [403]. Collisions between H_3^+ and electrons have been much studied because of the importance of dissociative recombination in this system [5,102]. However, the absence of low-lying curve resonances in the system means that, like dissociative recombination of the isoelectronic molecular ion HeH^+ [103], detailed consideration of non-adiabatic effects are necessary to model this process [104].

Like any ion, there are many resonance states in electron–H_3^+ collisions. These have been the subject of a number of studies which are summarized in Table 4. This table shows that the **R**-matrix and Kohn calculations based on the same

Table 4
Symmetry, resonance position (E^r in eV) and resonance width (Γ in eV) of the low-lying resonance of H_3^+ at its equilibrium geometry. Column A: 6-state **R**-matrix calculations [23]; Column B: 6-state Kohn variational calculation [404] (position of third resonance taken from figure 2) ; Column C: 64-state Molecular **R**-matrix with pseudo-states (MRMPS) calculation [187].

Symmetry	A		B		C	
	E^r	Γ	E^r	Γ	E^r	Γ
$^2E'$	9.12	0.64	9.1	0.64	8.74	0.58
$^2A_1'$	10.14	0.19	10.3	0.18	9.57	0.19
$^2A_2'$	11.11	0.0086	≈11.2		10.79	0.00065
$^2E''$					10.83	0.097
$^2E'$					10.95	0.10
$^2E'$					12.73	0.080
$^2A_1'$	12.85	0.026			12.72	0.050
$^2E'$					12.99	0.012
$^2E''$					13.04	0.027

6-state close-coupling expansion [23,404] give very similar results. Indeed the most significant difference is the ability of the **R**-matrix method resolve large numbers of resonances. However the inclusion of pseudo-states in the close-coupling expansion leads to a significant lowering of the resonances [187]. While some of this lowering is due to the somewhat lower target excitation threshold with which these Feshbach resonances are associated, there is a major contribution due to the improved treatment of polarization in the RMPS calculation. A close-coupling expansion based on the 6 physical states used in these studies yields 91% of the parallel polarizability but only 3% of the perpendicular polarizability; in contract the RMPS study gives more that 98% of both of these [26]. The result in terms of quantum defects is a systematic lowering of the real part of the quantum defect of each resonance by about 0.05; such a lowering is consistent with comparisons made with resonances in other ionic targets [212].

The headline aim of the RMPS calculations for H_3^+ was to study electron impact ionization [26,187]. Although molecular RMPS studies have given excellent results for this process with other systems [105,187], there were until recently no measurements for H_3^+. However Lecointre et al. [405] have recently reported electron impact dissociation of D_3^+ ions leading to the formation of D^+ and D_2^+ products i.e. simultaneous dissociation and ionization. This study does not agree particularly well with the RMPS calculations; however experimentally the D_3^+ is prepared hot and it would seem that the comparison between theory and experiment is not really like-for-like.

Electron impact rotational excitation (and de-excitation) of H_3^+ is likely to be a significant process in interstellar space not least because non-thermal distributions of H_3^+ are beginning to be observed [406]. Study of rotational excitation of H_3^+ and other symmetric top molecular ions, necessitated extending [407] the standard the mixed **R**-matrix — Coulomb–Born treatment which has been used extensively for linear molecules. As for most linear systems [362], it was found that short-range interactions, ignored in the standard Coulomb–Born theory, are crucial for studying electron impact rotational excitation of H_3^+. In particular, it was found [408] that electron collisions could help create and maintain non-thermal populations of H_3^+ levels.

Faure et al. [202] compared the **R**-matrix, adiabatic nuclei calculations described above with rovibrational quantum defect theory calculations based on the treatment of Kokoouline and Greene [409]. The adiabatic nuclei excitation cross sections were, somewhat surprisingly, shown to be accurate down to threshold, except in the presence of large oscillating Rydberg resonances. Furthermore, rotational rates were found to compete or even dominate those of dissociative recombination [410]. Recently the same workers have extended their calculations to also consider rotationally resolved electron impact vibrational excitation [411].

6.3. Collisions with larger molecules

Much recent work on electron collisions has concentrated on extending calculations to larger molecules. In this there has been special emphasis on the study of biomolecules with, in particular, a view to better understanding radiation damage. Some studies have also focused on clusters [306,307]. There is, of course, an inherent problem with such studies using the **R**-matrix method in that the division of space into an inner and outer region is based on the use of a spherical (or near-spherical [109]) inner region. To be tractable this inner region needs to be of modest size: with current GTO basis sets for the continuum orbital a calculation studying energies up to 20 eV is restricted to about $a = 15\ a_0$ or less. Given that the target wave function has to be entirely contained within this sphere, there is a clear constraint on the physical size of the target molecule that can be considered.

None-the-less multicenter **R**-matrix calculations have been successfully performed for electron collisions with a number of small organic molecules including: alkanes [167,412], cyclopropane [224,262], formaldehyde [413], tetrahydrofuran [244,269], methanol [414], glycine [415] and uracil [166]. The motivation for these studies varies.

R-matrix studies on methane have concentrated on issues to do with the complete representation of polarization [167,412]. Elastic scattering from methane displays a pronounced minimum in the cross section, usually called a Ramsauer minimum, at low energies. This minimum is caused by a cancellation between the repulsive static potential and the

attractive polarization potential. While the static potential is easy to represent, converging the polarization potential for methane using a fully *ab initio* procedure is difficult [158,165]. Correctly representing the Ramsauer minimum is thus a good test of the model used to represent polarization. Recent multistate **R**-matrix calculations were found to give good results for the Ramsauer minimum for methane although calculations at a similar level were not so satisfactory for ethane and propane [167] suggesting that there is more work to be done on this problem. I note that although calculations using up to 64 target states in the close-coupling expansion have been used for these studies, an RMPS method has yet to be tried for these systems. It is to be anticipated that an RMPS calculation will give a more fully converged representation of polarization.

Another major aim in the studies cited above is the study of resonances in biological systems since these are thought to play an important role in radiation damage [3]. In fact the **R**-matrix study on electron collisions with tetrahydrofuran, a ring with chemical formula C_4H_8O, found some Feshbach resonances associated with electronically excited states of the molecule but failed to find any shape resonances [269]. These shape resonances were shown to be present in both a single center **R**-matrix study [244] and a complex Kohn variational calculation [416]. It would seem likely that the original multicentered **R**-matrix calculation did not include enough virtual (i.e. unoccupied target) orbitals in the scattering calculation to accommodate the shape resonance.

This supposition is supported by both **R**-matrix [166] and Schwinger variational [160] calculations on uracil, $C_4H_4N_2O_2$, the simplest base used in building large biomolecules. These calculations showed that the three low-lying $^2A''$ shape resonances could only be properly represented by using at least 5 virtual orbitals of that symmetry. Although shape resonances are found in static exchange calculations, their parameters are usually sensitive to the inclusion of polarization effects. This is certainly true for uracil for which it has so far proved difficult to develop a fully robust model which demonstrates that the treatment of polarization effects is fully converges [166].

7. Conclusion

Applications of the **R**-matrix method have come a long way since it was originally proposed as a method for the semi-empirical treatment of nuclear reactions by Wigner [34] more than sixty years ago. The use of an **R**-matrix calculations as the basis of an *ab initio* treatment of electron collisions with DNA [246] illustrate this. The **R**-matrix method is now routinely used to study low-energy collisions with small, and increasingly medium-sized, molecules. The provision of automated software for running **R**-matrix calculations [149] means that the method has become available to non-specialists. Given this and the recent development of a number of new **R**-matrix codes [71–74], the use of **R**-matrix methods for studying molecular processes should continue to grow.

Of course there remain unresolved issues and areas for improvement in the currently available methods. The treatment of polarization effects in low-energy electron collisions represents a long-standing and general problem with all electron–molecule scattering methods. That this remains an issue in all truly *ab initio* procedures is not altogether surprising given the difficulty of treating the closely related electron correlation problem in computationally simpler, bound state problems. Within an **R**-matrix framework, the use of the **R**-matrix with pseudo-states method (RMPS) [26,187] would appear to offer the best immediate hope for tackling the issue of polarization effects. Recent calculations for diatomic targets [105,189] have suggested that the RMPS method can provide a converged treatment of polarization even for highly polarizable molecules. However, even for electron collisions from the relatively small for C_2^- anion, it was not computationally feasible to do a full RMPS treatment of the problem [188] with the present implementation of the codes and present day computers. The use of an RMPS treatment for resolving problems with converging the treatment of polarization in larger molecules, such as uracil [166] or the alkanes [167], where the present results are not stable to treatments of polarization, remains something one can only aspire to.

On a somewhat longer timescale, it is notable that the use of wave functions which explicitly consider electron–electron coordinates for bound state problems has grown rapidly over the last decade [387,388]. Explicitly correlated functions give significantly better convergence of the electron correlation problem, even if their use is computationally very demanding. Such functions have yet to be used in electron–molecule scattering of any description but, given the close association of the inner region of an **R**-matrix calculation with quantum chemistry, it is to be anticipated that explicitly correlated functions will be used to address the polarization problem at some point. It should be noted that these functions are also necessary to allow for the formation of positronium in positron scattering calculations and provide a natural framework calculations of rates of positron annihilation [386].

The recent trend towards calculation with larger molecules clearly raises issues with the **R**-matrix method. Most of these calculations use a single set of Gaussian Type Orbitals (GTOs) placed on the origin, the center-of-mass of the system [261,263]. Linear dependence problems and other practical issues limit the range of energies and magnitude of the **R**-matrix radius, a, that can simultaneously be covered by a such a basis. For energies up to about 12 eV it has proved difficult to develop robust GTO basis sets for $a > 15\ a_0$, with practical calculations often limited to $a = 13\ a_0$. This limitation is not suffered by numerical basis sets [155,417]. The extension of B-spline basis sets [266] or some other similar more flexible representation of the continuum orbitals to the general electron–molecule problem will probably be required to resolve this problem.

The recent use of attosecond lasers as a probe of molecular properties has placed emphasis on developing theoretical treatments which employ the sort of detailed description of the molecular physics available via the **R**-matrix method and at the same time couple to a strong, time-dependent field. A time-dependent formulation of the **R**-matrix method was been

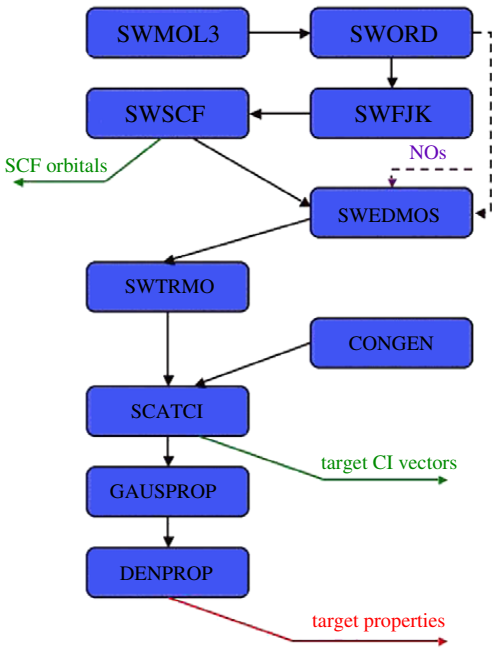

Fig. 12. Structure of a target calculation in the polyatomic UK Molecular **R**-matrix codes [227]. A natural orbital (NO) or indeed multi-configurational SCF (MC-SCF) orbital file is an optional input. Outputs are a file of target CI vectors for the inner region calculation and a file containing the target properties for the outer region calculation. G. Halmová, private communication.

developed some time ago by Burke and Burke [60]. Recently a time-dependent **R**-matrix procedure has been implemented for atoms in intense laser fields [139]; a similar molecular implementation must surely follow.

Acknowledgements

I thank Michal Tarana and Stephen Harrison for many helpful comments on the manuscript. I am also grateful to my many co-workers over the years for their collaboration and for providing results which I have freely quoted from in this article.

Appendix. The UK molecular R-matrix codes

The UK molecular **R**-matrix code [227] is now in use by a large number of different groups round the world [259,413–415, 418–424]. The codes themselves are freely available. The inner region code is actually a compound one with two distinct forms: the original version, which only treated scattering from diatomics, and a more general polyatomic code. An expert system, Quantemol-N [149], is also available to facilitate the use of the polyatomic version of the codes by non-experts. Below I give a brief description of the structure of the polyatomic code. The structure of the diatomic code, which is based on an adapted [231] version of the Alchemy quantum chemistry code [229,230], is very similar [226].

A.1. Inner region and target wave functions

The numerical treatment of the inner regions of flexible **R**-matrix codes is generally based on a quantum chemistry package. This is because, besides the generation of the target state wave function and properties which is a standard quantum chemistry problem, several of the other steps are related closely to those performed in an *ab initio* electronic structure calculation. The UK polyatomic **R**-matrix code is built about the Sweden Molecule quantum chemistry package of Almlöf and Taylor [232,233].

Fig. 12 shows the steps that are taken to generate target wave functions and associated properties as a prelude to a full scattering run. The first three modules, SWMOL3, SWORD and SWFJK perform the necessary integral evaluation, ordering and Fock-matrix building steps prior to the actual SCF calculation in SWSCF. These modules are all taken largely unchanged from the Sweden Molecule code as is the four-index transformation code SWTRMO which converts the integrals labelled in atomic orbitals to integrals over molecular orbitals which are used in the configuration interaction (CI) step of the calculation. Before this can be done SWEDMOS ensures that the orbital set being used is orthonormal by doing a simple Schmidt orthogonalization. Optionally the SCF step of the calculation can be skipped and orbitals can be read in from another source. As discussed in Section 5.2.2, the main options for other orbitals are natural orbitals (NOs) or Multi-Configuration

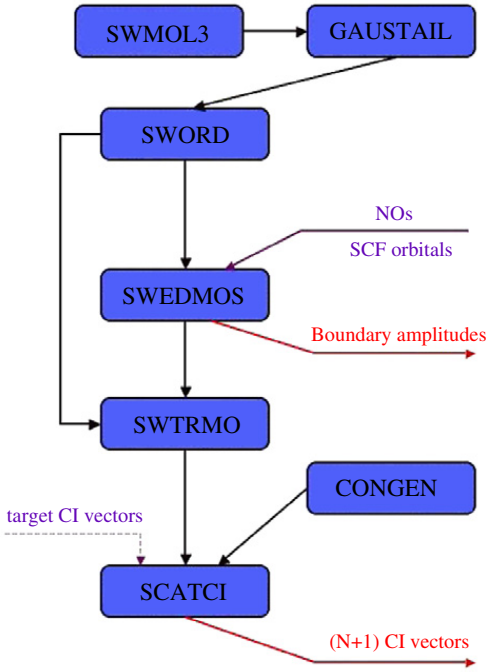

Fig. 13. Structure of the inner region calculation for the polyatomic UK Molecular **R**-matrix codes [227]. Inputs are target orbitals and CI vectors; outputs are the boundary amplitudes, the **R**-matrix poles and associated eigenvectors. G. Halmová, private communication.

SCF (MC-SCF) orbitals. In practice, the option of reading in orbitals from another quantum chemistry package, particularly MOLPRO [425], is being used increasingly as this approach offers more flexibility in defining the target and virtual orbitals.

The configuration generation program CONGEN is a heavily adapted version of program with the same purpose which originally came from the ALCHEMY program suite [229]. SCATCI is a specialist Hamiltonian matrix construction and diagonalization program discussed in Section 5.2.3 which is the workhorse of the inner region calculation. The target CI vectors produced by SCATCI form part of the input for the inner region scattering run along with the orthonormal target orbitals produced by SWEDMOS.

Modules GAUSPROP and DENPROP are concerned with calculating target properties, particularly diagonal and off-diagonal dipole and quadrupole moments. These properties, along with information on the geometry and the electronic states of the target considered, are written to the target properties file which is one of the inputs for the outer region calculation.

It should be noted that molecular RMPS calculations, see Section 5.3, involve running the target section of the code twice. The first run is a standard target run; the second run adds the pseudo-continuum orbitals to the basis and uses SWEDMOS to generate an appropriate orbital set. These are then used to generate target energies, wave functions and properties.

As shown in Fig. 13, a number of the modules used in calculating the target wave functions are also used for the inner region calculation but with some subtle differences. Thus the integrals over atomic orbitals are again computed by SWMOL3 but those which are marked as involving a continuum orbital are adjusted for the finite dimension of the **R**-matrix sphere using GAUSTAIL [69]. The orthogonalization procedure implemented in SWEDMOS combines both symmetric and Schmidt orthogonalization as described in Section 5.2.2. SWEDMOS also computes the amplitude of each continuum orbital as a function of partial wave on the **R**-matrix boundary; these from part of the input for the outer region.

CONGEN and SCATCI use a highly developed algorithm for solving the scattering problem [285,284], see Section 5.2.3. The output from this is the **R**-matrix pole energies, E_k^{N+1}, and associated wave functions, ϕ_k^{N+1}. In practice the wave functions are passed in the form of coefficients a_{ijk} and b_{ik}, see Eq. (14).

A.2. Outer region

Unlike the inner regions codes the outer region is run as a single program with a driver routine which specifies which modules are needed for a particular run. Fig. 14 shows the main but by no means all the modules available in this code; other modules available include POLYDCS [209] or DCS [426] for calculating differential cross sections, MCQD for calculating multichannel quantum defects from the above threshold **S**-matrix [110], ROTIONS [355] for calculating rotational excitation of ions, BORNCROS for adding a dipole Born correction to both elastic and inelastic cross sections [427], ALIGN for treating collisions with oriented (or aligned) molecules [380] and others.

Subroutine SWINTERF, or its diatomic equivalent INTERF, actually acts as the boundary between the inner region and outer region codes. It reads in the target properties, boundary amplitude, **R**-matrix pole positions and associated

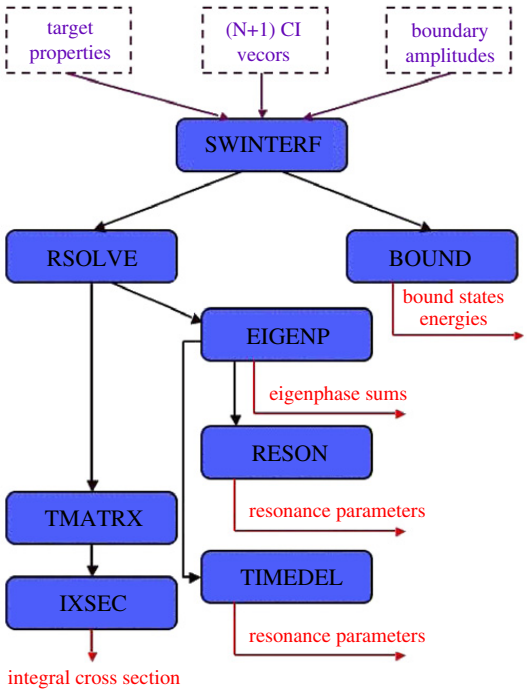

Fig. 14. The main modules used in the outer region of the polyatomic UK Molecular **R**-matrix codes [227] showing inputs and possible outputs. G. Halmová, private communication.

eigenvectors. From these it constructs a list of asymptotic channels with associated energies, the outer region potential coefficients, see Eq. (21), and assembles the information necessary to construct the **R**-matrix. This information is all written to a channels file and an **R**-matrix file. These files can conveniently be stored either to archive a given calculation or to move between different computers.

RSOLVE is the main workhorse of the outer region code; it calls RPROP2 [94] to propagate the **R**-matrices and then module CFASYM [99] to find the asymptotic solution which in turn uses COULFG [428] to provide Coulomb or Bessel functions for charged or neutral targets respectively. It should be noted that the present version of the code does not take advantage of developments that have been made for many-channel atomic problems [61]. The output from RSOLVE is a set of **K**-matrices produced on a grid of energies.

K-matrices are turned into **T**-matrices by TMATRX using the definition

$$\mathbf{T} = \frac{2\mathrm{i}\mathbf{K}}{1 - \mathrm{i}\mathbf{K}}. \tag{76}$$

The **T**-matrices are in turn used to give a cross section, σ, for going from target state i to target state i' using

$$\sigma(i \to i') = \frac{\pi}{k_i^2} \sum_S \frac{(2S+1)}{2(2S_i+1)} \sum_{\Gamma ll'} |T_{ill'l'}^{\Gamma S}|^2 \tag{77}$$

where $\frac{k_i^2}{2}$ is energy of scattering electron relative to the initial state which has spin S_i. The first sum in Eq. (77) runs over the total spin states of the collision system, S, and the second sum runs over the spatial symmetries, Γ, and the degenerate channels associated with the initial and final target states, denoted l and l' respectively.

Alternatively module EIGENP diagonalizes the **K**-matrix to give the eigenphase sum, see Eq. (32). These can then be analyzed for resonances using module RESON [314] which is actually written to recursively re-call RSOLVE using a fine grid in the region of a resonance. TIMEDEL [321] provides an alternative method fitting resonances, see Section 5.4.2.

BOUND searches for bound states using bound state boundary conditions and an adapted [347] version of method of Seaton [56].

References

[1] D.L. Huestis, S.W. Bougher, J.L. Fox, M. Galand, R.E. Johnson, J.I. Moses, J.C. Pickering, Space Sci. Rev. 139 (2008) 63–105.
[2] A. Luque, U. Ebert, W. Hundsdorfer, Phys. Rev. Lett. 101 (2008) 075005.
[3] B. Boudaïffa, P. Cloutier, D. Hunting, M.A. Huels, L. Sanche, Science 287 (2000) 1658–1660.
[4] J.M. Ajello, D.E. Shemansky, W.R. Pryor, A.I. Stewart, K.E. Simmons, T. Majeed, J.H. Waite, G.R. Gladstone, D. Grodent, Icarus 152 (2001) 151–171.
[5] W.D. Geppert, M. Larsson, Mol. Phys. 106 (2008) 2199–2226.

[6] A. Fuente, S. Garca-Burillo, A. Usero, M. Gerin, R. Neri, A. Faure, J.L. Bourlot, M. Gonzlez-Garca, J.R. Rizzo, T. Alonso-Albi, J. Tennyson, Astron. Astrophys. 492 (2008) 675–684.
[7] M. Roellig, N.P. Abel, T. Bell, F. Bensch, J. Black, G.J. Ferland, B. Jonkheid, I. Kamp, M.J. Kaufman, J. Le Bourlot, F. Le Petit, R. Meijerink, O. Morata, V. Ossenkopf, E. Roueff, G. Shaw, M. Spaans, A. Sternberg, J. Stutzki, W.-F. Thi, E.F. van Dishoeck, P.A.M. van Hoof, S. Viti, M.G. Wolfire, Astron. Astrophys. 467 (2007) 187–206.
[8] M.J. Brunger, S.J. Buckman, Phys. Rep. 357 (2002) 215–458.
[9] C. Winstead, V. McKoy, Adv. At. Mol. Phys. 43 (2000) 111–145.
[10] K. Bartschat, Comput. Phys. Comm. 75 (1993) 219–258.
[11] C. Champion, J. Hanssen, P.A. Hervieux, J. Chem. Phys. 121 (2004) 9423–9429.
[12] G. Cooper, E. Christensen, A.P. Hitchcock, J. Chem. Phys. 127 (2007) 084315.
[13] W.M. Huo, F.A. Gianturco (Eds.), Computational Methods for Electron Molecule Collisions, Plenum Press, New York, 1995.
[14] B.I. Schneider, T.N. Rescigno, Phys. Rev. A 37 (1988) 3749–3754.
[15] T.N. Resigno, C.W. McCurdy, A.E. Orel, B.H. Lengsfield III, in: W.M. Huo, F. Gianturco (Eds.), Computational Methods for Electron Molecule Collisions, Plenum Press, New York, 1995, pp. 1–44.
[16] K. Takatsuka, V. McKoy, Phys. Rev. A 24 (1981) 2473–2480.
[17] K. Takatsuka, V. McKoy, Phys. Rev. A 30 (1984) 1734–1740.
[18] C. Winstead, Q.Y. Sun, P.G. Hipes, M.A.P. Lima, V. McKoy, Aust. J. Phys. 45 (1992) 325–336.
[19] H.D. Meyer, Chem. Phys. Lett. 223 (1994) 465–468.
[20] B.I. Schneider, L. Collins, J. Phys. B: At. Mol. Opt. Phys. 18 (1985) L857–L863.
[21] K.L. Baluja, C.J. Noble, J. Tennyson, J. Phys. B: At. Mol. Phys. 18 (1985) L851–L855.
[22] M.A.P. Lima, T.L. Gibson, W.M. Huo, V. McKoy, J. Phys. B: At. Mol. Opt. Phys. 18 (1985) L865–L870.
[23] A. Faure, J. Tennyson, J. Phys. B: At. Mol. Opt. Phys. 35 (2002) 1865–1873.
[24] C.W. McCurdy, T.N. Rescigno, W.A. Isaacs, D.E. Manolopoulos, Phys. Rev. A 57 (1998) 3511–3517.
[25] S. Chiesa, M. Mella, G. Morosi, Phys. Rev. A 66 (2002) 042502.
[26] J.D. Gorfinkiel, J. Tennyson, J. Phys. B: At. Mol. Opt. Phys. 37 (2004) L343–L350.
[27] J.C. Light, R.B. Walker, J. Chem. Phys. 65 (1976) 4272–4282.
[28] R.B. Walker, J.C. Light, Ann. Rev. Phys. Chem. 31 (1980) 401–433.
[29] J. Gerratt, Phys. Rev. A 30 (1984) 1643–1660.
[30] C.J. Bocchetta, J. Gerratt, J. Chem. Phys. 82 (1985) 1351–1362.
[31] M. Mohan, K.F. Milfeld, R.E. Wyatt, Mol. Phys. 70 (1990) 1085–1095.
[32] G.J. Tawa, S.L. Mielke, D.G. Truhlar, D.W. Schwenke, J. Chem. Phys. 100 (1994) 5751–5777.
[33] W. Hu, G.C. Schatz, J. Chem. Phys. 125 (2006) 132301.
[34] E.P. Wigner, Phys. Rev. 70 (1946) 15–33.
[35] E.P. Wigner, Phys. Rev. 70 (1946) 606–618.
[36] E.P. Wigner, L. Eisenbud, Phys. Rev. 72 (1947) 29–41.
[37] P.L. Kapur, R. Peierls, Proc. R. Soc. London A 166 (1938) 277–295.
[38] W.E. Meyerhof, Phys. Rev. 129 (1963) 692–702.
[39] I.I. Fabrikant, J. Phys. B: At. Mol. Phys. 18 (1985) 1873–1879.
[40] W.E. Meyerhof, G. Laricchia, J. Phys. B: At. Mol. Opt. Phys. 30 (1997) 2221–2238.
[41] J.W. Humberston, P. VanReeth, M.S.T. Watts, W.E. Meyerhof, J. Phys. B: At. Mol. Opt. Phys. 30 (1997) 2477–2493.
[42] R.S. Wilde, G.A. Gallup, I.I. Fabrikant, J. Phys. B: At. Mol. Opt. Phys. 32 (1999) 663–673.
[43] H. Hotop, M.W. Ruf, M. Allan, I.I. Fabrikant, Adv. At. Mol. Phys. 49 (2003) 85–216.
[44] M. Tarana, P. Wielgus, S. Roszak, I.I. Fabrikant, Phys. Rev. A 79 (2009) 052712.
[45] A.M. Lane, R.G. Thomas, Rev. Modern Phys. 30 (1958) 257–353.
[46] R.F. Barrett, B.A. Robson, W. Tobocman, Rev. Modern Phys. 55 (1983) 155–243.
[47] H. Derrien, L.C. Leal, N.M. Larson, Nucl. Sci. Eng. 160 (2008) 149–167.
[48] A.J. Bartlett, J.A. Tostevin, I.J. Thompson, Phys. Rep. C 78 (2008) 054603.
[49] J.L. Jackson, Phys. Rev. 83 (1951) 301–304.
[50] R.K. Nesbet, R.S. Oberoi, Phys. Rev. A 6 (1972) 1855–1862.
[51] U. Fano, C.M. Lee, Phys. Rev. Lett. 31 (1973) 1573–1576.
[52] P.G. Burke, A. Hibbert, W.D. Robb, J. Phys. B: At. Mol. Phys. 4 (1971) 153–161.
[53] P.G. Burke, W.D. Robb, Adv. At. Mol. Phys. 11 (1975) 143–214.
[54] P.G. Burke, K.A. Berrington (Eds.), Atomic and Molecular Processes, an R-matrix Approach, Institute of Physics Publishing, Bristol, 1993.
[55] D.G. Hummer, K.A. Berrington, W. Eissner, A.K. Pradhan, H.E. Saraph, J.A. Tully, Astron. Astrophys. 279 (1993) 298–309.
[56] M.J. Seaton, J. Phys. B: At. Mol. Opt. Phys. 18 (1985) 2111–2131.
[57] The Opacity Project Team, M.J. Seaton, The Opacity Project, vol. 1, Insitute of Physics Publishing, 1995.
[58] The Opacity Project Team, K.A. Berrington, The Opacity Project, vol. 2, Insitute of Physics Publishing, 1994.
[59] P.G. Burke, V.M. Burke, K.M. Dunseath, J. Phys. B: At. Mol. Opt. Phys. 27 (1994) 5341–5373.
[60] P.G. Burke, V.M. Burke, J. Phys. B: At. Mol. Opt. Phys. 30 (1997) L383–L391.
[61] A.G. Sunderland, C.J. Noble, V.M. Burke, P.G. Burke, Comput. Phys. Comm. 145 (2002) 311–340.
[62] B. Schneider, Chem. Phys. Lett. 31 (1975) 237–241.
[63] B.I. Schneider, Phys. Rev. A 11 (1975) 1957–1962.
[64] B.I. Schneider, P.J. Hay, Phys. Rev. A 13 (1976) 2049–2056.
[65] P.G. Burke, I. Mackey, I. Shimamura, J. Phys. B: At. Mol. Phys. 10 (1977) 2497–2512.
[66] P.G. Burke, J.F. Williams, Phys. Rep. 34 (1977) 325–369.
[67] C.J. Noble, P.G. Burke, S. Salvini, J. Phys. B: At. Mol. Phys. 15 (1982) 3779–3786.
[68] B.M. Nestmann, R.K. Nesbet, S.D. Peyerimhoff, J. Phys. B: At. Mol. Opt. Phys. 24 (1991) 5133–5149.
[69] L.A. Morgan, C.J. Gillan, J. Tennyson, X. Chen, J. Phys. B: At. Mol. Opt. Phys. 30 (1997) 4087–4096.
[70] W.M. Huo, D. Brown, Phys. Rev. A 60 (1999) 295–305.
[71] P. Kolorenc, M. Cizek, J. Horacek, G. Mil'nikov, H. Nakamura, Phys. Scr. 65 (2002) 328–335.
[72] M. Telmini, C. Jungen, Phys. Rev. A 68 (2003) 062704.
[73] M. Hiyama, N. Kosugi, J. Theor. Comput. Chem. 4 (2005) 35–47.
[74] S. Tonzani, Comput. Phys. Comm. 176 (2007) 146–156.
[75] T. Jayasekera, M.A. Morrison, K. Mullen, Phys. Rev. B 74 (2006) 235308.
[76] P. Huang, E.A. Carter, Ann. Rev. Phys. Chem. 59 (2008) 261–290.
[77] J.J.M. Michiels, J.E. Inglesfield, C.J. Noble, V.M. Burke, P.G. Burke, Phys. Rev. Lett. 78 (1997) 2851–2854.
[78] P.G. Burke, K. Higgins, J.E. Inglesfield, Phil. Trans. Roy. Soc. A 357 (1999) 1143–1160.
[79] D. Teillet-Billy, D.T. Stibbe, J. Tennyson, J.P. Gauyacq, Surf. Sci. 443 (1999) 57–68.
[80] C. Bloch, Nuclear Phys. 4 (1957) 503.
[81] P.G. Burke, M.J. Seaton, J. Phys. B: At. Mol. Opt. Phys. 17 (1984) L683–L687.
[82] A.M. Arthurs, A. Dalgarno, Proc. Phys. Soc. London A 256 (1960) 540–551.

[83] R. Fandreyer, P.G. Burke, L.A. Morgan, C.J. Gillan, J. Phys. B: At. Mol. Opt. Phys. 26 (1993) 3625–3637.
[84] D. Shafir, S. Novotny, H. Buhr, S. Altevogt, A. Faure, M. Grieser, A.G. Harvey, O. Heber, J. Hoffmann, H. Kreckel, L. Lammich, I. Nevo, H. Pedersen, H. Rubinstein, I.F. Schneider, D. Schwalm, J. Tennyson, A. Wolf, D. Zajfman, Phys. Rev. Lett. 102 (2009) 223202.
[85] M.A. Morrison, Adv. At. Mol. Phys. 24 (1988) 51–156.
[86] R. Zhang, A. Faure, J. Tennyson, Phys. Scr. 80 (2009) 015301.
[87] D.E. Manolopoulos, R.E. Wyatt, Chem. Phys. Lett. 152 (1988) 123.
[88] D.E. Manolopoulos, M. D'Mello, R.E. Wyatt, J. Chem. Phys. 91 (1989) 6096.
[89] D. Brown, J.C. Light, J. Chem. Phys. 101 (1994) 3723–3728.
[90] G. Danby, J. Tennyson, J. Phys. B: At. Mol. Opt. Phys. 23 (1990) 1005–1016; J. Phys. B: At. Mol. Opt. Phys. 23 (1990) 2471 (erratum).
[91] M. Tarana, B.M. Nestmann, J. Horacek, Phys. Rev. A 79 (2009) 012716.
[92] B.M. Nestmann, T. Beyer, Chem. Phys. 343 (2008) 281–291.
[93] K.L. Baluja, P.G. Burke, L.A. Morgan, Comput. Phys. Comm. 27 (1982) 299–307.
[94] L.A. Morgan, Comput. Phys. Comm. 31 (1984) 419–422.
[95] P.G. Burke, H.M. Schey, Phys. Rev. 126 (1962) 147.
[96] M.A. Crees, Comput. Phys. Comm. 19 (1980) 103–137.
[97] M.A. Crees, Comput. Phys. Comm. 23 (1981) 181–198.
[98] M. Gailitis, J. Phys. B: At. Mol. Opt. Phys. 9 (1976) 843.
[99] C.J. Noble, R.K. Nesbet, Comput. Phys. Comm. 33 (1984) 399.
[100] W. Domcke, Phys. Rep. 208 (1991) 97–188.
[101] A.I. Florescu-Mitchell, J.B.A. Mitchell, Phys. Rep. 430 (2006) 277–374.
[102] M. Larsson, A.E. Orel, Dissociative Recombination of Molecular Ions, Cambridge University Press, 2008.
[103] B.K. Sarpal, J. Tennyson, L.A. Morgan, J. Phys. B: At. Mol. Opt. Phys. 27 (1994) 5943–5953.
[104] C.H. Greene, V. Kokoouline, Philos. Trans. R. Soc. Lond. A 364 (2006) 2965–2980.
[105] G. Halmová, J. Tennyson, Phys. Rev. Lett. 100 (2008) 213202.
[106] D.T. Stibbe, J. Tennyson, J. Phys. B: At. Mol. Opt. Phys. 30 (1997) L301–L307.
[107] C. Jungen (Ed.), Molecular Applications of Quantum Defect Theory, Taylor and Francis, 1996.
[108] M. Arif, C. Jungen, A.L. Roche, J. Chem. Phys. 106 (1997) 4102–4118.
[109] S. Bezzaouia, M. Telmini, C. Jungen, Phys. Rev. A 70 (2004) 012713.
[110] J. Tennyson, J. Phys. B: At. Mol. Opt. Phys. 21 (1988) 805–816.
[111] I. Shimamura, C.J. Noble, P.G. Burke, Phys. Rev. A 41 (1990) 3545–3554.
[112] J. Tennyson, At. Data Nucl. Data Tables 64 (1996) 253–277.
[113] N. Vinci, J. Tennyson, J. Phys. B: At. Mol. Opt. Phys. 37 (2004) 2011–2031.
[114] J.N. Bardsley, J. Phys. B: At. Mol. Phys. 1 (1968) 365–380.
[115] L.A. Morgan, P.G. Burke, J. Phys. B: At. Mol. Opt. Phys. 21 (1988) 2091–2105.
[116] M. McCartney, P.G. Burke, L.A. Morgan, C.J. Gillan, J. Phys. B: At. Mol. Opt. Phys. 23 (1990) L415–L418.
[117] L.A. Morgan, P.G. Burke, C.J. Gillan, J. Phys. B: At. Mol. Opt. Phys. 23 (1990) 99–113.
[118] H.T. Thümmel, R.K. Nesbet, S.D. Peyerimhoff, J. Phys. B: At. Mol. Opt. Phys. 26 (1993) 1233–1251.
[119] K. Pfingst, H.T. Thümmel, S.D. Peyerimhoff, J. Phys. B: At. Mol. Opt. Phys. 25 (1992) 2107–2119.
[120] H.T. Thümmel, R.K. Nesbet, S.D. Peyerimhoff, J. Phys. B: At. Mol. Opt. Phys. 25 (1992) 4553–4579.
[121] P.G. Burke, K.A. Berrington, C.V. Sukumar, J. Phys. B: At. Mol. Phys. 14 (1981) 289–305.
[122] P.G. Burke, C.J. Noble, P. Scott, Proc. R. Soc. London A 410 (1987) 289–310.
[123] T.T. Scholz, J. Phys. B: At. Mol. Opt. Phys. 24 (8) (1991) 2127–2146.
[124] I. Rabadán, J. Tennyson, J. Phys. B: At. Mol. Opt. Phys. 29 (1996) 3747–3761.
[125] I. Rabadán, J. Tennyson, J. Phys. B: At. Mol. Opt. Phys. 30 (1997) 1975–1988; J. Phys. B: At. Mol. Opt. Phys. 31 (1998) 4485–4487 (erratum).
[126] J. Tennyson, J. Phys. B: At. Mol. Phys. 20 (1987) L375–L378.
[127] P.G. Burke, in: F.A. Gianturco (Ed.), Atomic and Molecular Collision Theory, Plenum Press, New York, 1982, pp. 69–122.
[128] B.K. Sarpal, J. Tennyson, J. Phys. B: At. Mol. Opt. Phys. 25 (1992) L49–L55.
[129] P.G. Burke, K.T. Taylor, J. Phys. B: At. Mol. Opt. Phys. 8 (1975) 2620–2639.
[130] J. Tennyson, C.J. Noble, P.G. Burke, Int. J. Quantum Chem. 29 (1986) 1033–1042.
[131] J. Tennyson, N. Chandra, Comput. Phys. Comm. 46 (1987) 99–105.
[132] U. Fano, D. Dill, Phys. Rev. A 6 (1972) 185–192.
[133] D.C.S. Allison, P.G. Burke, W.D. Robb, J. Phys. B: At. Mol. Phys. 5 (1972) 55–65.
[134] P.G. Burke, P. Francken, C.J. Joachain, J. Phys. B: At. Mol. Opt. Phys. 24 (1991) 761–790.
[135] J. Colgan, D.H. Glass, K. Higgins, P.G. Burke, Comput. Phys. Comm. 114 (1998) 27–41.
[136] C.J. Joachain, J. Modern Opt. 54 (2007) 1859–1882.
[137] P.G. Burke, J. Colgan, D.H. Glass, K. Higgins, J. Phys. B: At. Mol. Opt. Phys. 33 (2000) 143–167.
[138] J. Colgan, D.H. Glass, K. Higgins, P.G. Burke, J. Phys. B: At. Mol. Opt. Phys. 34 (2001) 2089–2106.
[139] H.W. van der Hart, M.A. Lysaght, P.G. Burke, Phys. Rev. A 76 (2007) 043405.
[140] J.N. Cooper, E.A.G. Armour, M. Plummer, J. Phys. B: At. Mol. Opt. Phys. 41 (2008) 245201.
[141] B.K. Sarpal, K. Pfingst, B.M. Nestmann, S.D. Peyerimhoff, J. Phys. B: At. Mol. Opt. Phys. 29 (1996) 857–873; J. Phys. B: At. Mol. Opt. Phys. 29 (1996) 1877 (erratum).
[142] K. Pfingst, B.M. Nestmann, S.D. Peyerimhoff, J. Phys. B: At. Mol. Opt. Phys. 27 (1994) 2283–2296.
[143] R.J. Buenker, S.D. Peyerimhoff, Theor. Chim. Acta 35 (1974) 33–58.
[144] R.J. Buenker, S.D. Peyerimhoff, Theor. Chim. Acta 39 (1975) 217–228.
[145] R.J. Buenker, S.D. Peyerimhoff, W. Butscher, Mol. Phys. 35 (1978) 771–791.
[146] C.J. Gillan, C.J. Noble, P.G. Burke, J. Phys. B: At. Mol. Opt. Phys. 23 (1990) L407–L413.
[147] B.M. McLaughlin, C.J. Gillan, P.G. Burke, J.S. Dahler, Phys. Rev. A 47 (1993) 1967–1980.
[148] J. Tennyson, J. Phys. B: At. Mol. Opt. Phys. 29 (1996) 6185–6201.
[149] J. Tennyson, D.B. Brown, J.J. Munro, I. Rozum, H.N. Varambhia, N. Vinci, J. Phys. Conf. Series 86 (2007) 012001.
[150] J.D. Gorfinkiel, A. Faure, S. Taioli, C. Piccarretta, G. Halmová, J. Tennyson, Euro. J. Phys. D 35 (2005) 231–237.
[151] N.F. Zobov, O.L. Polyansky, C.R. Le Sueur, J. Tennyson, Chem. Phys. Lett. 260 (1996) 381–387.
[152] K. Chakrabarti, J. Tennyson, J. Phys. B: At. Mol. Opt. Phys. 42 (2009) 105204.
[153] V.M. Burke, P.G. Burke, N.S. Scott, Comput. Phys. Comm. 69 (1992) 76–98.
[154] T.N. Rescigno, B.H. Lengsfield III, C.W. McCurdy, S.D. Parker, Phys. Rev. A 45 (1992) 7800–7809.
[155] S. Tonzani, C.H. Greene, J. Chem. Phys. 122 (2005) 014111.
[156] R. McWeeny, Methods of Molecular Quantum Mechanics, 2nd ed., Academic Press, London, 1989.
[157] M. Tarana, J. Horáček, J. Chem. Phys. 127 (2007) 154319.
[158] B.H. Lengsfield III, T.N. Rescigno, C.W. McCurdy, Phys. Rev. A 44 (1991) 4296–4308.
[159] C.S. Trevisan, A.E. Orel, T.N. Rescigno, Phys. Rev. A 68 (2003) 062707.
[160] C. Winstead, V. McKoy, J. Chem. Phys. 125 (2006) 174304.
[161] J. Tennyson, C.J. Noble, S. Salvini, J. Phys. B: At. Mol. Phys. 17 (1984) 905–912.

[162] I. Bray, A.T. Stelbovics, Phys. Rev. A 46 (1992) 6995–7011.
[163] D.V. Fursa, I. Bray, J. Phys. B: At. Mol. Opt. Phys. 30 (1997) 757–785.
[164] G. Halmová, J.D. Gorfinkel, J. Tennyson, J. Phys. B: At. Mol. Opt. Phys. 39 (2006) 2849–2860.
[165] T.J. Gil, B.H. Lengsfield III, C.W. McCurdy, T.N. Rescigno, Phys. Rev. A 49 (1994) 2551–2560.
[166] A. Dora, L. Bryjko, T. van Mourik, J. Tennyson, J. Chem. Phys. (2009) 164307.
[167] H.N. Varambhia, J.J. Munro, J. Tennyson, Int. J. Mass Spectrometry 271 (2008) 1–7.
[168] M. Jones, J. Tennyson, J. Phys. B: At. Mol. Opt. Phys. 43 (2010) 045101.
[169] I. Bray, D.V. Fursa, A.S. Kadyrov, A.T. Stelbovics, in: M.L. Ge, C.H. Oh, K.K. Phua (Eds.), Statistical Physics, High Energy, Condensed Matter and Mathematical Physics, World Scientific, 2008, pp. 486–497.
[170] I. Bray, D.V. Fursa, A.S. Kheifets, A.T. Stelvobics, J. Phys. B: At. Mol. Opt. Phys. 35 (2002) R117.
[171] T. Scholz, P. Scott, P.G. Burke, J. Phys. B: At. Mol. Opt. Phys. 21 (1988) L139–L145.
[172] K. Bartschat, P.G. Burke, J. Phys. B: At. Mol. Phys. 20 (1987) 3191–3200.
[173] K. Bartschat, E.T. Hudson, M.P. Scott, P.G. Burke, V.M. Burke, J. Phys. B: At. Mol. Opt. Phys. 29 (1996) 115–123.
[174] M.S. Pinzola, F.J. Robicheaux, Phys. Rev. A 61 (2000) 052707.
[175] M.S. Pindzola, F. Robicheaux, S.D. Loch, J.C. Berengut, T. Topcu, J. Colgan, M. Foster, D.C. Griffin, C.P. Ballance, D.R. Schultz, T. Minami, N.R. Badnell, M.C. Witthoeft, D.R. Plante, D.M. Mitnik, J.A. Ludlow, U. Kleiman, J. Phys. B: At. Mol. Opt. Phys. 40 (2007) R39–R60.
[176] M. Pindzola, F. Robicheaux, J. Colgan, J. Phys. B: At. Mol. Opt. Phys. 38 (2005) L285–L290.
[177] A.A. Kernoghan, M.T. McAlinden, H.R.J. Walters, J. Phys. B: At. Mol. Opt. Phys., 28 (1995) 1079–1094.
[178] K. Bartschat, I. Bray, J. Phys. B: At. Mol. Opt. Phys. 29 (1996) L577–L583.
[179] P.G. Burke, J.F. Mitchell, J. Phys. B: At. Mol. Opt. Phys. 7 (1974) 665–673.
[180] A. Hibbert, M. Le Dourneuf, V.K. Lan, J. Phys. B: At. Mol. Phys. 10 (1977) 1015–1025.
[181] B.I. Schneider, Chem. Phys. Lett. 51 (1977) 578–581.
[182] L. Malegat, M. Vincke, C. Gillan, M. Le Dourneuf, J. Phys. B: At. Mol. Opt. Phys. 25 (1992) 727–739.
[183] C.J. Gillan, C.J. Noble, P.G. Burke, J. Phys. B: At. Mol. Opt. Phys. 21 (1988) L53–L59.
[184] R. Fandreyer, P.G. Burke, J. Phys. B: At. Mol. Opt. Phys. 29 (1996) 339–343.
[185] J. Tennyson, J. Phys. B: At. Mol. Phys. 19 (1986) 4255–4263.
[186] R.K. Nesbet, S. Mazevet, M.A. Morrison, Phys. Rev. A 64 (2001) 034702.
[187] J.D. Gorfinkiel, J. Tennyson, J. Phys. B: At. Mol. Opt. Phys. 38 (2005) 1607–1622.
[188] G. Halmová, J.D. Gorfinkiel, J. Tennyson, J. Phys. B: At. Mol. Opt. Phys. 41 (2008) 155201.
[189] M. Tarana, J. Tennyson, J. Phys. B: At. Mol. Opt. Phys. 41 (2008) 205204.
[190] R. Zhang, J. Franz, K.L. Baluja, J. Tennyson, (in preparation).
[191] Y.K. Kim, M.E. Rudd, Phys. Rev. A 50 (1994) 3945.
[192] H. Deutsch, K. Becker, S. Matt, T.D. Märk, Int. J. Mass Spec. 197 (2000) 37.
[193] W.M. Huo, Phys. Rev. A 64 (2001) 042719.
[194] X. Yang, M. Lin, B. Zhang, Chem. Phys. Lett. 382 (2003) 160–166.
[195] J.J. Chang, J. Phys. B: At. Mol. Phys. 8 (1975) 2327–2335.
[196] M.J. Seaton, J. Phys. B: At. Mol. Opt. Phys. 20 (1987) 6363–6378.
[197] N.R. Badnell, J. Phys. B: At. Mol. Opt. Phys. 41 (2008) 175202.
[198] I.P. Grant, J. Phys. B: At. Mol. Opt. Phys. 41 (2008) 055002.
[199] H.E. Saraph, Comput. Phys. Comm. 15 (1978) 247–258.
[200] N.F. Lane, Rev. Modern Phys. 52 (1980) 29–119.
[201] D.M. Chase, Phys. Rep. 104 (1956) 838–842.
[202] A. Faure, V. Kokoouline, C.H. Greene, J. Tennyson, J. Phys. B: At. Mol. Opt. Phys. 39 (2006) 4261–4273.
[203] R.J.W. Henry, Phys. Rev. A 2 (1970) 1349–1358.
[204] N. Chandra, A. Temkin, Phys. Rev. A 13 (1976) 188–203.
[205] E.S. Chang, A. Temkin, Phys. Rev. Lett. 23 (1969) 399–403.
[206] E.S. Chang, U. Fano, Phys. Rev. A 6 (1972) 173–185.
[207] N. Chandra, Phys. Rev. A 16 (1977) 80–108.
[208] M.A. Morrison, W. Sun, in: W.M. Huo, F. Gianturco (Eds.), Computational Methods for Electron Molecule Collisions, Plenum Press, New York, 1995, pp. 131–190.
[209] N. Sanna, F.A. Gianturco, Comput. Phys. Comm. 114 (1998) 142–167.
[210] A. Jain, D.G. Thompson, Comput. Phys. Comm. 32 (1984) 367–383.
[211] D.T. Stibbe, J. Tennyson, Phys. Rev. Lett. 79 (1997) 4116–4119.
[212] I.F. Schneider, I. Rabadán, L. Carata, J. Tennyson, L.H. Andersen, A. Suzor-Weiner, J. Phys. B: At. Mol. Opt. Phys. 33 (2000) 4849–4861.
[213] M. Allan, J. Phys. B: At. Mol. Opt. Phys. 18 (1985) 4511–4517.
[214] L.A. Morgan, J. Phys. B: At. Mol. Opt. Phys. 19 (1986) L439–L445.
[215] B.I. Schneider, M. Le Dourneuf, P.G. Burke, J. Phys. B: At. Mol. Phys. 40 (1979) L365–369.
[216] R.K. Nesbet, Phys. Rev. A 54 (1996) 2899–2905.
[217] B.I. Schneider, M. Le Dourneuf, V.K. Lan, Phys. Rev. Lett. 43 (1979) 1926–1929.
[218] B.K. Sarpal, J. Tennyson, L.A. Morgan, J. Phys. B: At. Mol. Opt. Phys. 24 (1991) 1851–1866.
[219] I. Rabadán, J. Tennyson, L.A. Morgan, Chem. Phys. Lett. 285 (1998) 105–113.
[220] I. Rabadán, J. Tennyson, J. Phys. B: At. Mol. Opt. Phys. 32 (1999) 4753–4762.
[221] N. Vinci, N. de Ruette, F.O. Waffeu-Tamo, O. Motapon, M.F.A. Crumeyrolle, X. Urbain, J. Tennyson, I.F. Schneider, J. Phys: Conf. Ser. 4 (2005) 162–167.
[222] O. Motapon, M. Fifirig, A. Florescu, F.O. Waffeu-Tamo, O. Crumeyrolle, G. Varin-Breant, A. Bultel, P. Vervisch, J. Tennyson, I.F. Schneider, Plasma Phys. Sci. Technol. 15 (2006) 23–32.
[223] K. Pfingst, B.M. Nestmann, S.D. Peyerimhoff, in: W.M. Huo, F.A. Gianturco (Eds.), Computational Methods for Electron Molecule Collisions, Plenum Press, New York, 1995, pp. 293–308.
[224] A. Busalla, K. Blum, T. Beyer, B.M. Nestmann, J. Phys. B: At. Mol. Opt. Phys. 32 (1999) 791–814.
[225] M. Hanrath, B. Engels, Chem. Phys. 225 (1997) 197.
[226] C.J. Gillan, J. Tennyson, P.G. Burke, in: W. Huo, F.A. Gianturco (Eds.), Computational Methods for Electron-Molecule Collisions, 1995, pp. 239–254.
[227] L.A. Morgan, J. Tennyson, C.J. Gillan, Comput. Phys. Comm. 114 (1998) 120–128.
[228] P.G. Burke, J. Tennyson, Mol. Phys. 103 (2005) 2537–2548.
[229] A.D. McLean, in: W.A. Lester Jr. (Ed.), Potential Energy Surfaces in Chemistry, IBM Research Laboratory, San Jose, 1971, p. 87.
[230] A.D. McLean, M. Yoshimine, B. Lengsfield III, P.S. Bagus, B. Liu, in: E. Clementi (Ed.), Modern Techniques in Computational Chemistry, MOTECC-91, Escom, Leiden, 1991.
[231] C.J. Noble, The ALCHEMY Linear Molecule Integral Generator, Technical Report DL/SCI/TM33T, Daresbury Laboratory, 1982.
[232] J. Almlöf, P.R. Taylor, in: C.E. Dykstra (Ed.), Advanced Theories and Computational Approaches to the Electronic Structure of Molecules, Reidel, 1984.
[233] J. Almlöf, P.R. Taylor, in: E. Clementi (Ed.), Modern Techniques in Computational Chemistry, MOTECC-91, Escom, Leiden, 1991.
[234] M. Hiyama, N. Kosugi, Phys. Scr. T115 (2005) 136–139.
[235] M. Hiyama, N. Kosugi, J. Phys. B: At. Mol. Opt. Phys. 39 (2006) 1797–1811.
[236] C. Jungen, A.L. Roche, Can. J. Phys. 79 (2001) 287–298.

[237] R.W. Field, C.M. Gittins, N.A. Harris, C. Jungen, J. Chem. Phys. 122 (2005) 184314.
[238] C. Jungen, A.L. Roche, M. Arif, Phil. Trans. Roy. Soc. A 355 (1734) (1997) 1481–1504; Phil. Trans. Roy. Soc. A 355 (1997) 2520 (erratum).
[239] S. Raouafi, G.H. Jeung, C. Jungen, J. Chem. Phys. 115 (2001) 7450–7459.
[240] H. Gao, C. Jungen, C.H. Greene, Phys. Rev. A 47 (1993) 4877–4884.
[241] C. Jungen, F. Texier, J. Phys. B: At. Mol. Opt. Phys. 33 (2000) 2495–2510.
[242] R. Guerout, M. Jungen, C. Jungen, J. Phys. B: At. Mol. Opt. Phys. 37 (2004) 3043–3055.
[243] A. Osterwalder, A. Wuest, F. Merkt, C. Jungen, J. Chem. Phys. 121 (2004) 11810–11838.
[244] S. Tonzani, C.H. Greene, J. Chem. Phys. 125 (2006) 094504.
[245] S. Tonzani, C.H. Greene, J. Chem. Phys. 124 (2006) 054312.
[246] L. Caron, L. Sanche, S. Tonzani, C.H. Greene, Phys. Rev. A 78 (2008) 042710.
[247] R.K. Nesbet, C.J. Noble, L.A. Morgan, C.A. Weatherford, J. Phys. B: At. Mol. Phys. 17 (1984) L891–L895.
[248] P.G. Burke, C.J. Noble, S. Salvini, J. Phys. B: At. Mol. Phys. 16 (1983) L113–L120.
[249] G. Raseev, Comput. Phys. Comm. 20 (1980) 267–274.
[250] S. Salvini, P.G. Burke, C.J. Noble, J. Phys. B: At. Mol. Phys. 17 (1984) 2549–2561.
[251] L.A. Morgan, J. Tennyson, J. Phys. B: At. Mol. Opt. Phys. 26 (1993) 2429–2441.
[252] P.J.A. Buttle, Phys. Rev. 160 (1967) 719–729.
[253] P.G. Burke, C.J. Noble, in: L.C. Pritcharda, V. McKoy, A. Chutjian, S. Trajmar (Eds.), Swarm Studies and Inelastic Electron Molecule Collisions, Springer, New York, 1987, pp. 265–283.
[254] J. Tennyson, P.G. Burke, K.A. Berrington, Comput. Phys. Comm. 47 (1987) 207–212.
[255] S.E. Branchett, J. Tennyson, Phys. Rev. Lett. 64 (1990) 2889–2892.
[256] S.E. Branchett, J. Tennyson, L.A. Morgan, J. Phys. B: At. Mol. Opt. Phys. 23 (1990) 4625–4639.
[257] S.E. Branchett, J. Tennyson, L.A. Morgan, J. Phys. B: At. Mol. Opt. Phys. 24 (1991) 3479–3496.
[258] B.K. Antony, K.N. Joshipura, N.J. Mason, J. Tennyson, J. Phys. B: At. Mol. Opt. Phys. 37 (2004) 1061–1071.
[259] C.P. Ballance, K.A. Berrington, B.M. McLaughlin, J. Phys. B: At. Mol. Opt. Phys. 34 (2001) 3775–3787.
[260] F. Jensen, Introduction to Computational Chemistry, Wiley, Chircester, 1999.
[261] B.M. Nestmann, S.D. Peyerimhoff, J. Phys. B: At. Mol. Opt. Phys. 23 (1990) L773–777.
[262] T. Beyer, B.M. Nestmann, B.K. Sarpal, S.D. Peyerimhoff, J. Phys. B: At. Mol. Opt. Phys. 30 (1997) 3431–3444.
[263] A. Faure, J.D. Gorfinkiel, L.A. Morgan, J. Tennyson, Comput. Phys. Comm. 144 (2002) 224–241.
[264] H.W. van der Hart, J. Phys. B: At. Mol. Opt. Phys. 30 (1997) 453–465.
[265] O. Zatsarinny, Comput. Phys. Comm. 174 (2006) 273–356.
[266] I. Sanchez, F. Martin, J. Phys. B: At. Mol. Opt. Phys. 30 (1997) 679–692.
[267] H. Bachau, E. Cormier, P. Decleva, J.E. Hansen, F. Martin, Rep. Progr. Phys. 64 (2001) 1815–1943.
[268] O. Zatsarinny, K. Bartschat, J. Phys. B: At. Mol. Opt. Phys. 37 (2004) 2173–2189.
[269] D. Bouchiha, J.D. Gorfinkiel, L.G. Caron, L. Sanche, J. Phys. B: At. Mol. Opt. Phys. 39 (2006) 975–986.
[270] W.J. Hunt, W.A. Goddard III, Chem. Phys. Lett. 3 (1969) 414–418.
[271] A.W. Fliflet, V. McKoy, T.N. Rescigno, J. Phys. B: At. Mol. Phys. 12 (1979) 3281–3293.
[272] C.W. Bauschlicher Jr., J. Chem. Phys. 72 (1980) 880–885.
[273] M.H.F. Bettega, C. Winstead, V. McKoy, J. Chem. Phys. 112 (2000) 8806–8812.
[274] H.P. Pritchard, V. McKoy, M.A.P. Lima, Phys. Rev. A 41 (1990) 546–549.
[275] E.R. Davidson, Rev. Modern Phys. 44 (1972) 451–464.
[276] J.D. Gorfinkiel, L.A. Morgan, J. Tennyson, J. Phys. B: At. Mol. Opt. Phys. 35 (2002) 543–555.
[277] I. Rozum, N.J. Mason, J. Tennyson, J. Phys. B: At. Mol. Opt. Phys. 35 (2002) 1583–1591.
[278] I. Rozum, N.J. Mason, J. Tennyson, New J. Phys. 5 (2003) 1–155.
[279] J.J. Munro, N. Doss, J. Tennyson, S.-Y. Kang, (in preparation).
[280] N. Doss, J. Tennyson, J. Phys. B: At. Mol. Opt. Phys. 41 (2008) 125701.
[281] D.L. Cooper, K. Kirby, J. Chem. Phys. 87 (1987) 424–432.
[282] I. Rozum, N.J. Mason, J. Tennyson, J. Phys. B: At. Mol. Opt. Phys. 36 (2003) 2419–2432.
[283] K.A. Berrington, C.P. Ballance, J. Phys. B: At. Mol. Opt. Phys. 35 (2002) 2275–2289.
[284] J. Tennyson, J. Phys. B: At. Mol. Opt. Phys. 37 (2004) 1061–1071.
[285] J. Tennyson, J. Phys. B: At. Mol. Opt. Phys. 29 (1996) 1817–1828.
[286] B. Liu, M. Yoshimine, J. Chem. Phys. 74 (1981) 612–616.
[287] B. Liu, B.H. Lengsfield III, in: E. Clementi (Ed.), Modern Techniques in Computational Chemistry, MOTECC-91, Escom, Leiden, 1991.
[288] A.E. Orel, T.N. Rescigno, B.H. Lengsfield III, Phys. Rev. A 44 (1991) 4328–4335.
[289] C.J. Gillan, J. Tennyson, B.M. McLaughlin, P.G. Burke, J. Phys. B: At. Mol. Opt. Phys. 29 (1996) 1531–1547.
[290] J. Tennyson, Comput. Phys. Comm. 100 (1997) 26–30.
[291] L.A. Collins, B.I. Schneider, Phys. Rev. A 24 (1981) 2387–2401.
[292] J. Tennyson, G. Halmová, in: M. Plummer, G.D. Gorfinkiel, J. Tennyson (Eds.), Mathematical and Computational Methods in R-matrix Theory, CCP2, Daresbury, 2007, pp. 85–90.
[293] R.B. Lehoucq, D.C. Sorensen, C. Yang, ARPACK users' guide: solution of large-scale eigenvalue problems with implicitly restarted Arnoldi methods, SIAM, 1998.
[294] K.J. Maschhoff, D.C. Sorensen, Appled parallel computing in industrial problems and optimization, in: J. Wasniewski, J. Dongarra, K. Madson, D. Olsen (Eds.), in: Lecture notes in computer science, vol. 1184, Springer-Verlag, 1996.
[295] T. Beyer, B.M. Nestmann, S.D. Peyerimhoff, Chem. Phys. 255 (2000) 1–14.
[296] M.W. Schmidt, K. Ruedenberg, J. Chem. Phys. 71 (1992) 3951–3962.
[297] S. Wilson, Theor. Chim. Acta 57 (1980) 53–61.
[298] P.G. Burke, C.J. Noble, A.G. Sunderland, V.M. Burke, Phys. Scr. T100 (2002) 55–63.
[299] V.M. Burke, C.J. Noble, Comput. Phys. Comm. 85 (1995) 471–500.
[300] A.G. Sunderland, J.W. Heggarty, C.J. Noble, N.S. Scott, Comput. Phys. Comm. 114 (1998) 183–194.
[301] V.M. Burke, C.J. Noble, V. Faro-Maza, A. Maniopoulou, N.S. Scott, Comput. Phys. Comm. 180 (2009) 2450–2451.
[302] T. Grimm-Bosbach, H.T. Thümmel, R.K. Nesbet, S.D. Peyerimhoff, J. Phys. B: At. Mol. Opt. Phys. 29 (1996) L105–L112.
[303] L.G. Caron, L. Sanche, Phys. Rev. Lett. 91 (2003) 113201.
[304] L. Caron, L. Sanche, Phys. Rev. A 70 (2004) 032719.
[305] L. Caron, D. Bouchiha, J.D. Gorfinkiel, L. Sanche, Phys. Rev. A 76 (2007) 032716.
[306] D. Bouchiha, L.G. Caron, J.D. Gorfinkiel, L. Sanche, J. Phys. B: At. Mol. Opt. Phys. 41 (2008) 045204.
[307] S. Caprasecca, J.D. Gorfinkiel, D. Bouchiha, L.G. Caron, J. Phys. B: At. Mol. Opt. Phys. 42 (2009)) 095205.
[308] B.I. Schneider, Phys. Rev. A 24 (1981) 1–3.
[309] C.J. Noble, M. Dörr, P.G. Burke, J. Phys. B: At. Mol. Opt. Phys. 26 (1993) 2983–3000.
[310] L. Quigley, K. Berrington, J. Phys. B: At. Mol. Opt. Phys. 29 (1996) 4529–4542.
[311] B.M. Nestmann, J. Phys. B: At. Mol. Opt. Phys. 31 (1998) 3929–3948.
[312] G. Breit, E. Wigner, Phys. Rev. 49 (1936) 519–531.
[313] A.U. Hazi, Phys. Rev. A 19 (1979) 920–922.

[314] J. Tennyson, C.J. Noble, Comput. Phys. Comm. 33 (1984) 421–424.
[315] K. Bartschat, P.G. Burke, Comput. Phys. Comm. 41 (1986) 75–84.
[316] D.W. Busby, P.G. Burke, V.M. Burke, C.J. Noble, N.S. Scott, Comput. Phys. Comm. 114 (1998) 243–270.
[317] N.S. Scott, A. McMinn, P.G. Burke, V.M. Burke, C.J. Noble, Comput. Phys. Comm. 78 (1993) 67–76.
[318] P.G. Burke, Adv. At. Mol. Phys. 4 (1968) 174–219.
[319] F.T. Smith, Phys. Rev. 114 (1960) 349–356.
[320] D.T. Stibbe, J. Tennyson, J. Phys. B: At. Mol. Opt. Phys. 29 (1996) 4267–4283.
[321] D.T. Stibbe, J. Tennyson, Comput. Phys. Comm. 114 (1998) 236–242.
[322] C.P. Ballance, B.M. McLaughlin, K.A. Berrington, J. Phys. B: At. Mol. Opt. Phys. 31 (1998) L655–L665.
[323] L.A. Morgan, Phys. Rev. Lett. 80 (1998) 1873–1875.
[324] J. Tennyson, L.A. Morgan, Phil. Trans. A 357 (1999) 1161–1173.
[325] L. Quigley, K. Berrington, J. Pelan, Comput. Phys. Comm. 114 (1998) 225–235.
[326] C.P. Ballance, B.M. McLaughlin, O. Nagy, K.A. Berrington, P.G. Burke, J. Phys. B: At. Mol. Opt. Phys. 31 (1998) L305–L314.
[327] C.P. Ballance, K.A. Berrington, B.M. McLaughlin, Phys. Rev. A 60 (1999) R4217–R4220.
[328] D.T. Stibbe, J. Tennyson, Chem. Phys. Lett. 308 (1999) 532–536.
[329] T. Sommerfeld, U.V. Riss, H.D. Meyer, L.S. Cederbaum, B. Engels, H.U. Suter, J. Phys. B: At. Mol. Opt. Phys. 31 (1998) 4107–4122.
[330] K. Houfek, T.N. Rescigno, C.W. McCurdy, Phys. Rev. A 77 (2008) 012710.
[331] T. Beyer, B.M. Nestmann, S.D. Peyerimhoff, J. Phys. B: At. Mol. Opt. Phys. 33 (2000) 4657–4672.
[332] T. Beyer, B.M. Nestmann, S.D. Peyerimhoff, J. Phys. B: At. Mol. Opt. Phys. 34 (2001) 3703–3716.
[333] B.M. Nestmann, V. Brems, A. Dora, S. Kumar, J. Phys. B: At. Mol. Opt. Phys. 38 (2005) 75–81.
[334] B.M. Nestmann, S.V.K. Kumar, S.D. Peyerimhoff, Phys. Rev. A 71 (2005) 012705.
[335] V. Brems, T. Beyer, B.M. Nestmann, H.D. Meyer, L.S. Cederbaum, J. Chem. Phys. 117 (2002) 10635–10647.
[336] P. Kolorenč, V. Brems, J. Horáček, Phys. Rev. A 72 (2005) 012708.
[337] D.T. Stibbe, J. Tennyson, J. Phys. B: At. Mol. Opt. Phys. 31 (1998) 815–844.
[338] J. Tennyson, C.J. Noble, J. Phys. B: At. Mol. Phys. 18 (1985) 155–165.
[339] D.J. Haxton, Z.Y. Zhang, C.W. McCurdy, T.N. Rescigno, Phys. Rev. A 69 (2004) 062713.
[340] D.T. Stibbe, J. Tennyson, New J. Phys. 1 (1998) 2.
[341] R.W. Brankin, J.R. Dormand, I. Gladwell, P. Prince, W.L. Seward, ACM Trans. Math. Soft. 15 (1989) 31–40.
[342] G.V. Mil'nikov, H. Nakamura, J. Phys. B: At. Mol. Opt. Phys. 34 (24) (2001) L791–L794.
[343] G. Danby, J. Tennyson, Phys. Rev. Lett. 61 (1988) 2737–2739.
[344] M.A. Hayes, C.J. Noble, J. Phys. B: At. Mol. Opt. Phys. 31 (1998) 3609–3619.
[345] S.E. Branchett, J. Tennyson, J. Phys. B: At. Mol. Opt. Phys. 25 (1992) 2017–2026.
[346] B.K. Sarpal, J. Phys. B: At. Mol. Opt. Phys. 26 (1993) 4145–4154.
[347] B.K. Sarpal, S.E. Branchett, J. Tennyson, L.A. Morgan, J. Phys. B: At. Mol. Opt. Phys. 24 (1991) 3685–3699.
[348] G. Theodorakopoulos, S.C. Farantos, R.J. Buenker, S.D. Peyerimhoff, J. Phys. B: At. Mol. Phys. 17 (1984) 1453–1462.
[349] M.C. van Hemert, S.D. Peyerimhoff, J. Chem. Phys. 94 (1991) 4369–4383.
[350] W. Ketterle, J. Chem. Phys. 93 (1990) 6935–6941.
[351] C.W. Clark, Phys. Rev. A 30 (1984) 750–757.
[352] N.T. Padial, D.W. Norcross, L.A. Collins, J. Phys. B: At. Mol. Opt. Phys. 14 (1981) 2901–2909.
[353] F.A. Gianturco, A. Jain, Phys. Rep. 143 (1986) 347–425.
[354] D.W. Norcross, N.T. Padial, Phys. Rev. A 25 (1982) 226–338.
[355] I. Rabadán, J. Tennyson, Comput. Phys. Comm. 114 (1998) 129–141.
[356] I. Rabadán, B.K. Sarpal, J. Tennyson, J. Phys. B: At. Mol. Opt. Phys. 31 (1998) 2077–2090.
[357] A. Faure, H.N. Varambhia, T. Stoecklin, J. Tennyson, Mon. Not. R. Astron. Soc. 382 (2007) 840–848.
[358] A.J. Lim, I. Rabadán, J. Tennyson, Mon. Not. R. Astron. Soc. 306 (1999) 473–478.
[359] I. Jimenez-Serra, J. Martin-Pintado, S. Viti, S. Martin, A. Rodriguez-Franco, A. Faure, J. Tennyson, Astrophys. J. 650 (2006) L135–L138.
[360] D.A. Neufeld, A. Dalgarno, Phys. Rev. A 40 (1989) 633–637.
[361] I. Rabadán, B.K. Sarpal, J. Tennyson, Mon. Not. R. Astron. Soc. 299 (1998) 171–175.
[362] A. Faure, J. Tennyson, Mon. Not. R. Astron. Soc. 325 (2001) 443–448.
[363] B.K. Sarpal, J. Tennyson, Mon. Not. R. Astron. Soc. 263 (1993) 909–912.
[364] V. Ngassam, O. Motapon, A. Florescu, L. Pichl, I.F. Schneider, A. Suzor-Weiner, Phys. Rev. A 68 (2003) 032704.
[365] S. Krohn, Z. Amitay, A. Baer, D. Zajfman, M. Lange, L. Knoll, J. Levin, D. Schwalm, R. Wester, A. Wolf, Phys. Rev. A 62 (2000) 032713.
[366] O. Motapon, F.O.W. Tamo, X. Urbain, I.F. Schneider, Phys. Rev. A 77 (2008) 052711.
[367] A. Faure, J.D. Gorfinkiel, J. Tennyson, Mon. Not. Roy. astr. Soc. 347 (2004) 323–333.
[368] H.N. Varambhia, M. Gupta, A. Faure, K.L. Baluja, J. Tennyson, J. Phys. B: At. Mol. Opt. Phys. 42 (2009) 095204.
[369] A. Faure, J.D. Gorfinkiel, J. Tennyson, J. Phys. B: At. Mol. Opt. Phys. 37 (2004) 801–807.
[370] Y. Itikawa, N. Mason, J. Phys. Chem. Ref. Data 34 (2005) 1–22.
[371] D.M. Campbell, P.S. Farago, Nature 318 (1985) 52–53.
[372] S. Mayer, J. Kessler, Phys. Rev. Lett. 74 (1995) 4803–4806.
[373] K.W. Trantham, M.E. Johnston, T.J. Gay, Can. J. Phys. 74 (1996) 925–928.
[374] K. Blum, D. Thompson, Adv. At. Mol. Opt. Phys. 38 (1998) 39–86.
[375] R.P. Nordbeck, K. Blum, C.J. Noble, P.G. Burke, J. Phys. B: At. Mol. Opt. Phys. 26 (1993) 3611–3623.
[376] M. Tashiro, Phys. Rev. A 77 (2008) 012723.
[377] G. Wöste, C. Fullerton, K. Blum, D. Thompson, J. Phys. B: At. Mol. Opt. Phys. 27 (1994) 2625–2637.
[378] H. Niikura, P.B. Corkum, Adv. At. Mol. Opt. Phys. 54 (2007) 511–548.
[379] A.G. Harvey, J. Tennyson, J. Modern Opt. 54 (2007) 1099–1106.
[380] A.G. Harvey, J. Tennyson, J. Phys. B: At. Mol. Opt. Phys. 42 (2009) 095101.
[381] A.-T. Le, R.R. Lucchese, S. Tonzani, T. Morishita, C.D. Lin, Phys. Rev. A 80 (2009) 013401.
[382] A.G. Harvey, O. Smirnova, J. Tennyson, (in preparation).
[383] M. Charlton, J.W. Humberston, Positron Physics, Cambridge University Press, 2000.
[384] K.L. Baluja, R. Zhang, J. Franz, J. Tennyson, J. Phys. B: At. Mol. Opt. Phys. 40 (2007) 3515–3524.
[385] J. Franz, F.A. Gianturco, K.L. Baluja, J. Tennyson, R. Carey, R. Montuoro, R.R. Lucchese, T. Stoecklin, P. Nicholas, T.L. Gibson, Nucl. Instr. Meths. Phys. Res. B 266 (2008) 425–434.
[386] E.A.G. Armour, J.W. Humberston, Phys. Rep. 204 (1991) 165–251.
[387] W. Klopper, F.R. Manby, S. Ten-No, E.F. Valeev, Int. Rev. Phys. Chem. 25 (2006) 427–468.
[388] S. Hoefener, D.P. Tew, W. Klopper, T. Helgaker, Chem. Phys. 356 (2009) 25–30.
[389] J. Franz, K.L. Baluja, R. Zhang, J. Tennyson, Nucl. Instr. Meths. Phys. Res. B 266 (2008) 419–424.
[390] K.R. Hoffman, M.S. Dababneh, Y.F. Hsieh, W.E. Kauppila, V. Pol, J.H. Smart, T.S. Stein, Phys. Rev. A 25 (1982) 1393–1403.
[391] M. Charlton, T.C. Griffith, G.R. Heyland, G.L. Wright, J. Phys. B: At. Mol. Opt. Phys. 16 (1983) 323–341.
[392] G.O. Morell, R.G. Parr, J. Chem. Phys. 71 (1979) 4139–4141.
[393] H. Cho, Y.-S. Park, H. Tanaka, S.J. Buckman, J. Phys. B: At. Mol. Opt. Phys. 37 (2004) 625.

[394] M.A. Khakoo, H. Silva, J. Muse, M.C.A. Lopes, C. Winstead, V. McKoy, Phys. Rev. A 78 (2008) 052710.
[395] K. Jung, T. Antoni, R. Müller, K.-H. Kochem, H. Ehrhardt, J. Phys. B: At. Mol. Opt. Phys. 15 (1982) 3535–3555.
[396] L.A. Morgan, J. Phys. B: At. Mol. Opt. Phys. 31 (1998) 5003–5011.
[397] S. Taioli, J. Tennyson, J. Phys. B: At. Mol. Opt. Phys. 39 (2006) 4379–4392.
[398] T.J. Gil, T.N. Rescigno, C.W. McCurdy, B.H. Lengsfield III, Phys. Rev. A 49 (1994) 2642–2650.
[399] D.J. Haxton, T.N. Rescigno, C.W. McCurdy, Phys. Rev. A 72 (2005) 022705.
[400] D.J. Haxton, T.N. Rescigno, C.W. McCurdy, Phys. Rev. A 75 (2007) 012711.
[401] D.J. Haxton, T.N. Rescigno, C.W. McCurdy, Phys. Rev. A 78 (2008) 040702.
[402] C. Piccarreta, Ph.D. Thesis, University of London, 2007.
[403] J. Tennyson, Rep. Progr. Phys. 57 (1995) 421–476.
[404] A.E. Orel, K.C. Kulander, Phys. Rev. Lett. 71 (1993) 4315–4318.
[405] J. Lecointre, M.O.A. El Ghazaly, J.J. Jureta, D.S. Belic, X. Urbain, P. Defrance, J. Phys. B: At. Mol. Opt. Phys. 42 (2009) 075201.
[406] T. Oka, T.R. Geballe, M. Goto, T. Usuda, B.J. McCall, Astrophys. J. 632 (2005) 882–893.
[407] A. Faure, J. Tennyson, J. Phys. B: At. Mol. Opt. Phys. 35 (2002) 3945–3956.
[408] A. Faure, L. Wiesenfeld, P. Valiron, J. Tennyson, Philos. Trans. R. Soc. Lond. A 364 (2006) 4379–4392.
[409] V. Kokoouline, C.H. Greene, Phys. Rev. A 68 (2003) 012703.
[410] A. Faure, V. Kokoouline, C.H. Greene, J. Tennyson, J. Phys. Conf. Series 192 (2009) 012016.
[411] V. Kokoouline, A. Faure, J. Tennyson, C.H. Greene, Mon. Not. R. Astron. Soc. (in press).
[412] B.M. Nestmann, K. Pfingst, S.D. Peyerimhoff, J. Phys. B: At. Mol. Opt. Phys. 27 (1994) 2297–2308.
[413] S. Kaur, K.L. Baluja, J. Phys. B: At. Mol. Opt. Phys. 38 (2005) 3917–3933.
[414] D. Bouchiha, J.D. Gorfinkiel, L.G. Caron, L. Sanche, J. Phys. B: At. Mol. Opt. Phys. 40 (2007) 1259–1270.
[415] M. Tashiro, J. Chem. Phys. 129 (2008) 164308.
[416] C.S. Trevisan, A.E. Orel, T.N. Rescigno, J. Phys. B: At. Mol. Opt. Phys. 39 (2006) L255–L260.
[417] J. Tennyson, C.J. Noble, J. Phys. B: At. Mol. Phys. 19 (1986) 4025–4033.
[418] K.L. Baluja, A.Z. Msezane, J. Phys. B: At. Mol. Opt. Phys. 35 (2002) 437–444.
[419] K.L. Baluja, J.A. Tossell, J. Phys. B: At. Mol. Opt. Phys. 37 (2004) 609–623.
[420] M. Tashiro, K. Morokuma, Phys. Rev. A 75 (2007) 012720.
[421] M. Gupta, K.L. Baluja, Euro. Phys. J. D 41 (2007) 475–483.
[422] B. Yan, S.-F. Pan, J.-H. Yu, Chinese Physics 16 (2007) 1956–1958.
[423] R. Curik, C.H. Greene, Mol. Phys. 105 (2007) 1565–1574.
[424] D.J. Haxton, C.H. Greene, Phys. Rev. A 78 (2008) 052704.
[425] H.-J. Werner, P.J. Knowles, R. Lindh, F.R. Manby, M. Schütz, et al. Molpro, version 2008.1, a package of ab initio programs, see http://www.molpro.net 2008.
[426] L. Malegat, Comput. Phys. Comm. 60 (1990) 391–404.
[427] S. Kaur, K.L. Baluja, J. Tennyson, Phys. Rev. A 77 (2008) 032718.
[428] A.R. Barnett, Comput. Phys. Comm. 27 (1982) 147–166.